Electronic Supplementary Information

Merging Electrocatalytic Alcohol Oxidation with C-N Bond Formation by Electrifying Metal-Ligand Cooperative Catalysts

Sitthichok Kasemthaveechok,[a] Patrice Gérardo[b] and Niklas von Wolff[a]*

[a]Université Paris-Cité, Laboratoire d'Electrochimie Moléculaire, CNRS UMR 7591, F-75013 Paris, France.

[b]Université Paris-Cité, Laboratoire de Chimie et Biochimie, Pharmacologiques et Toxicologiques, CNRS UMR 8601, F-75006 Paris, France.

Email: niklas.von-wolff@u-paris.fr

Table of Contents

1 General information

All manipulations unless stated otherwise were performed using Schlenk or glovebox techniques under dry argon or nitrogen atmosphere, respectively. THF was dried over Na/benzophenone, freshly distilled prior to use and stored under nitrogen atmosphere over molecular sieves (4Å). Anhydrous deuterated solvents were purchased from Eurisotop and stored over 4Å molecular sieves. All commercial chemicals were purchased from suppliers and used as received. **Ru-2** and **Ru-3** were synthesized according to literature procedures.[1,2] GC-MS analyses were performed on a Shimadzu QP-2020 equipped with a capillary column (Shimadzu, SH-Rtx-Wax, fused silica column with crossband polar polyethylene glycol phase, 60 m × 0.32 mm × 0.5 µm film thickness). Temperature program: start temperature 120 °C, heating rate 15 °C/min, end temperature 240 °C for 32-67 min, run total 40-75 mn. ^{1}H and ^{13}C NMR spectra were recorded at room temperature on an AVANCE III 400 BRUKER at Laboratoire Interfaces Traitements Organisation et DYnamique des Systèmes (ITODYS), Université Paris-Cité or on a Magritek Spinsolve 80^{ULTRA}. For high-resolution mass-spectrometry (HR-MS), analytes were passed using direct Flow Injection Analysis (FIA) with a Shimadzu nexera X2 HPLC system, equipped with a Shimadzu PDA prominence at 0.3ml/min eluted with 100% Methanol. The HPLC system is coupled, for the detection, with a Thermo scientific exactive, orbitrap mass spectrometer. This high-resolution mass spectrometer operated in negative and positive electrospray ionization mode with a probe voltage of 4.6 KV and a capillary temperature of 275°C. Data acquisition and analysis were performed with Xcalibur software version 2.2.0

Chemical shifts δ are given in ppm and coupling constants *J* in Hz. Chemical shifts for ^{1}H NMR spectra are referenced relative to residual protium in the deuterated solvent (^{1}H δ = 7.26 ppm, $CDCl_3$, δ = 5.32 ppm, CD_2Cl_2). ^{13}C shifts are referenced to deuterated solvent (δ = 77.2 ppm for $CDCl_3$, δ = 53.8 ppm for CD_2Cl_2). The following abbreviations are used for describing NMR spectra: s (singlet), d (doublet), t (triplet), td (triplet of doublets), ddd (doublet of doublets of doublets), vd (virtual doublet), vt (virual triplet), br (broad). Thin-layer chromatography (TLC) was performed on aluminum sheets precoated with Merck 5735 Kieselgel 60F254. Column chromatography was carried out with Merck 5735 Kieselgel 60F (0.040-0.063 mm mesh).

2 Electrochemistry

If not stated otherwise, electrosynthesis was conducted via controlled potential electrolysis (CPE) using an AUTOLAB potentiostat (Metrohm) with a three-electrode set-up in a home-made divided H-cell (6 mL for working compartment), using a leak-free Ag/AgCl-reference electrode, a Pt-mesh counter electrode and a graphite/carbon cloth working electrode under an argon atmosphere. Cyclic voltammetry was performed using a SCE reference electrode, a platinum wire counter electrode and a 3mm glassy carbon working electrode, that was polished (diamant paste), washed and sonicated prior to use.

2.1 General procedure for CPE

A homemade H-cell was charged with degassed alcohol, base and amine substrate in a working compartment, while the same concentration of basic aqueous solution was charged in the counter compartment. A homemade carbon working electrode (Figure S1, carbon felt on graphite rod) was used as the anode and a Pt-mesh as cathode. The reaction mixture was electrolyzed under a constant potential electrolysis of 0.3 V vs Ag/AgCl for 6 hours (for condition and catalyst screening) or 2F mol (76 C for substrate scope). The reaction mixture and working electrode was then washed and extracted with water, dichloromethane, dried over $MgSO_4$ and then concentrated under reduced pressure (*see work up procedure for more details*, *vide infra*). This crude reaction mixture was diluted to 10 mL with dichloromethane and product quanitification was done using GC-MS with mesitylene as an internal standard (*ca.* 5 µL). To obtain NMR and isolated yields, the solution was purified by silica gel chromatography column (5% Et_3N/Heptane).

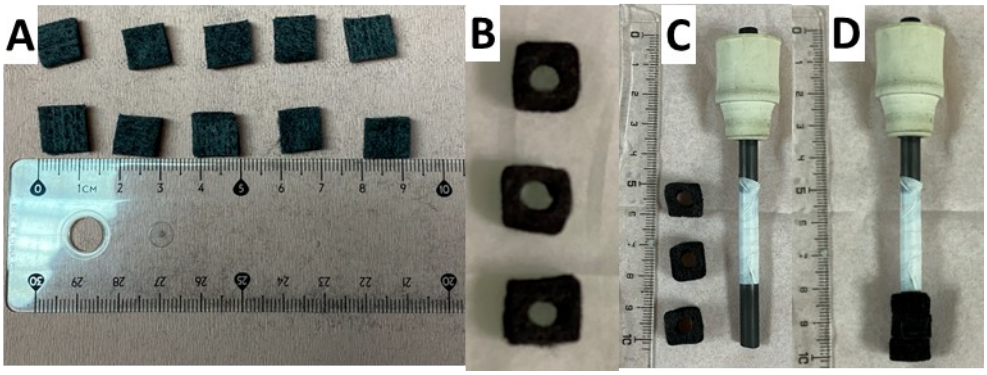

Figure S1: Preparation of homemade carbon working electrode: A) Cut carbon felt from the carbon felt sheet in a cuboid shape of ca. 1x1x0.5 cm. B) A hole with a diameter of ϕ ca. 5 mm was cut out from the center. C) A graphite-rod (6mm diameter) electrode was covered with PTFE-tape to leave a blank 2cm piece of the electrode, on which the carbon felt pieces (3) were mounted. D) Finished anode ensemble of graphite-rod and carbon felt cuboids.

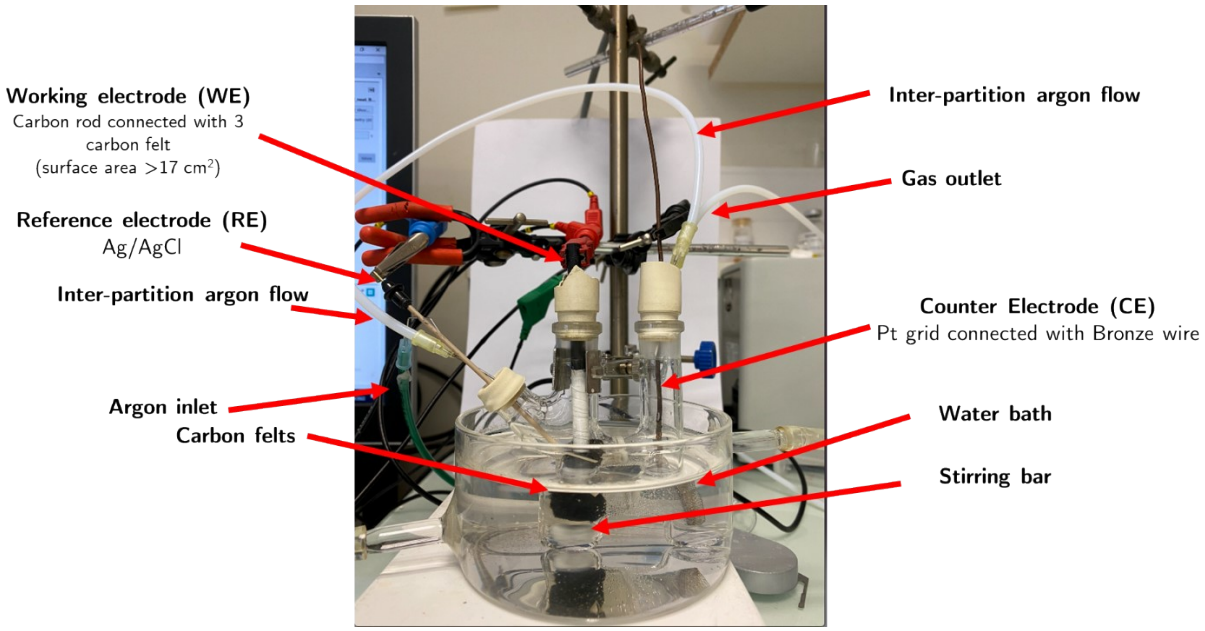

Figure S2. To the assembled electrolysis cell, an argon line is attached with a loop connecting working and counter compartment to balance pressure. The cell is degassed by Ar-bubbling through the solvent for roughly 5-10 minutes. After the Ar-purge, the entry needle is raised above the reaction solution and a slow Ar flow remains, to eliminate any formed H_2 from the counter electrode so as to prevent H_2 crossover and pressure built-up.

2.2 Workup procedure

The cap of the working compartment is unplugged and the solution is poured into 30 mL of water in separation funnel and extracted with DCM (3 x 10 mL). The organic layer is then dried over $MgSO_4$ and the solvent is removed under reduced pressure. The residual material (mostly remaining BnOH derivatives) is transferred to a 10 mL volumetric flask and diluted to 10 mL with dichloromethane and 5 µL of mesitylene are added as internal standard. The mixture is then analyzed by GC-MS.

2.3 Cleaning Procedure

The porous homemade C-felts and graphite rod are sonicated for 5 minutes each with these following solutions: 1) 0.1 M aq. HCl 2) deionized water 3) acetone 4) dichloromethane. Then, the electrodes are dried with compressed air.

The H-cell is washed by the following solutions. 1) 0.1 M aq. HCl 2) deionized water 3) acetone 4) dichloromethane and then dried with compressed air.

2.4 General procedure for CV

Cyclic voltammetry was performed in a oven-dried, home-made thermostated glass cell (25 °C) in a three electrode set-up under argon. The working electrode (3 mm glassy carbon) was polished using diamond paste, washed with ultra-pure water (milliQ), acetone, sonicated in acetone for 5 mn, rinsed with water and acetone and dried with compressed air prior to use. The reference electrode (sat. calomel, SCE) was separated from the working compartment by a ceramic frit. A platinum grid was used as counter-electrode. CVs were run with a AUTOLAB potentiostat (Metrohm) and ohmic drop was compensated using positive feedback. Unless otherwise stated, the electrolyte was tetrabutyl ammonium hexafluorophosphate (recrystallized from ethanol and dried under high vacuum) in THF (0.1 M). Unless otherwise stated, the scan rate was 0.1 V/s. CVs are referenced to the ferrocene/ferrocenium couple by adding ferrocene to the solution at the end of experiment.

3 Benzyl alcohol impurities and aerobic oxidation

During the screening using neat benzyl alcohol as substrate, we observed a steady excess in faradaic efficiency as well as high excess in the benzaldehyde portion. The observed issue with commercial benzyl alcohol is the presence of benzaldehyde traces (which promptly react with the amine to form the corresponding imine) and its corresponding benzyl benzoate in solution (**Figure S3a**, **Figure S4**). This observation was described elsewhere in the literature.[3] Moreover, alkaline solutions of benzyl alcohol may

significantly increase the amount of aerobic benzaldehyde produced over time (see **Figure S3a**). Generally, the amount of benzaldehyde and benzyl benzoate is negligible if used in dilute solutions. In the case of a neat solution however, this amount has an effect and cannot be neglected (**Figure S3b**). Therefore, in our experiments, the benzyl alcohol alkali solution was prepared and used as soon as possible, which is generally less than a week. All batches of alkaline BnOH solution used in the experiments were analyzed by GC-MS and the amount of amine added was corrected for initially present aldehyde and ester. Results along the manuscript correspond to product formation/F.E. after subtraction of background autooxidation.

Calculation of yield and F.E. of the product will be as followed.

$$Yield = \frac{OP\ (mmol) - PAB\ (mmol)}{IPA\ (mmol) - PAB\ (mmol)} \times 100\% \quad (1)$$

$$F.E. = \frac{OP\ (mmol)\ + TAP\ (mmol) + \ 2 \times OEP(mmol)\ -\ PAB\ (mmol) - 2 \times PAE(mmol)}{C\ (mmol)/_2} \times 100\%$$

OP = Observed imine product (mmol) PAB = Pre-observed aldehyde in BnOH (mmol)

PAE = Pre-observed ester in BnOH (mmol) IPA = Input amine substrate (mmol)

C = Charged passed TAP = Total aldehyde product (mmol)

OEP = Observed ester product (mmol)

Note: IPA is adjusted for initially present aldehyde product (PAB), *i.e.* IPA = 0.38 mmol + PAB, for all reactions in Scheme 3, 4, 5 and 6 of the manuscript. For all other reactions, IPA is equal to the indicated amine concentration. For all reactions, the product yield is recalculated by subtracting imine formation from initially present benzaldehyde to avoid false high yields due to benzyl alcohol aerobic-oxidation.

Calculation example:

Table 1, entry 1: F.E. =

$$F.E. = \frac{0.390\ mmol\ +\ 0.142\ mmol\ +\ 0\ .044\ mmol\ -\ 0.133\ mmol - 0.044\ mmol}{0.788\ mmol\ e^-/_2} \times 100\% = 101\%$$

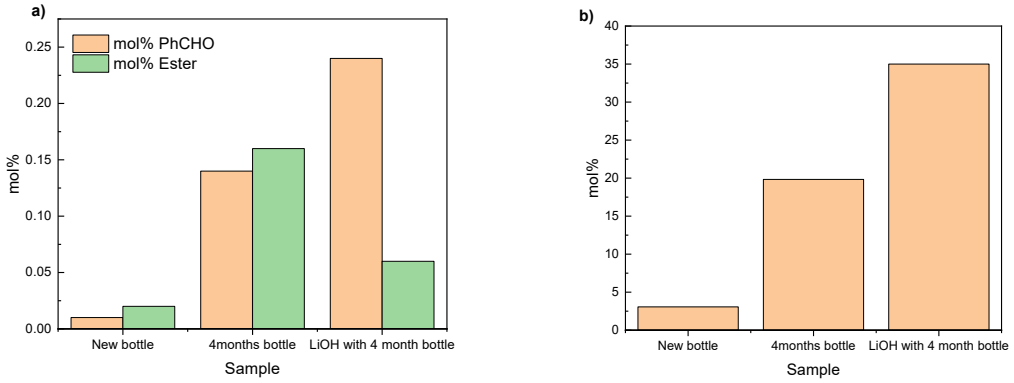

Figure S3. a) Quantitative amount of benzaldehyde and benzyl benzoate traces in pure BnOH and alkali BnOH samples. b) Corresponding amount of amine promptly consumed by the benzaldehyde traces in the pre-electrolysis solution under neat BnOH conditions.

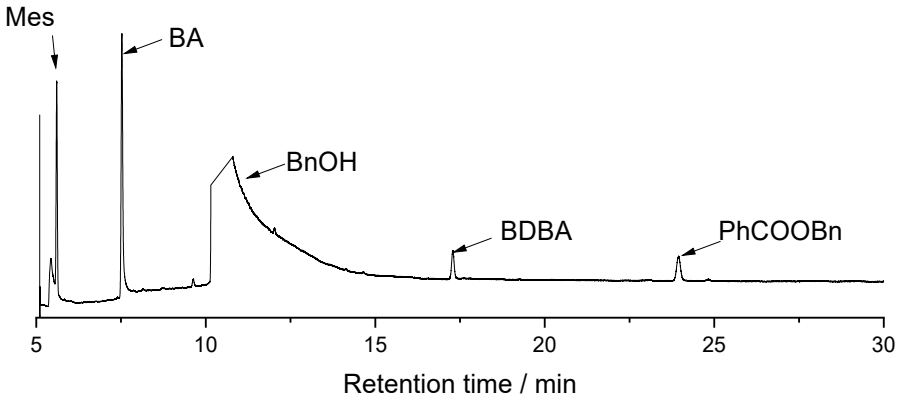

Figure S4. Chromatogram of commercial benzyl alcohol solution. BA = Benzaldehyde; BDBA = benzaldehyde dibenzyl acetal; PhCOOBn = benzyl benzoate.

4 Reaction optimization

Cation effects in the case of electrocatalytic water oxidation are well-documented[4–7] and their effect on the molecular EAO was hence investigated (Table SI). The efficacy of hydroxide bases of the alkali metal decreases down the group (entries 1-4) with Cs^+ giving however slightly better results than potassium. Switching to dianionic bases or using bases commonly employed in electrosynthesis or those that have been used for the activation of alcohols for HAT-chemistry[8,9] was not productive. The organic TMA (tetramethyl ammonium) cation increased the imine yield, however at the cost of lower F.E. attributed to the presence of excess water. Increasing base loading gave slightly better results, again with water decreasing F.E.

Table S1. Imine bond formation coupling between benzyl alcohol and *n*-hexylamine using ruthenium-based metal-ligand corporate catalyst (**Ru-1**): Testing of different bases (electrolyte).

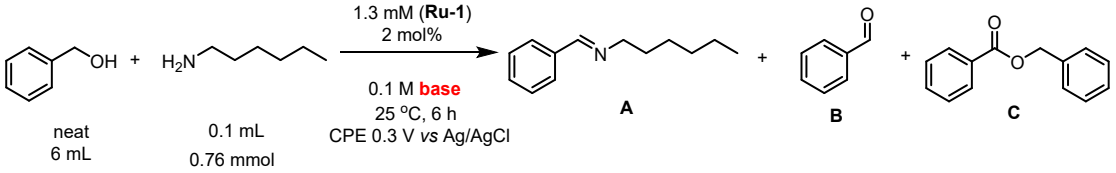

Entry	Base	Conversion BnOH (mmol)	F.E. distribution (%)			GC yield (Imine, %)	Faradaic efficiency (%)
			A	B	C		
1	LiOH	0.35	94	1	9	44	105
2	NaOH	0.31	92	2	8	41	102
3	KOH	0.20	99	2	6	28	102
4	CsOH	0.26	101	2	11	34	108
5	Cs_2CO_3	0.11	24	1	7	13	160
6	Li_2CO_3	0.04	55	0	58	4	565
7	KOPiv	0	0	0	0	0	0
8	$TBAH_2PO_4$	0.14	76	11	0	52	87
9	TMAOH*	0.34	68	1	14	63	83
10	0.2 M LiOH†	0.34	82	69	1	9	89
11	0.2 M TMAOH†	0.35	92	80	0	10	90

* Contains 10% H_2O, † Contains 20% H_2O

Table S2. Imine bond formation coupling between benzyl alcohol and *n*-hexylamine using ruthenium-based metal-ligand corporate catalyst (**Ru-1**): Testing of different electrolyte concentration.

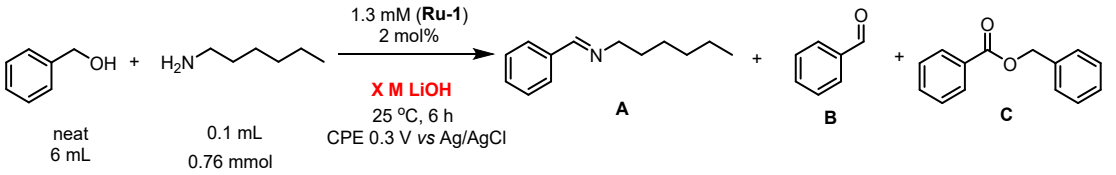

Entry	[LiOH] / **M**	Conversion BnOH (mmol)	F.E. distribution (%)			GC yield (Imine, %)	Faradaic efficiency (%)
			A	**B**	**C**		
1	0.1 M	0.35	94	1	9	44	105
2	0.2 M	0.49	75	5	8	62	88
3	0.5 M	0.29	97	1	2	32	99
4	1.0 M	0.26	98	1	1	29	101

Table S3. Imine bond formation coupling between benzyl alcohol and *n*-hexylamine using ruthenium-based metal-ligand corporate catalyst (**Ru-1**): Testing of different solvents.

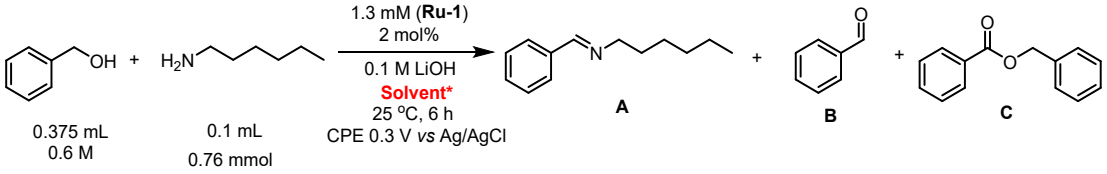

Entry	Solvent	Conversion BnOH (mmol)	F.E. distribution (%)			GC yield (Imine, %)	Faradaic efficiency (%)
			A	B	C		
1	neat	0.35	94	1	9	44	105
2	1,4-dioxane/H_2O (7:1)	0.17	31	1	0	22	32
3	CH_2Cl_2/H_2O (7:1)	0.15	70	0	7	15	77
4	$PhCF_3/H_2O$ (7:1)	0.03	863	0	117	4	980
5	THF/H_2O (7:1)	0.23	25	0	1	28	26
6[a]	*t*-AmOH	0.03	35	0	0	4	35
7[a,b]	1,4 dioxane	0.003	9	2	0	0.4	11
8[a]	$MeNO_2$	0.003	0.4	0	1.3	0.1	2

[a] 0.1 mL (0.2 M) of BnOH is used instead of standard condition, [b] LiOH is replaced by KOPiv due to solubility issue.

Table S4. Imine bond formation coupling between benzyl alcohol and *n*-hexylamine using ruthenium-based metal-ligand corporate catalyst (**Ru-1**): Testing of different benzyl alcohol concentration.

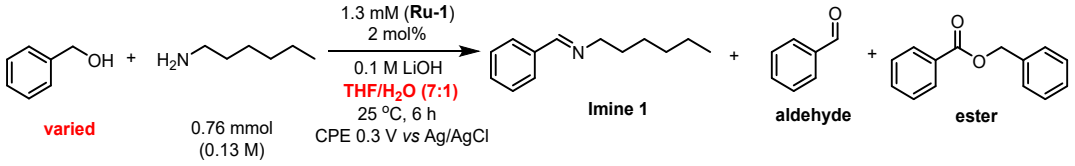

Entry	Solvent	Conversion BnOH (mmol)	F.E. distribution (%)			GC yield (Imine, %)	Faradaic efficiency (%)
			A	B	C		
1	neat	0.35	94	1	9	44	105
2	0.6 M BnOH	0.23	25	0	1	28	26
3	1.6 M BnOH	0.22	51	1	3	26	55
4	3.0 M BnOH	0.22	67	1	7	26	74

Table S5: Blank experiments compared to standard conditions in terms of amine conversion, as well as product selectivity. (neat 0.2 M LiOH/BnOH (6 mL), 50 µL hexylamine, 25°C, 6 hours, 1.3 mM catalyst, CPE 0.3 V vs Ag/AgCl ; the presence of two latter conditions is indicated in the table)

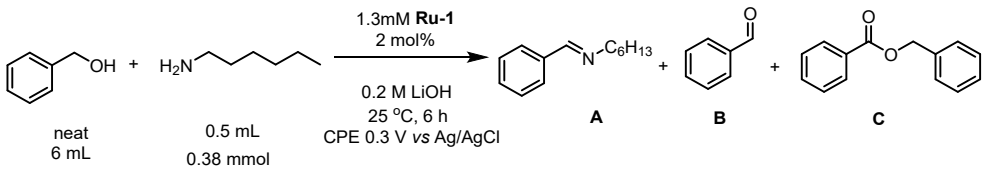

Entry	Catalyst	Applied potential	Conversion BnOH (mmol)	Product observed (µmol)			GC yield (Imine, %)	Faradaic efficiency (%)
				A	B	C		
1	•	•	0.40	257	142	0	>99	101

2	•	-	0.04	29	9	0	7	-
3	-	•	0.04	45	0	0	11	10
4	-	-	0	0	0	0	0	-
5	Replaced by **TEMPO**	•	0.02	9	6	0	2.5	73

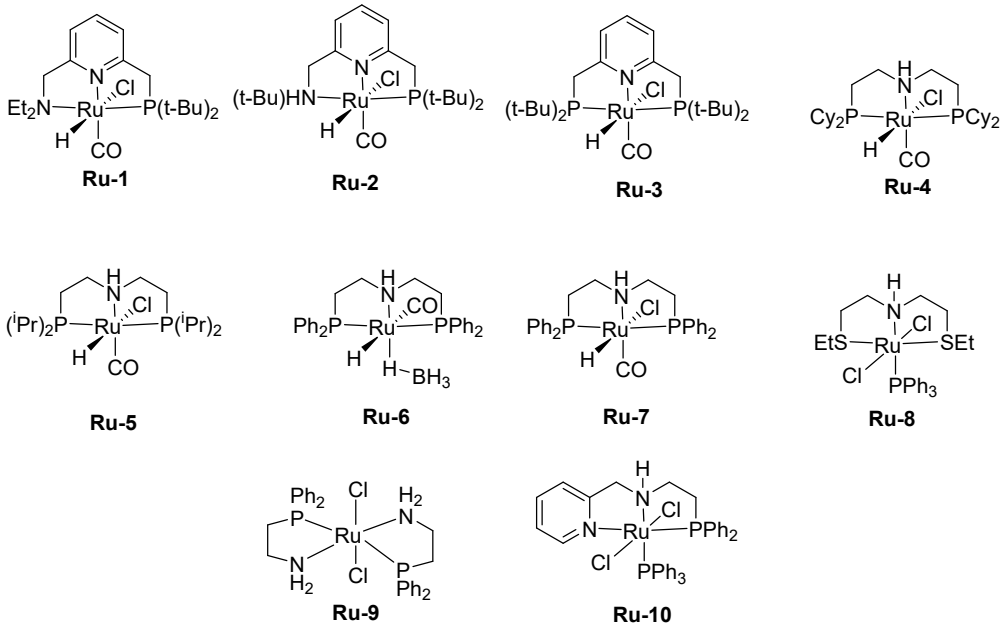

Scheme S1: Range of catalyst that were successfully tested for the reaction.

Table S6: Results of different catalyst screened in the study in standard condition (neat 0.2 M LiOH/BnOH (6 mL), 50 µL hexylamine, 1.3 mM catalyst, CPE 0.3 V vs Ag/AgCl, 25°C, 2F mol amine)

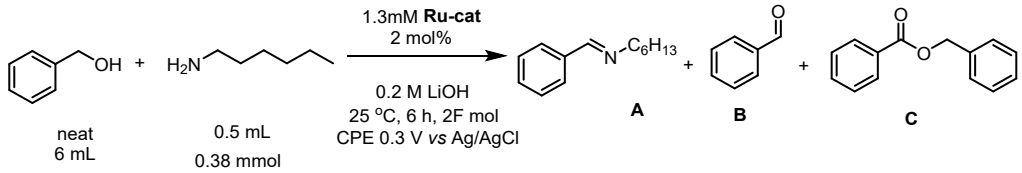

Entry	Catalyst	Conversion BnOH (mmol)	F.E. distribution (%)			GC yield (Imine, %)	Faradaic efficiency (%)
			A	B	C		
1	**Ru-1**	0.40	65	36	0	>99	101
2	**Ru-2**	0.34	67	18	0	>99	85
3	**Ru-3**	0.33	74	9	Trace	99	83
4	**Ru-4**	0.24	41	19	0	65	60
5	**Ru-5**	0.28	56	14	0	90	70
6	**Ru-6**	0.27	58	11	0	93	69
7	**Ru-7**	0.28	60	12	0	97	72
8	**Ru-8**	0.29	57	10	7	90	73
9	**Ru-9**	0.26	46	22	0	74	68
10	**Ru-10**	0.28	59	12	Trace	93	71
11	**TEMPO**	0.02	44	29	0	2.5	73

Table S7 Results of different alcohol derivatives screened in the study in standard condition (3 M alcohol, 0.2 M LiOH/(THF/H_2O – 7:1 v/v) (6 mL), 0.38 mmol n-hexylamine, 1.3 mM catalyst, CPE 0.3 V vs Ag/AgCl, 25°C, 2F mol amine)

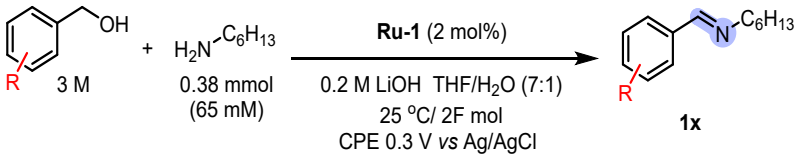

Entry	Alcohol	Conversion	Imine Selectivity		F.E. (%)
		BnOH (mmol)	GC yield (%)	NMR yield (%)	
1*	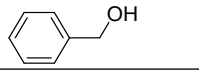	0.40	>99	66	101
1a	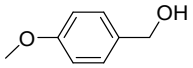	0.31	82	61	79
1b	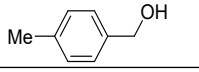	0.36	88	77	94
1c	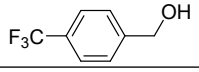	0.27	64	81	69
1d	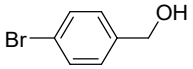	0.22	N/A	48	56
1e	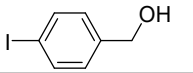	0.17	N/A	42[a]	45
1f	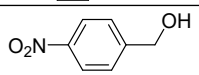	0.06	52	68	53
1g	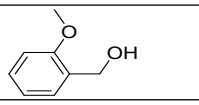	0.18	51	61	47
1h	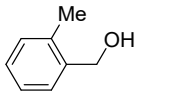	0.22	44	44	64
1i	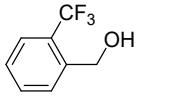	0.28	75	65	75
1j	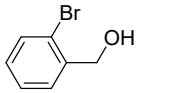	0.16	N/A	45	42
1k	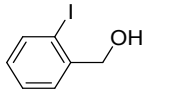	0.23	50	58	59
1l	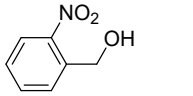	0.21	21	11	17
1m	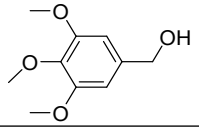	0.39	72	40	100

* Reaction in neat condition, [a] Isolated yield

Note: conversion of BnOH was calculated based on combined amount between benzaldehyde, imine, and benzyl benzoate.

Table S8: Results of different amine derivatives screened in the study in standard condition (neat 0.2 M LiOH/BnO H (6 mL), 0.38 mmol amine, 1.3 mM catalyst, CPE 0.3 V vs Ag/AgCl, 25°C, 2F mol amine)

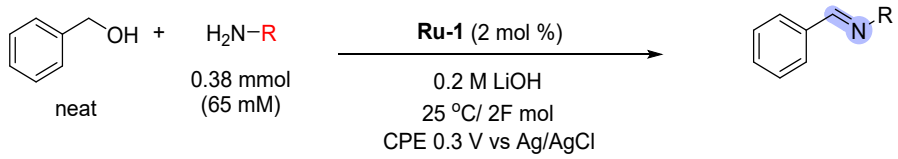

Entry	Amine	Conversion	Yield (%)		F.E. (%)
		BnOH (mmol)	Imine (GC)	Imine (NMR)	
1	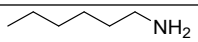	0.40	>99	66	101
2	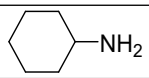	0.43	65	63	99
3	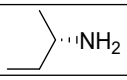	0.38	>99	nd	98
4		0.25	44	65	64
5	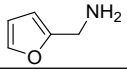	0.44	88	40	110
6	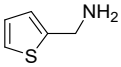	0.31	75	97	80
7	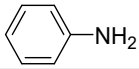	0.14	23	nd	35
7a	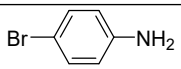	0.23	0	nd	58
7b	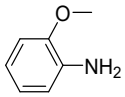	0.12	0	nd	30
7c	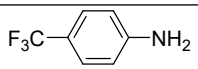	0.22	3	nd	55
7d	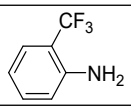	0.17	0	nd	20
8	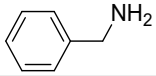	0.41	>99	79	105
9	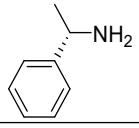	0.42	>99	88	107
10	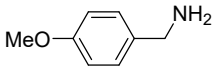	0.43	>99	26	108
11	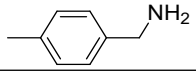	0.43	>99	28	110
12	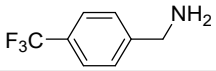	0.34	99	81	88
13	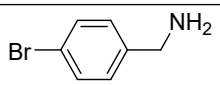	0.41	97	95	103
14	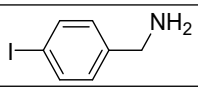	0.34	50	35	87

15	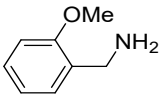	0.34	83	63	88
16	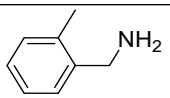	0.41	>99	60	106
17	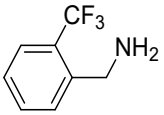	0.39	87	60	101
18	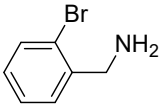	0.46	>99	45	110
19	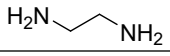	0.25	57	nd	64
20 (diimine)	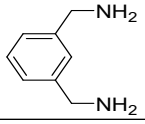	0.27	nd	53	68
20b (monoimine)				21	
21	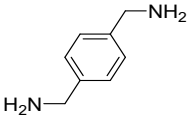	0.37	nd	84	95

Note: conversion of BnOH was calculated based on combined amount between benzaldehyde, imine, and benzyl benzoate.

5 Reuse and recyclability test

5.1 4.5 mmol scale reaction (reuse of reaction mixture after 2F mol)

A general condition for CPE has been used. A homemade H-cell was charged with degassed 1.9 mL of 0.2 M LiOH/BnOH, 4.1 mL of 0.2 M LiOH/(THF/H_2O – 7:1) and 0.1 mL of hexylamine (0.76 mmol) to a working compartment, while the counter compartment was charged with 0.2 M LiOH/H_2O. 4 mg of **Ru-1** catalyst (1 mol%) was added to the working compartment. The reaction mixture was electrolyzed under a constant potential electrolysis of 0.3 V vs Ag/AgCl for 2F mol (respective to amine, 151 C). After the electrolysis, the working compartment was charged again with degassed hexylamine (0.76 mmol), followed by **Ru-1** catalyst (8 µmol) and the electrolysis was continued for 2F mol. This procedure has been repeated for 5 consecutive rounds (total amount of 4.5 mmol hexylamine and 24 mg of **Ru-1**). The solution was passed to the work-up procedure (*vide supra*) and filtrated by column chromatography (5% Et_3N/heptane) to obtain 300 mg of **1** (33% yield). After obtaining the target imine, the column was flushed with 5% MeOH/Acetone to obtain 1.45 g of the leftover benzyl alcohol (74% recovery).

5.2 Recyclability test

A general condition for CPE has been used. A homemade H-cell was charged with degassed 1.75 mL of 4-CF_3BnOH, 4.25 mL of 0.2 M LiOH/(THF/H_2O – 7:1) and 50 µL of hexylamine (0.38 mmol) to a working compartment, while the counter compartment was charged with 0.2 M LiOH/H_2O. 4 mg of **Ru-1** catalyst (1 mol%) was added to the working compartment. The reaction mixture was electrolyzed under a constant potential electrolysis of 0.3 V vs Ag/AgCl for 2F mol (respective to amine, 76 C). The solution was passed to the work-up procedure (*vide supra*) and filtrated by column chromatography (5% Et_3N/heptane) to obtain 52 mg of **1** (53% yield). After obtaining the target imine, the column was then flushed with 5% MeOH/Acetone to obtain 2.07 g of the leftover 4-CF_3BnOH (92% recovery).

6 Synthesis of authentic samples Ru-OH and Ru-OBn

The synthesis of **Ru-OH** and **Ru-OBn** is achieved following reported pathways.[10,11] In short, **Ru-1** was treated with 1.2 eq. of KO*t*-Bu to afford the dearomatized intermediate. After filtration over celite, evaporation of the solvent and extraction with pentane, the dearomatized intermediate was treated with either excess BnOH or D_2O to afford **Ru-OBn** and **Ru-OH** respectively.

7 Thermochemistry and oxidation chemistry of simple alcohols and amines

Tabulated data for the calculation of the Gibbs free energy of formation ($\Delta_f G^0$), the Gibbs free Energy of reaction ($\Delta_r G^0 = \sum \Delta_f G^0_{product} - \sum \Delta_f G^0_{starting\ material}$), as well as theoretical cell potential (E_{cell}) and oxidation potential (E_{Anode}) for the dehydrogenation reactions of specific alcohols and amines (for which tabulated data was found) are given in Tables S9 and S10.

Table S9 Gibbs free energy of formation values that is used for the calculation of standard redox potentials. Data was obtained from the NIST website (https://www.nist.gov/), or from the KDB database (https://www.cheric.org/research/kdb/)

	$\Delta_f H^0_{liquide}$(kJ/mol)	S^0(kJ/mol.K)	$\Delta_f G^0$(kJ/mol)	Source
BnOH	-154,9	0,217	-219,5	NIST
Benzaldehyde	-87,1	0,221	-153,1	NIST
Methylamine			32,3	KDB
HCN	135,1 ($\Delta_f H^0_{gas}$)	0,202	75,0	NIST
Water			-228,8	KDB
Benzoic acid	-384,8	0,166	-434,2	NIST

Table S10 Gibbs free energy of reaction, standard redox potentials, as well as half reaction potentials for selected dehydrogenation reactions.

Reaction	$\Delta_r G^0$(kJ/mol)	E_{cell} (V vs NHE)	E_{anode} (=$E_{NHE} - E_{cell}$, $in\ V$)
$PhCH_2OH \rightleftharpoons PhCHO + H_2$	66,4	-0,344	+0,344
$PhCH_2OH + H_2O \rightleftharpoons PhCO_2H + 2H_2$	14,1	-0,036	+0,03666
$CH_3NH_2 \rightleftharpoons HCN + 2H_2$	42,7	-0,111	+0,111

From Table S10, it is evident that both the oxidation (dehydrogenation) of benzyl alcohol to benzoic acid, as well the dehydrogenation of a simple primary amine to the corresponding nitrile are thermodynamically more favorable, than benzyl alcohol dehydrogenation to benzaldehyde. To probe that amine oxidation on an electrode is also kinetically favored over benzyl alcohol oxidation, we run the respective anodic CV scans in THF (Figure S5). From the CV response, we see that amine oxidation starts around 0.1 V *vs* Fc/Fc^+, whereas benzyl alcohol is oxidized at much higher potential (starting around 0.7 V *vs* Fc/Fc^+) at a

glassy carbon electrode. In order to avoid parasitic amine oxidation, catalysts with a working potential around 0 V *vs* Fc/Fc^+, should be chosen.

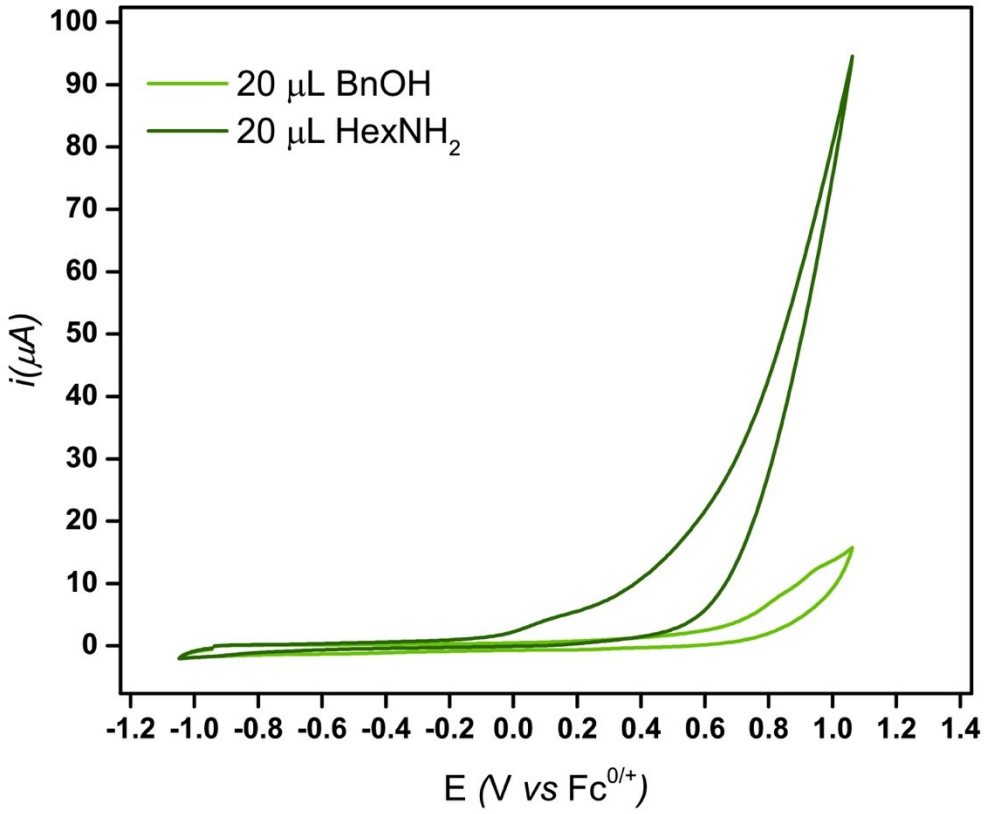

Figure S5. Cyclic voltammograms (0.1 V/s, 3 mm GC) in 0.1 M $TBAPF_6$ in THF of 20 μL (63 mM) of benzyl alcohol (light green) and 20 μL (51 mM) of hexyl amine (dark green).

8 Cyclic voltammetry studies

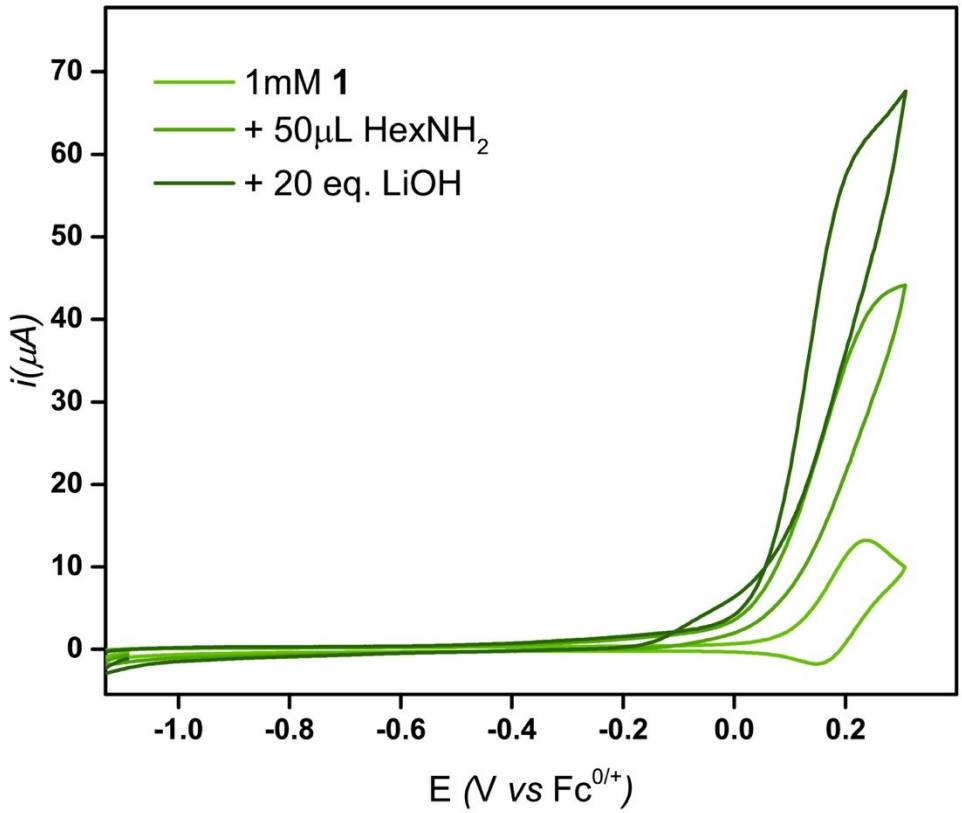

Figure S6. Cyclic voltammograms (0.1 V/s, 3 mm GC) in 0.1 M $TBAPF_6$ in THF of 1 mM **1** alone (light green), in the presence of 50 μL hexylamine (green, 72 mM) and in the presence of 50 μL hexylamine as well as 60 mM LiOH (dark green, equivalents of LiOH were added as 1 M solution in H_2O).

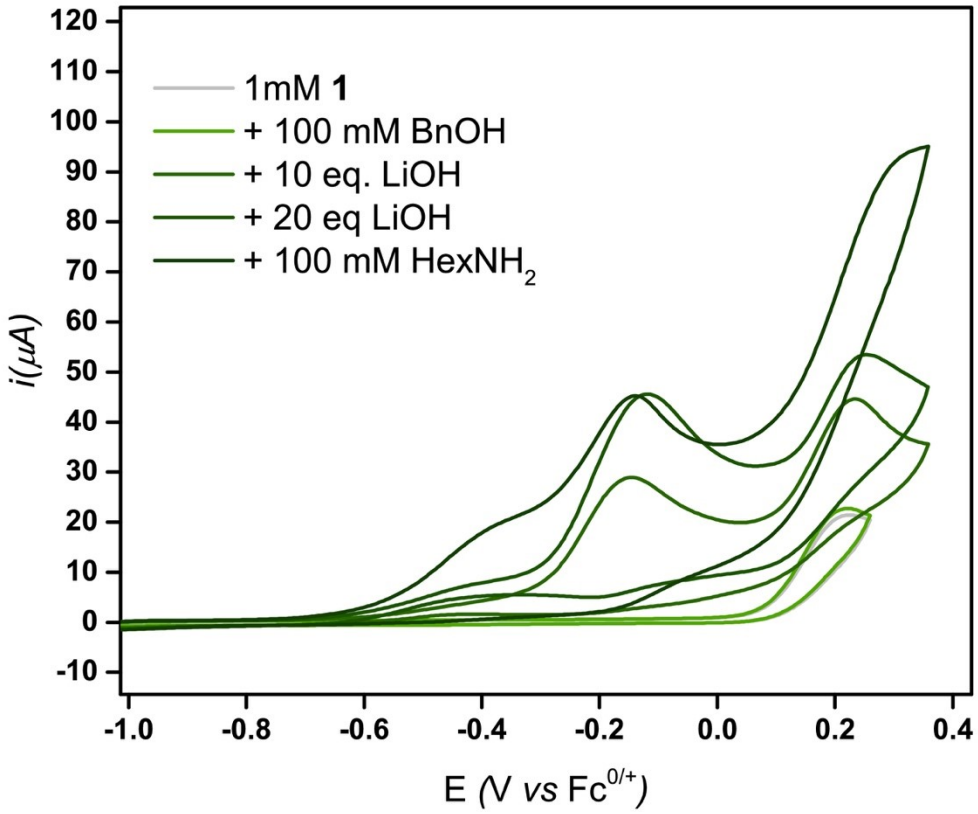

Figure S7. Cyclic voltammograms (0.1 V/s, 3 mm GC) in 0.1 M $TBAPF_6$ in 7:1 THF/H_2O of 1 mM **1** alone (light grey), in the presence (i) 100 mM BnOH (ii) 100 mM BnOH and 10 mM LiOH (iii) 100 mM BnOH, 20 mM LiOH (iv) 100 mM BnOH, 20 mM LiOH, 100 mM $HexNH_2$ (i-iv: from light to dark green, equivalents of LiOH were added as 1 M solution in H_2O).

In the absence of water/base, **1** shows a quasi-reversible one electron oxidation wave (Ru(II)/Ru(III) at roughly 0.2 V vs $Fc^{0/+}$, in agreement with what we already described in our previous paper (Figure S6).[12] At this potential, **1** is capable to induce mediated oxidation of hexyl amine, which is more pronounced in the presence of base (see Figure S7). Importantly, under these conditions, no dearomatization or formation of the amido- or alkoxo-complex is observed (compare also to our previous paper).[12] Hence, at the oxidation potential of **1**, simple outer-sphere oxidation of the amine occurs, albeit at potentials significantly lower than in the absence of **1** (compare Figure S5). The situation is different when switching to conditions used for CPE. As can be seen in Figure S7, in the presence of water, the oxidation of **1** becomes irreversible (grey trace). At this potential, **1** is not able to oxidize BnOH to a significant extend and the slight increase in current is attributed to outer-sphere non-specific oxidation of BnOH by **1** (Figure S7 (i)). Addition of 10 or 20 equivalents of base (LiOH) gives rise to new waves around -0.4 V and -0.2 V, which are characteristic of the dearomatization (wave at -0.4 V) and formation of alkoxide/hydride species (wave at -0.2V, compare to our previous paper[12]). This implies, that in the presence of excess LiOH and BnOH the active alkoxide species is indeed formed, which is not the case in the presence of amine alone. This is in agreement with our proposed mechanism, which highlights that the more acidic alcohol is deprotonated, leading to the formation of alkoxide species, that thermally evolve to the key hydride intermediate (see Scheme 7 of the main manuscript). Addition of amine to this mixture seems to favor somewhat the dearomatization and the wave at -0.2 V shifts slightly cathodically, which might be indicative of favoring the hydride formation by intercepting any concomitantly formed aldehyde (compare to Scheme 7). Its noteworthy, that under these conditions, some **1** still remains and promotes unselective amine oxidation. For alkyl alcohols, formation of the alkoxide species is less-favored and thus remaining **1** can promote undesired side-reactivity. Lowering the working potential, successfully suppresses this reactivity.

9 Energy efficiency

One of the advantages of electrochemistry is the ease with which we can control and monitor the energy input into the system. Hence, energy consumption can be easily addressed by monitoring key parameters.
In our home-made cell, we generally have cell voltages below 10 V and currents in the range of 5-20 mA under CPE conditions. If we take the 20 mA upper limit, the 76C (2F) needed for full conversion are passed after 63 min. With 200 mW power (10 V, 20 mA), the energy input is thus 760 J (0.2 W x 3800 s) or 2000 kJ/mol.

Calculating the energy necessary for the thermal activation is less straightforward and is thus roughly approximated. A commercial lab-scale heating plate (e.g. IKA Plate RCT Digital) has a maximum power of 600 W (heating up to 310 °C). Thermal imine formation is run at >110 °C[13] and we thus approximate the necessary power to 213 W. Although these reactions are in general run for more than 24 h, we approximate that 10 min will be sufficient to heat the oil bath to the desired temperature and that no further heat loss during the 24 h period will take place. The thermal energy input in the system is thus 128 kJ (213 W x 600 s), or 12'800 kJ/mol (10 mmol scale).

While the energy consumption of the electrochemical approach can be easily adjusted by lowering the cell voltage (e.g. membrane *vs.* ceramic frit, distance between electrodes, surface area of the counter electrode), our approximated energy consumption for the thermal approach is a rough lower bound and likely higher (mainting temperature throughout the 24 h etc.). This crude approximation thus highlights that electrochemical approaches might yield in an order of magnitude gain in energy efficiency, when compared to classical thermal systems.

10 Product characterizations

Symbol	Denote
○	Mesitylene (internal standard)
△	Benzyl alcohol
□	Benzaldehyde impurities
*	All the cut peaks in GC is the alcohol substrate signal

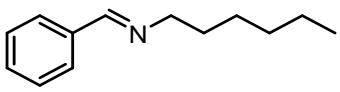

1

***N*-hexyl-1-phenylmethanimine** (**1**): ^{1}H NMR (400 MHz, $CDCl_3$) δ 8.18 (s, 1H), 7.69 – 7.59 (m, 2H), 7.37 – 7.29 (m, 3H), 3.52 (td, J = 7.1, 1.4 Hz, 2H), 1.76 – 1.51 (m, 2H), 1.35 – 1.08 (m, 6H), 0.80 (t, J = 2.9 Hz, 3H). ^{13}C NMR (101 MHz, $CDCl_3$) δ 160.74, 136.48, 130.48, 128.62, 128.09, 61.91, 31.77, 30.99, 27.13, 22.71, 14.16. NMR data are in accordance with literature values.[13]

GC-MS trace

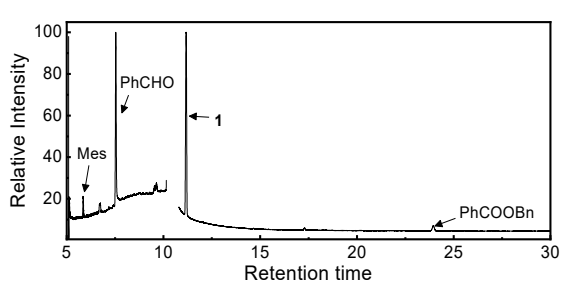

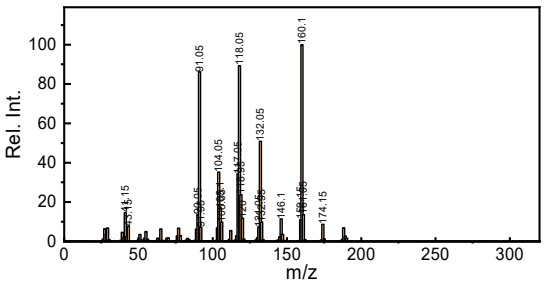

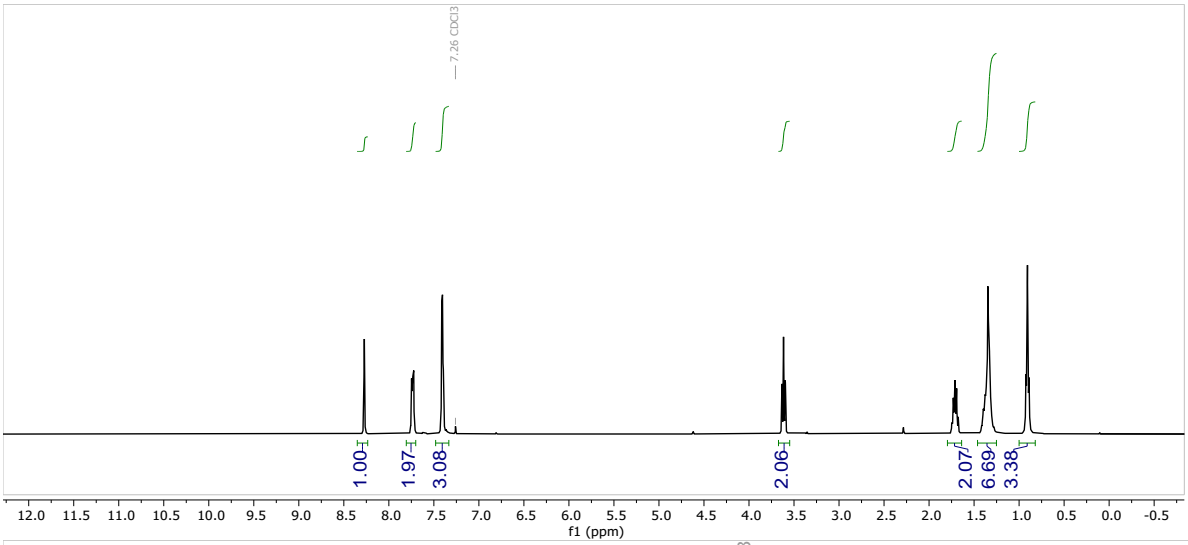

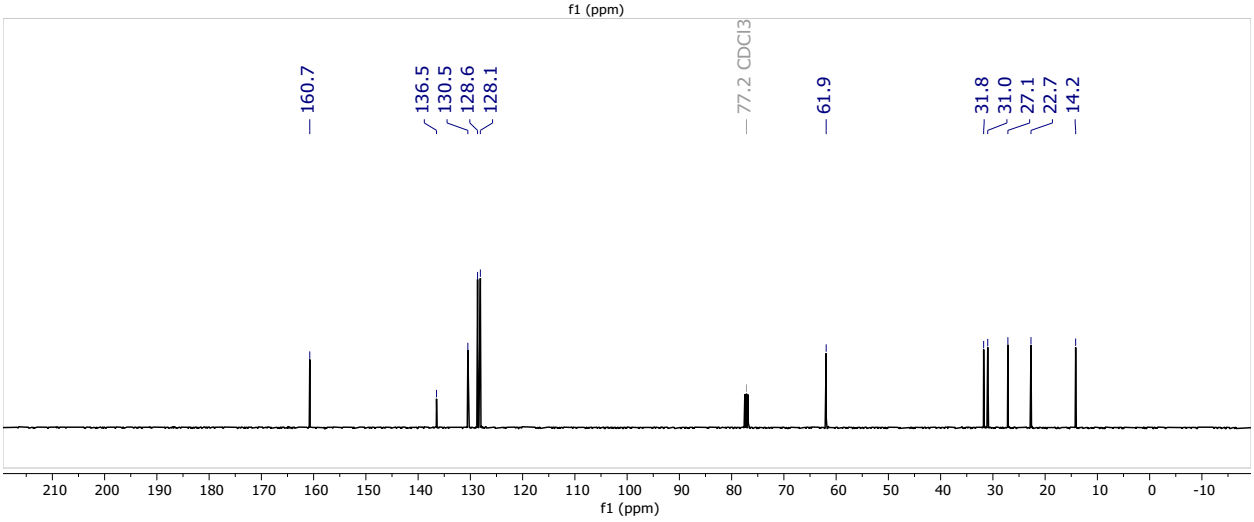

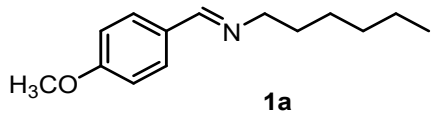

1a

***N*-hexyl-1-(4-methoxyphenyl)methanimine** (**1a**): ^{1}H NMR (400 MHz, $CDCl_3$) δ 8.12 (s, 1H), 7.59 (d, J = 8.7 Hz, 2H), 6.85 (d, J = 8.8 Hz, 2H), 3.76 (s, 3H), 3.49 (td, J = 7.1, 1.3 Hz, 2H), 1.66 – 1.55 (m, 2H), 1.38 – 1.19 (m, 6H), 0.87 – 0.77 (m, 3H). NMR data are in accordance with literature values.[13]

GC-MS trace

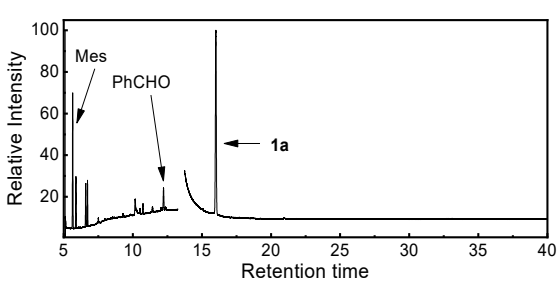

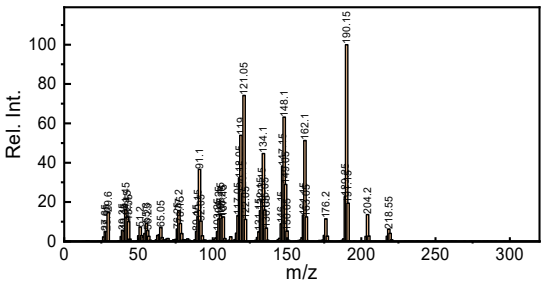

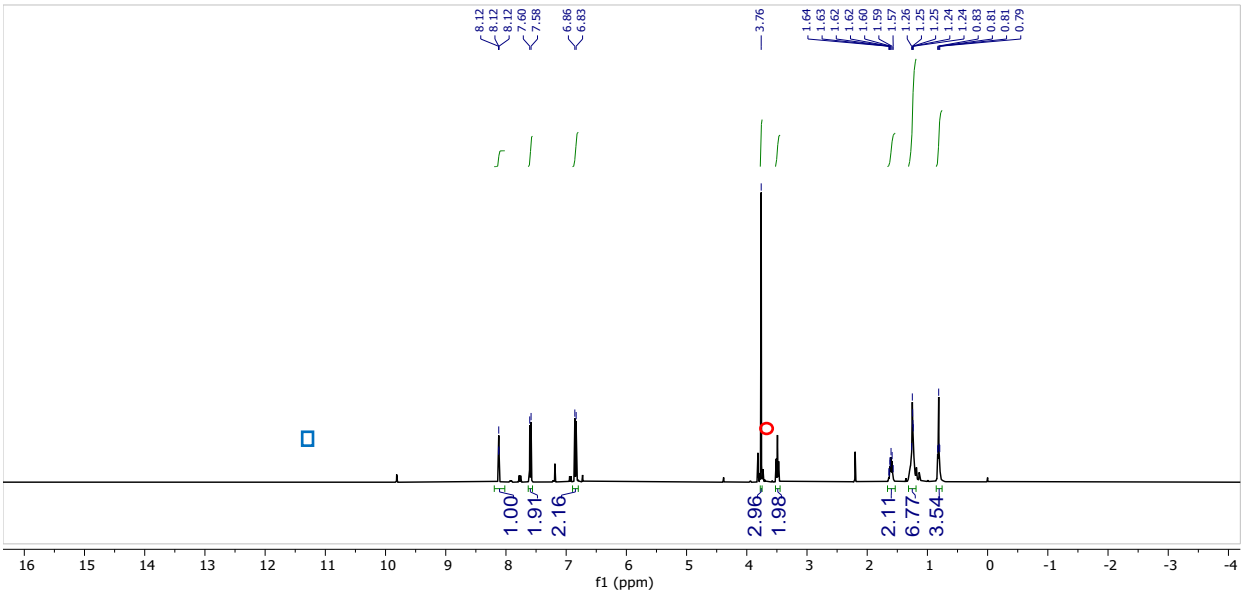

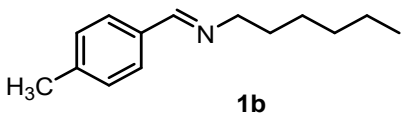

1b

***N*-hexyl-1-(4-methylphenyl)methanimine** (**1b**): ^{1}H NMR (400 MHz, $CDCl_3$) δ 8.23 (d, J = 1.4 Hz, 1H), 7.64 – 7.58 (m, 2H), 7.21 (d, J = 7.9 Hz, 2H), 3.59 (td, J = 7.1, 1.4 Hz, 2H), 2.38 (s, 3H), 1.75 – 1.60 (m, 2H), 1.35 – 1.30 (m, 6H), 0.91 – 0.87 (m, 3H). NMR data are in accordance with literature values.[14]

GC-MS trace

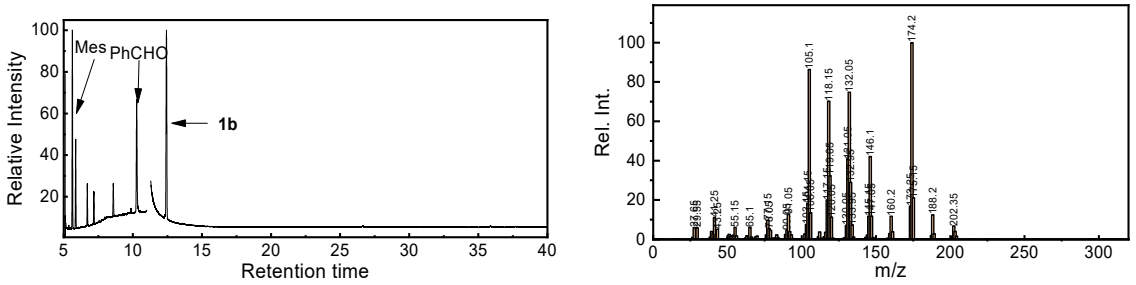

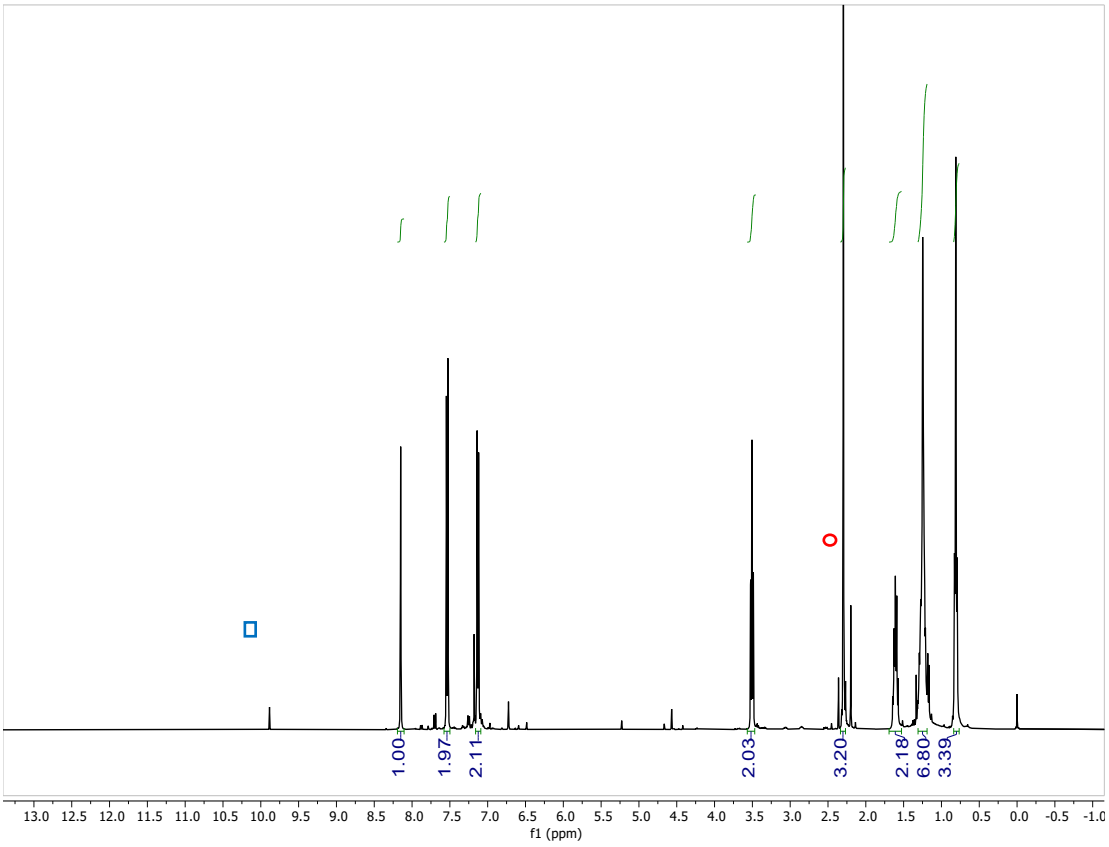

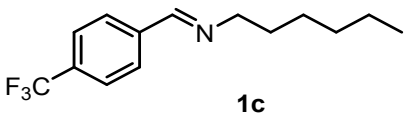

1c

***N*-hexyl-1-(4-trifluoromethylphenyl)methanimine** (**1c**): ^{1}H NMR (400 MHz, $CDCl_3$) δ 8.23 (s, 1H), 7.75 (d, *J* = 8.0 Hz, 3H), 7.58 (d, *J* = 8.1 Hz, 3H), 3.56 (td, *J* = 7.1, 1.4 Hz, 4H), 1.63 (dq, *J* = 8.3, 6.9 Hz, 3H), 1.40 – 1.20 (m, 6H), 0.85 – 0.78 (m, 3H). ^{19}F NMR (376 MHz, $CDCl_3$) δ -62.77. ^{13}C NMR (101 MHz, $CDCl_3$) δ 159.4, 139.6, 132.2 (d, *J* = 32.5 Hz), 125.7 (q, *J* = 3.8 Hz), 124.1 (d, *J* = 172 Hz), 62.0, 31.8, 30.9, 27.2, 22.8, 14.2. NMR data are in accordance with literature values.[15]

GC-MS trace

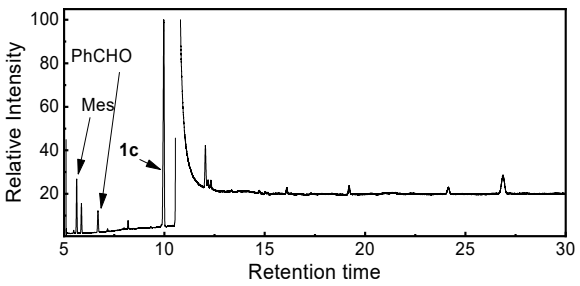
Relative Intensity
PhCHO
Mes
1c
Retention time

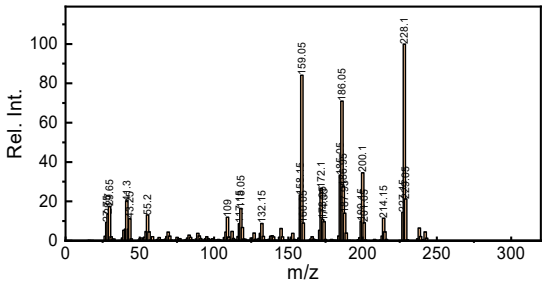
Rel. Int.
m/z

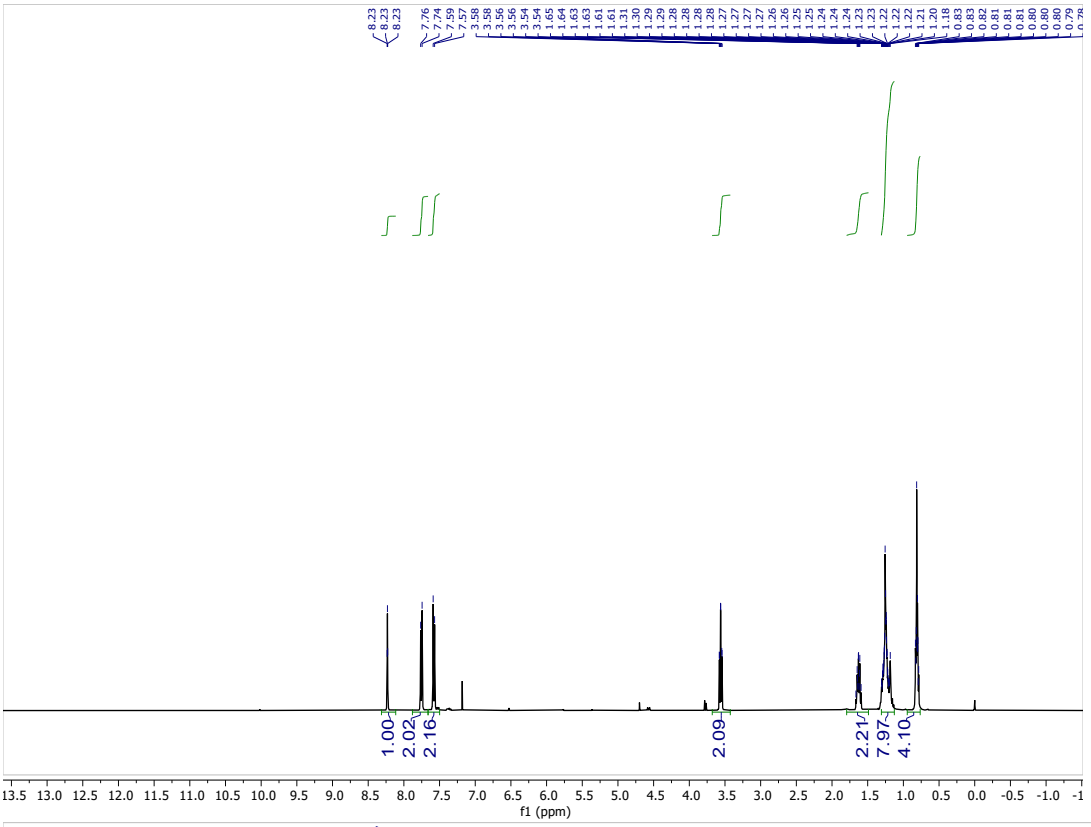
1.00
2.02
2.16
2.09
2.21
7.97
4.10
f1 (ppm)

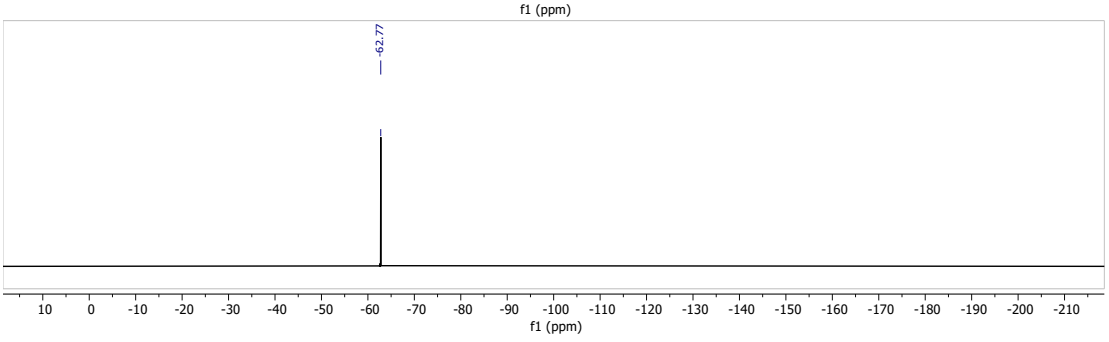
-62.77
f1 (ppm)

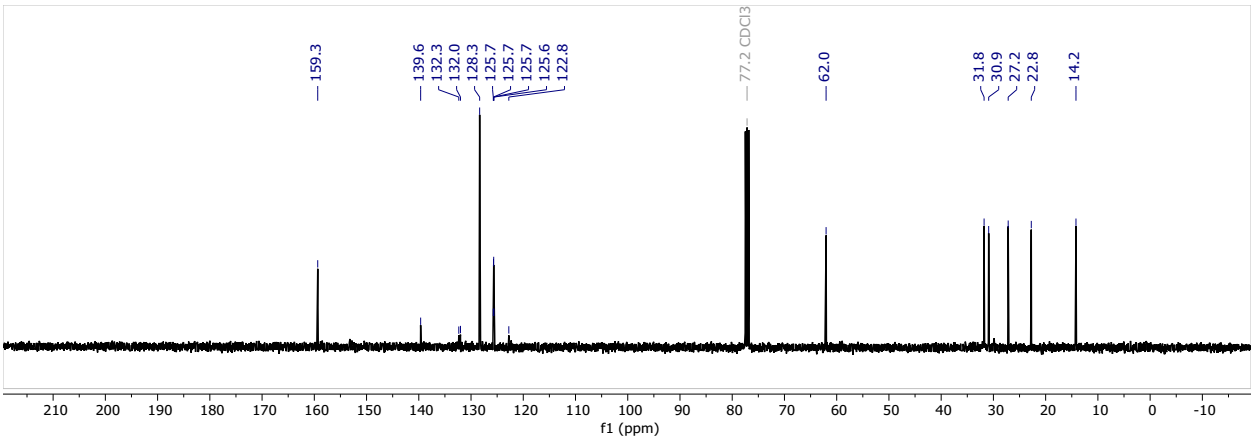

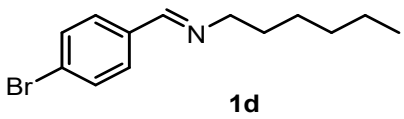

1d

***N*-hexyl-1-(4-bromophenyl)methanimine** (**1d**): ^{1}H NMR (400 MHz, $CDCl_3$) δ 8.13 (d, *J* = 1.5 Hz, 1H), 7.52 (d, *J* = 8.6 Hz, 2H), 7.46 (d, *J* = 8.7 Hz, 2H), 3.51 (td, *J* = 7.1, 1.4 Hz, 2H), 1.66 – 1.56 (m, 2H), 1.28 – 1.21 (m, 6H), 0.81 (m, 3H). NMR data are in accordance with literature values.[14]

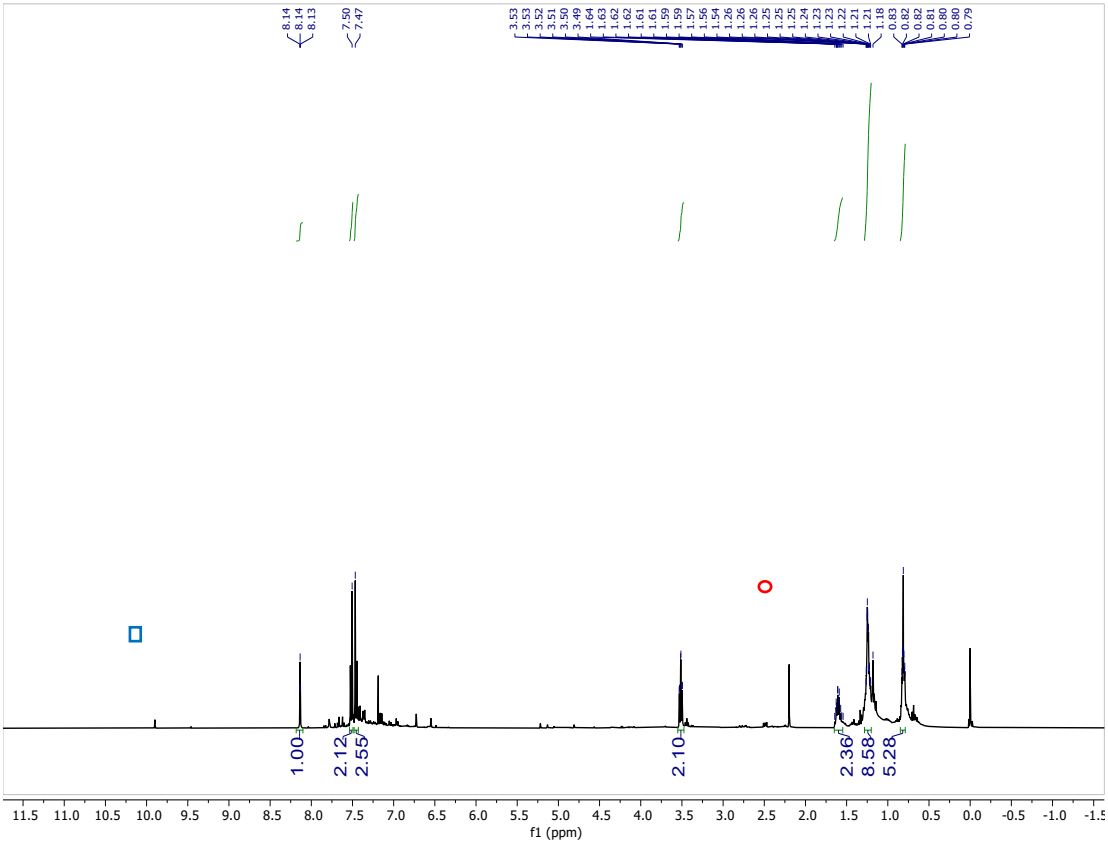

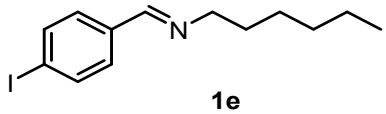

1e

***N*-hexyl-1-(4-iodophenyl)methanimine** (**1e**): ^{1}H NMR (400 MHz, $CDCl_3$) δ 8.11 (s, 1H), 7.71 – 7.63 (m, 2H), 7.41 – 7.33 (m, 2H), 3.51 (td, J = 7.1, 1.4 Hz, 2H), 1.61 (p, J = 7.0 Hz, 2H), 1.29 – 1.20 (m, 6H), 0.85 – 0.76 (m, 3H). ^{13}C NMR (101 MHz, $CDCl_3$) δ 159.6, 137.8, 135.8, 129.5, 96.9, 61.8, 31.6, 30.8, 27.0, 22.6, 14.1.

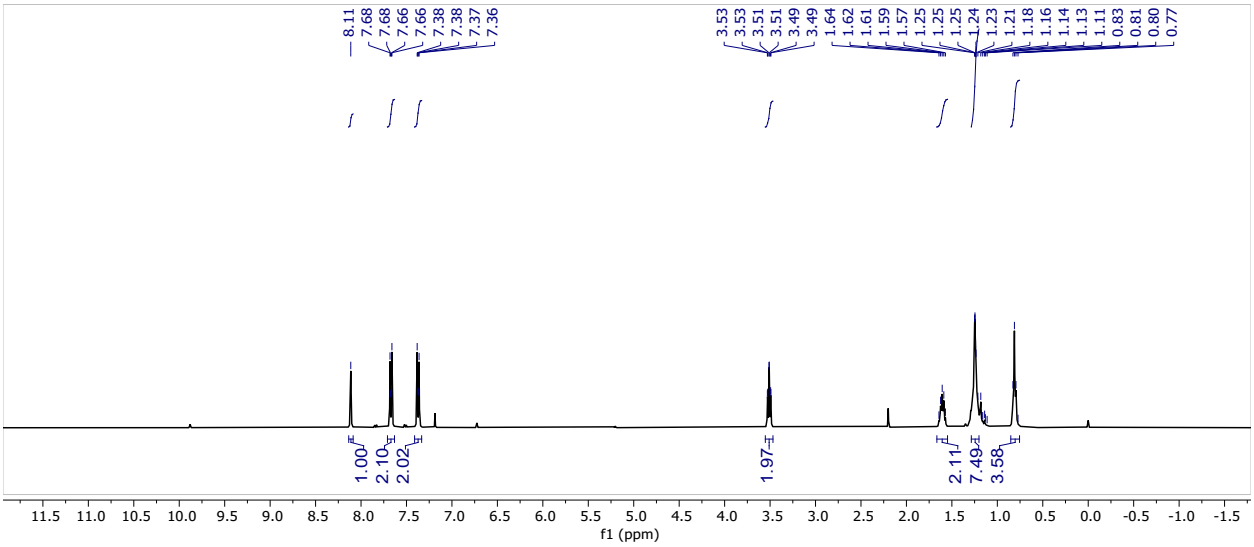

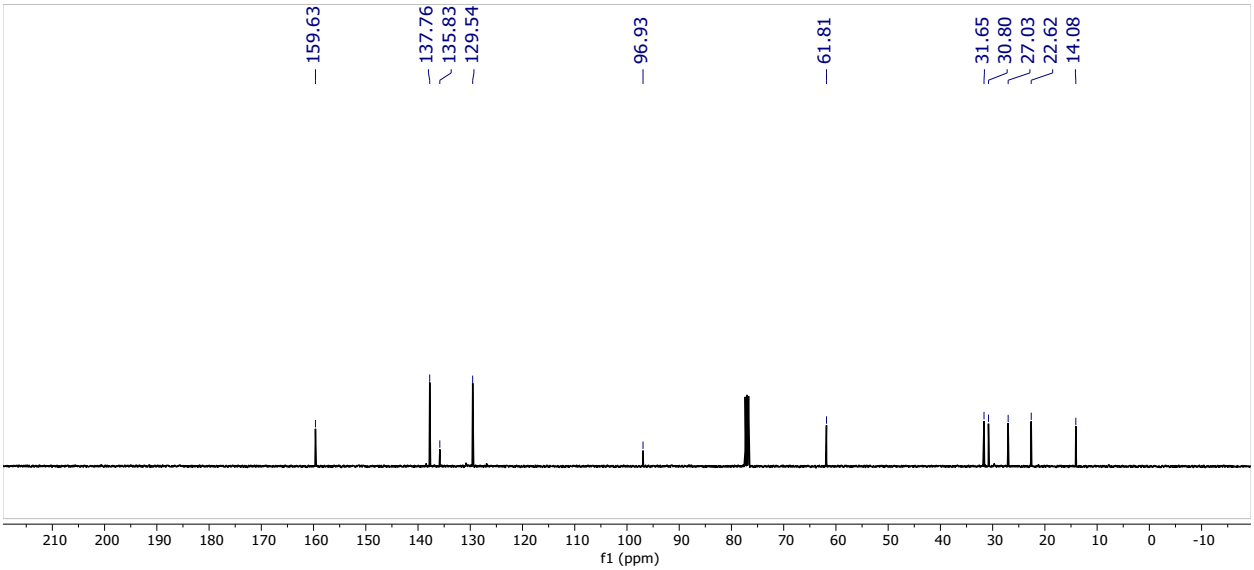

HR-MS: Exact mass ($[M+H]^+$): 316.05567. Found: 316.05494

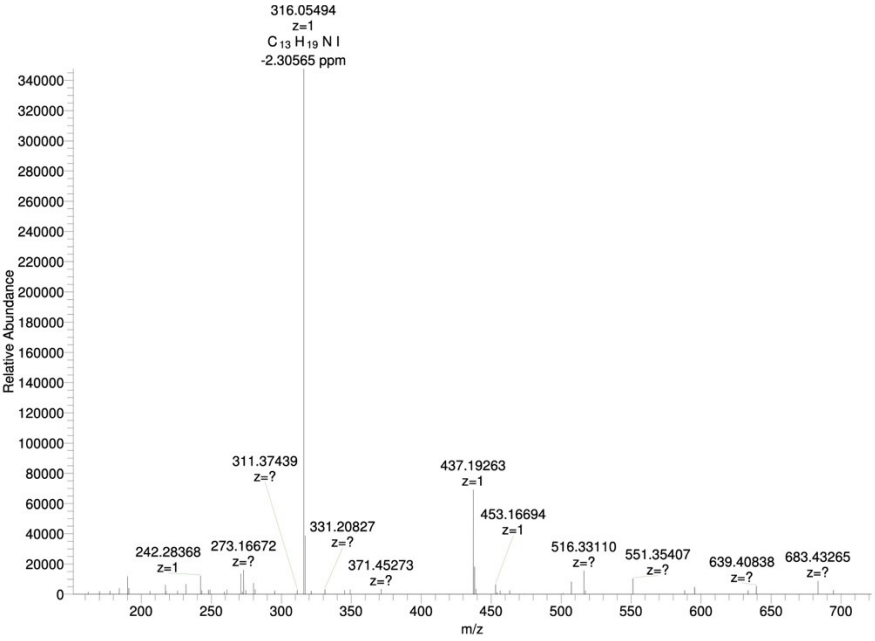

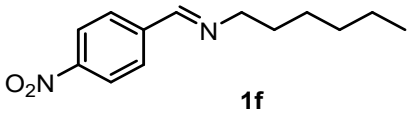

1f

***N*-hexyl-1-(4-nitrophenyl)methanimine** (**1f**): ^{1}H NMR (400 MHz, $CDCl_3$) δ 8.35 (d, J = 1.5 Hz, 1H), 8.29 – 8.23 (m, 2H), 7.88 (d, J = 8.8 Hz, 2H), 3.66 (td, J = 7.0, 1.4 Hz, 2H), 1.71 (p, J = 7.0 Hz, 3H), 1.38 – 1.27 (m, 6H), 0.91 – 0.86 (m, 4H). NMR data are in accordance with literature values.[16]

GC-MS trace

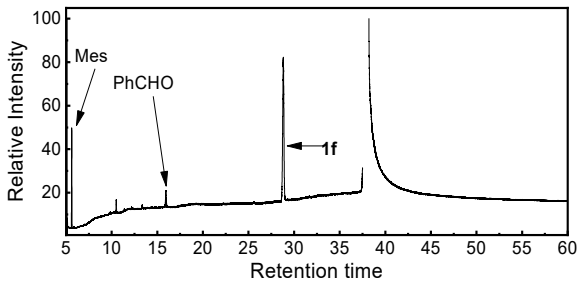

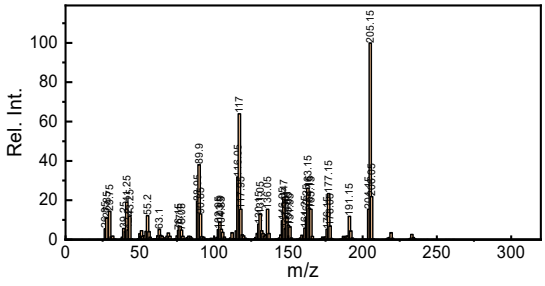

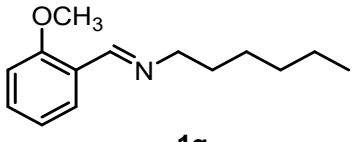

1g

***N*-hexyl-1-(2-methoxyphenyl)methanimine** (**1g**): ^{1}H NMR (400 MHz, $CDCl_3$) δ 8.69 (d, *J* = 1.5 Hz, 1H), 7.93 (dd, *J* = 7.7, 1.8 Hz, 1H), 7.36 (ddd, *J* = 8.2, 7.3, 1.8 Hz, 1H), 6.97 (t, *J* = 7.5 Hz, 1H), 6.91 (dd, *J* = 8.4, 1.0 Hz, 1H), 3.87 (s, 3H), 3.61 (td, *J* = 7.1, 1.4 Hz, 2H), 1.69 (dq, *J* = 14.4, 6.1 Hz, 2H), 1.34 – 1.24 (m, 6H), 0.91 – 0.87 (m, 3H). NMR data are in accordance with literature values.[15]

GC-MS trace

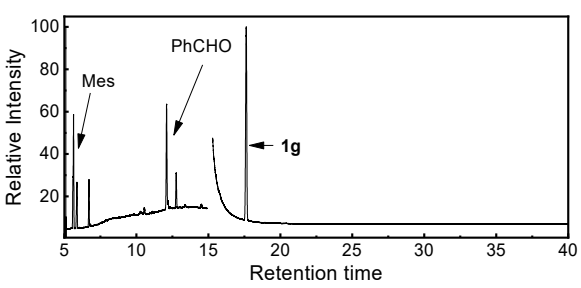

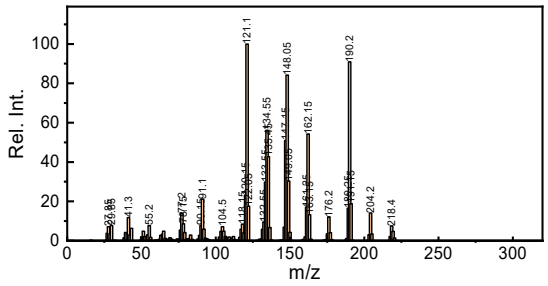

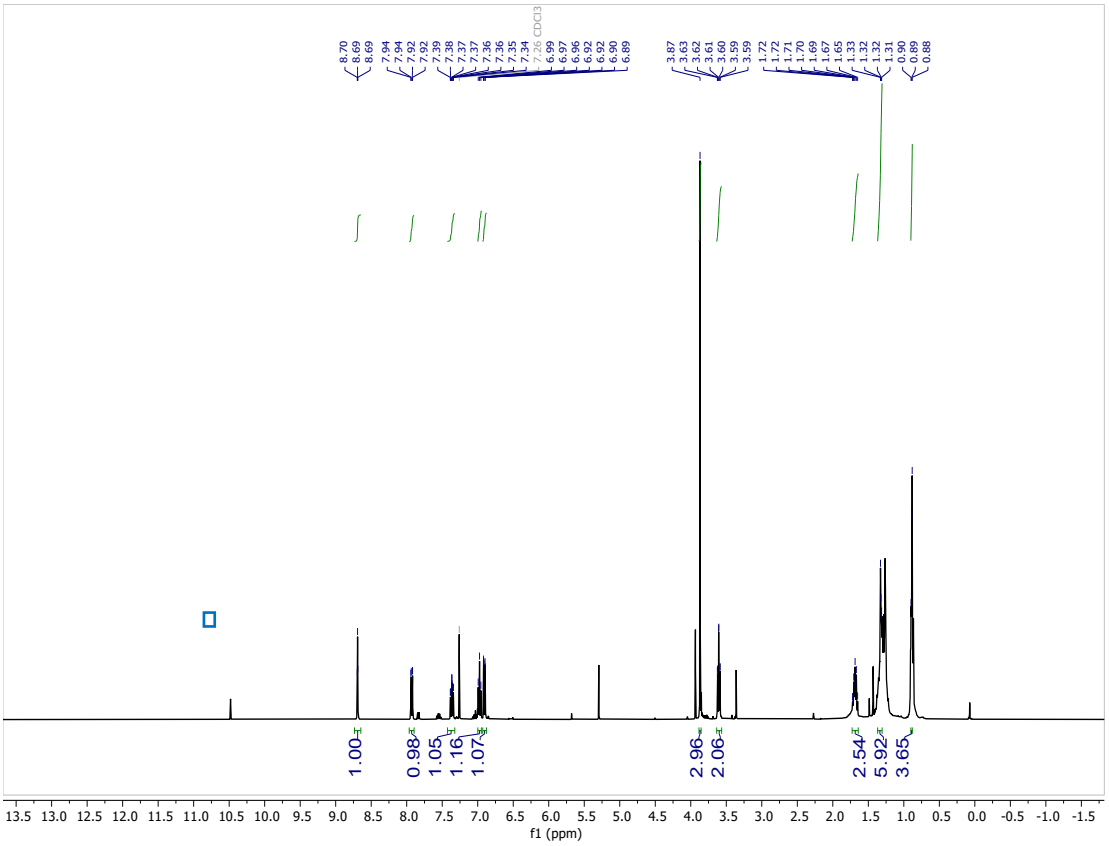

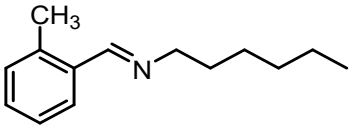

1h

***N*-hexyl-1-(2-methylphenyl)methanimine** (**1h**): ^{1}H NMR (400 MHz, $CDCl_3$) δ 8.50 (t, *J* = 1.0 Hz, 1H), 7.77 (dd, *J* = 7.6, 1.6 Hz, 1H), 7.20 (dd, *J* = 7.4, 1.7 Hz, 1H), 7.15 (td, *J* = 7.3, 1.5 Hz, 1H), 7.09 (ddt, *J* = 7.5, 1.5, 0.7 Hz, 1H), 3.54 (td, *J* = 7.0, 1.4 Hz, 2H), 2.42 (s, 3H), 1.68 – 1.57 (m, 2H), 1.38 – 1.11 (m, 6H), 0.84 – 0.80 (m, 3H). ^{13}C NMR (20.12 MHz, $CDCl_3$): δ 159.03 (1C, NH=*C*R), 137.15 (1C, quat. arom.), 134.36 (1C, quat. arom.), 130.60 (1C, arom.), 129.81 (1C, arom.), 127.40 (1C, arom.), 126.02 (1C, arom.), 62.19 (1C, NCH_2R), 31.63 (1C, CH_2), 30.95 (1C, CH_2), 26.98 (1C, CH_2), 22.58 (1C, CH_2), 19.16 (1C, Bn-CH_3), 13.99 (1C, CH_3).

GC-MS trace

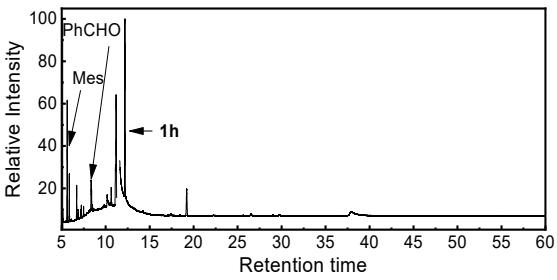
PhCHO
Mes
1h
Relative Intensity
Retention time

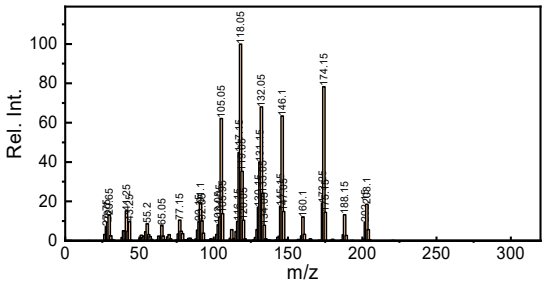
Rel. Int.
m/z
118.05
105.05
132.05
146.1
174.15
77.15
55.2
160.1
188.15

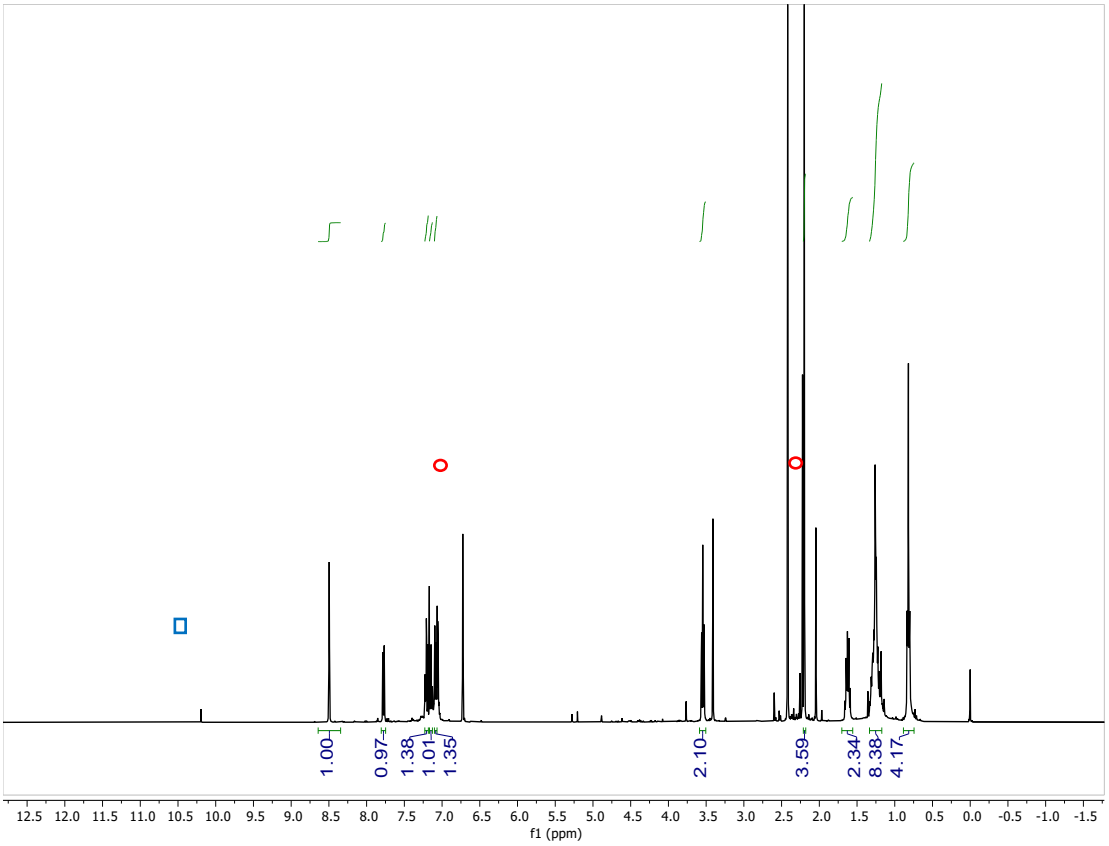
1.00
0.97
1.38
1.01
1.35
2.10
3.59
2.34
8.38
4.17
f1 (ppm)

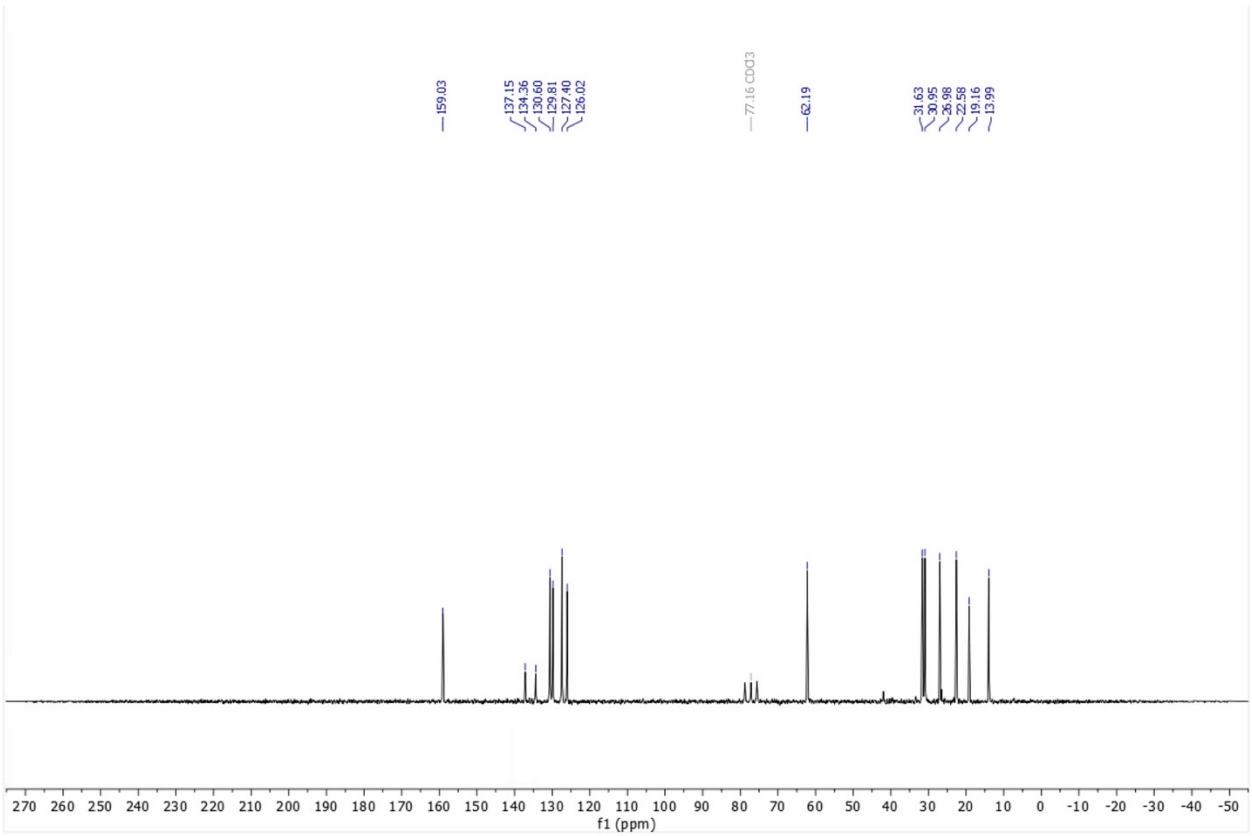

HR-MS: Exact mass ($[M+H]^+$): 204.17468. Found: 204.17413

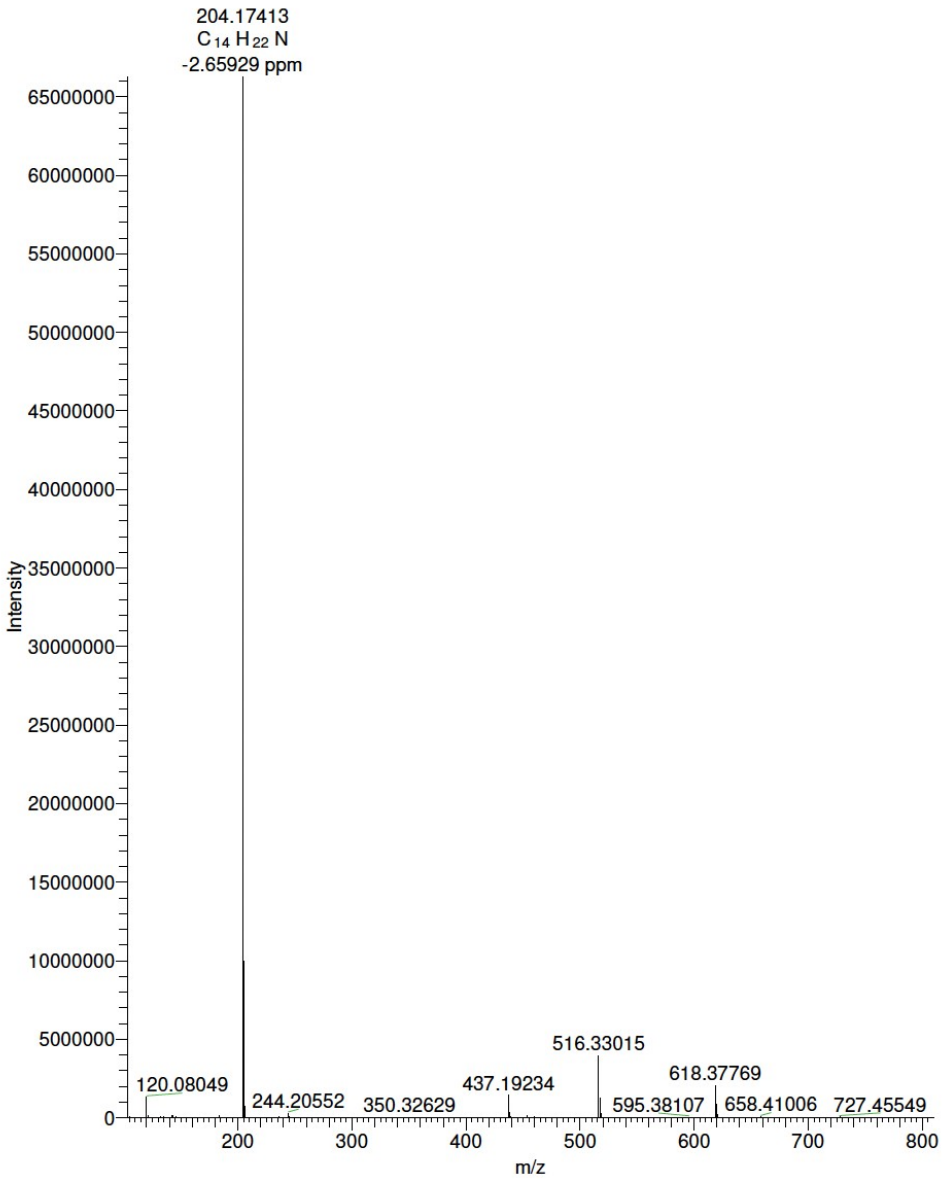
204.17413
C 14 H 22 N
-2.65929 ppm
Intensity
m/z
120.08049
244.20552
350.32629
437.19234
516.33015
595.38107
618.37769
658.41006
727.45549

ATR-IR

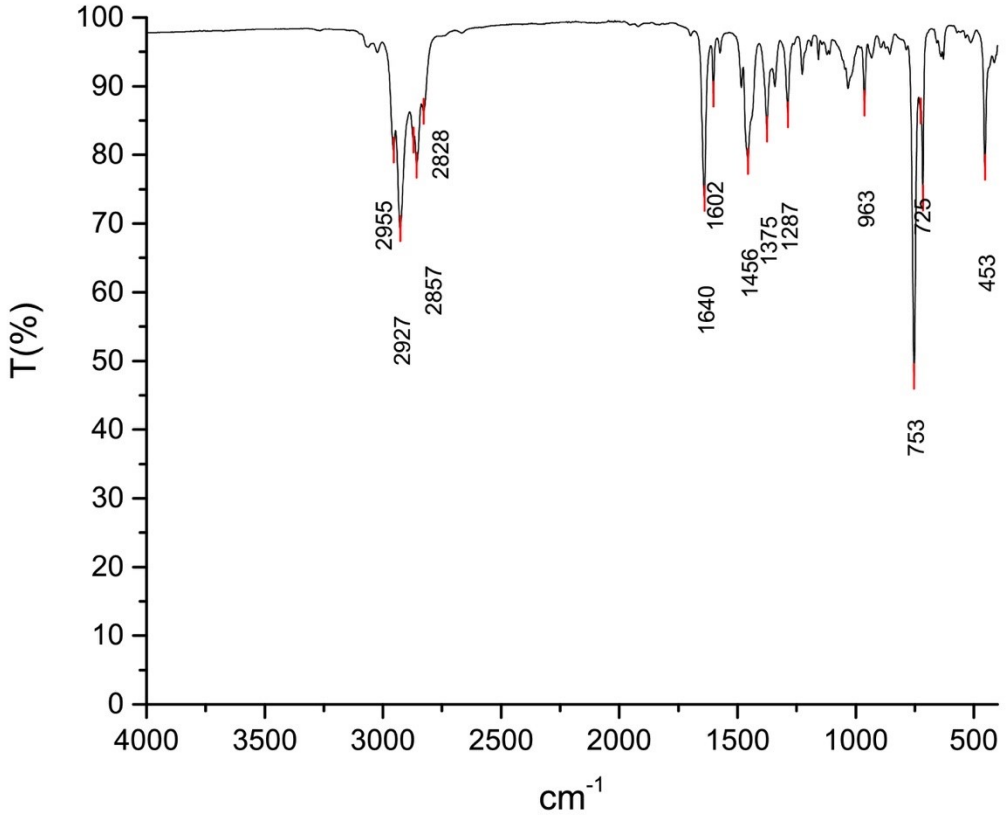

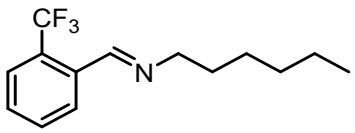

1i

***N*-hexyl-1-(2-trifluoromethylphenyl)methanimine** (**1i**): ^{1}H NMR (400 MHz, $CDCl_3$) δ 8.54 (q, *J* = 2.2 Hz, 1H), 8.10 (d, *J* = 7.8 Hz, 1H), 7.59 (d, *J* = 7.8 Hz, 1H), 7.50 (dd, *J* = 14.8, 7.2 Hz, 1H), 7.40 (t, *J* = 7.5 Hz, 1H), 3.58 (td, *J* = 7.0, 1.4 Hz, 2H), 1.69 – 1.57 (m, 2H), 1.35 – 1.14 (m, 7H), 0.81 (td, *J* = 5.5, 2.2 Hz, 3H). ^{19}F NMR (376 MHz, $CDCl_3$) δ -57.38. ^{13}C NMR (101 MHz, $CDCl_3$) δ 157.1, 132.0, 129.8, 128.3, 125.5, 125.5, 62.0, 31.6, 30.7, 26.9, 22.6, 14.0.

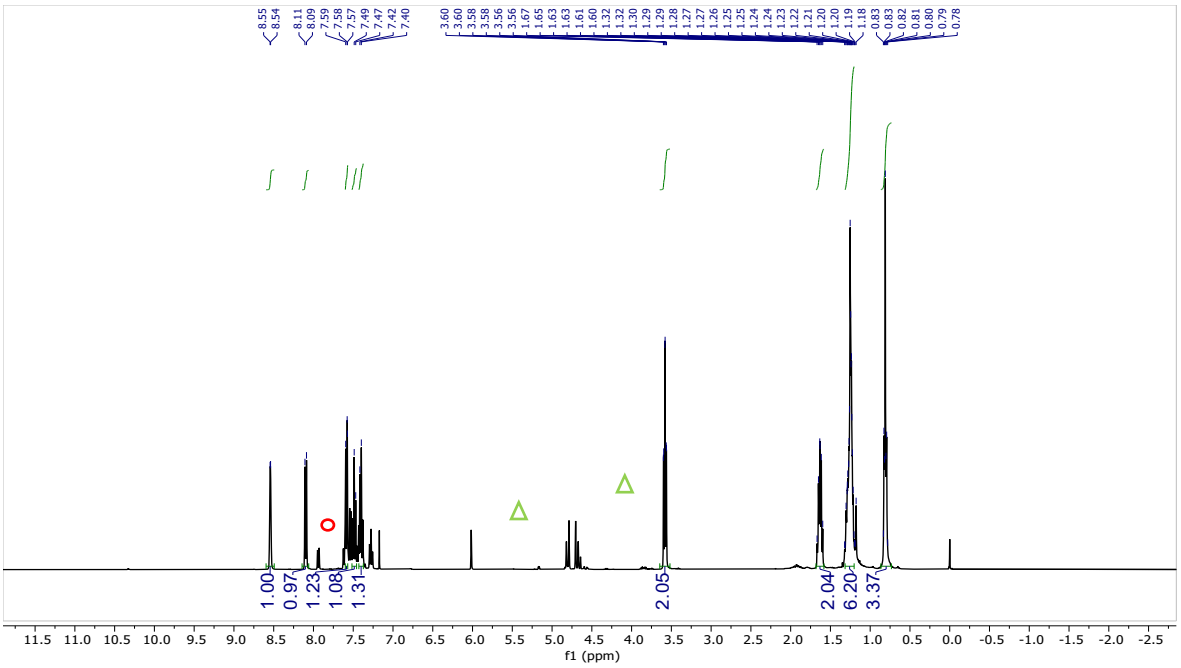
8.55
8.54
8.11
8.09
7.59
7.58
7.57
7.49
7.47
7.42
7.40
3.60
3.60
3.58
3.58
3.56
3.56
1.67
1.65
1.63
1.63
1.61
1.60
1.32
1.32
1.30
1.29
1.29
1.28
1.27
1.27
1.26
1.25
1.25
1.24
1.24
1.23
1.22
1.21
1.20
1.20
1.19
1.18
0.83
0.82
0.81
0.80
0.79
0.78
1.00
0.97
1.23
1.08
1.31
2.05
2.04
6.20
3.37
11.5 11.0 10.5 10.0 9.5 9.0 8.5 8.0 7.5 7.0 6.5 6.0 5.5 5.0 4.5 4.0 3.5 3.0 2.5 2.0 1.5 1.0 0.5 0.0 -0.5 -1.0 -1.5 -2.0 -2.5
f1 (ppm)

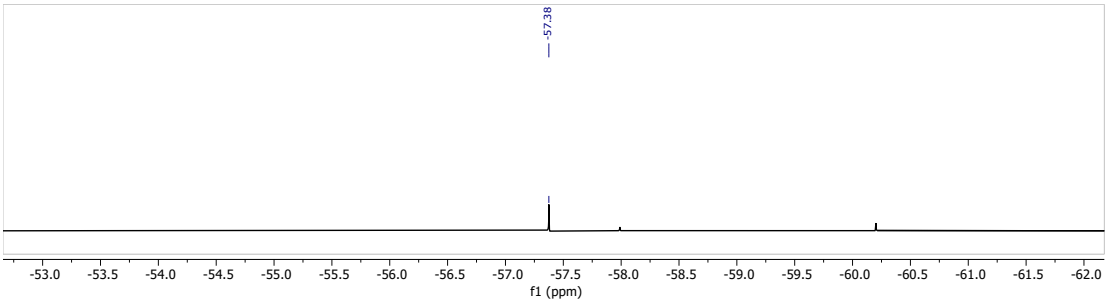
-57.38
-53.0 -53.5 -54.0 -54.5 -55.0 -55.5 -56.0 -56.5 -57.0 -57.5 -58.0 -58.5 -59.0 -59.5 -60.0 -60.5 -61.0 -61.5 -62.0
f1 (ppm)

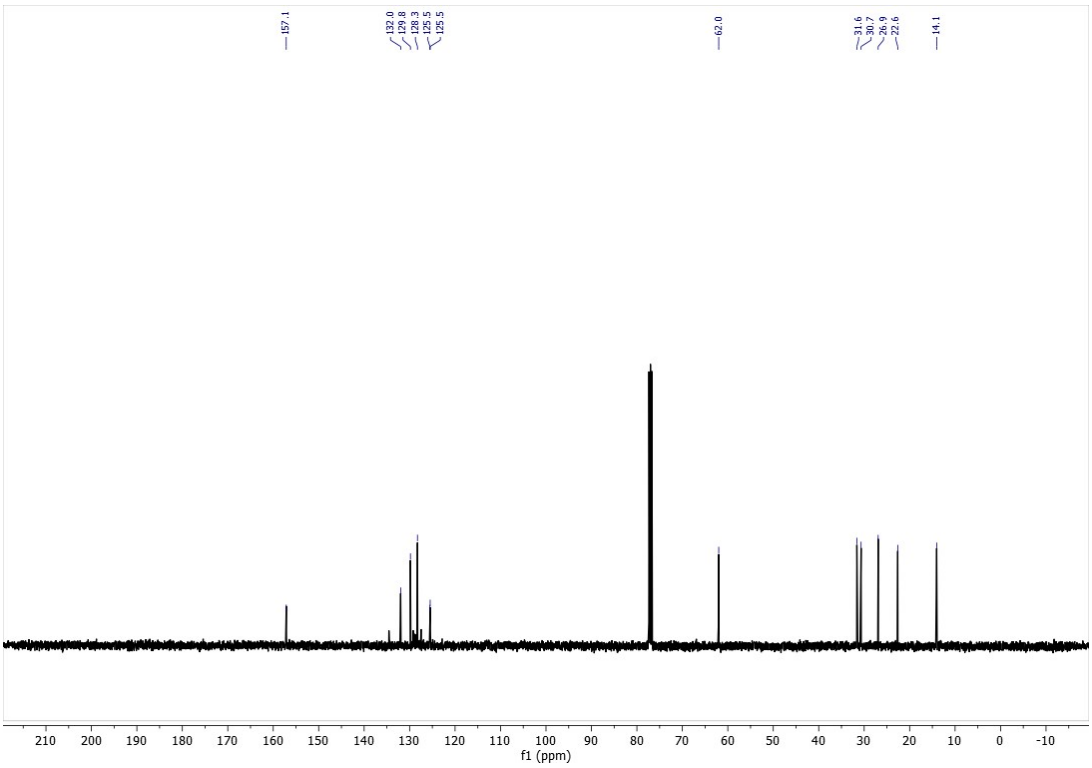
157.1
132.0
129.8
128.3
125.5
125.5
62.0
31.6
30.7
26.9
22.6
14.1
f1 (ppm)

GC-MS trace

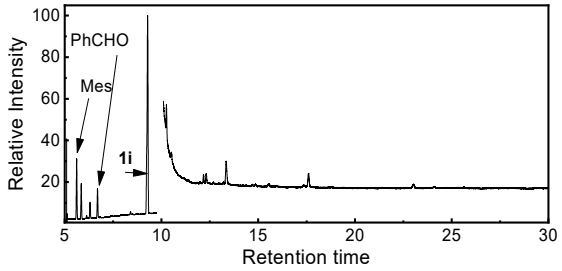
PhCHO
Mes
1i
Relative Intensity
Retention time

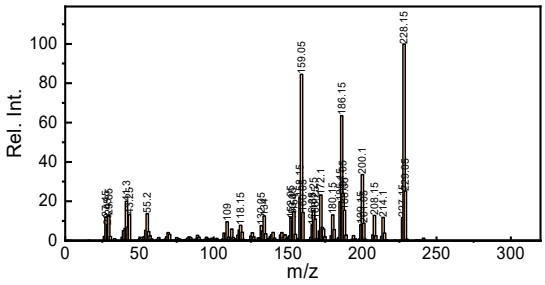
Rel. Int.
m/z
159.05
186.15
228.15
200.1

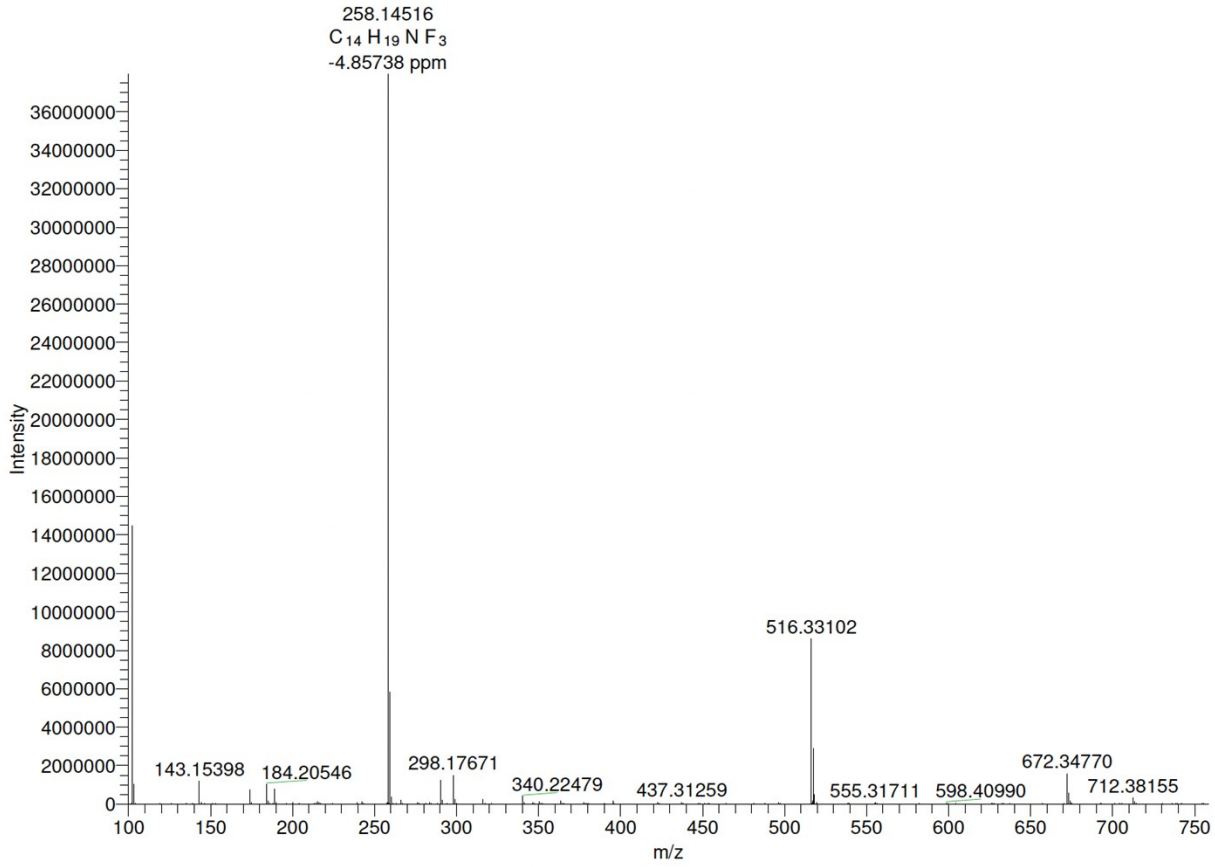

HR-MS: Exact mass ($[M+H]^+$): 258.14641. Found: 258.14516

ATR-IR

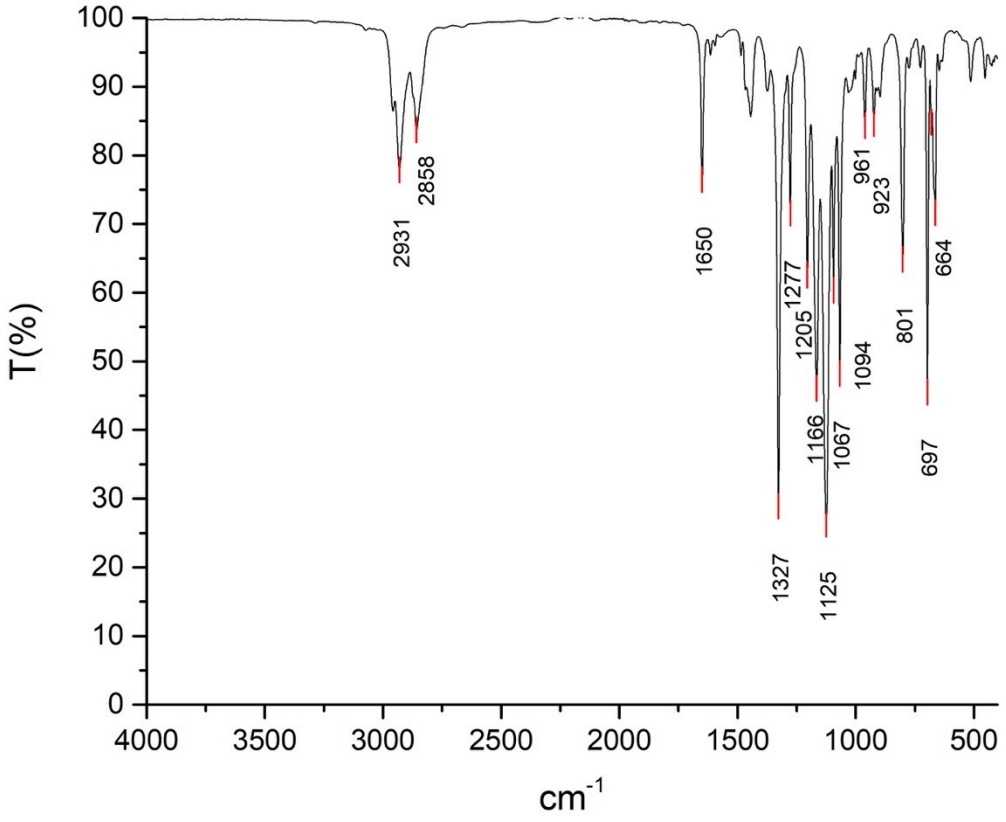

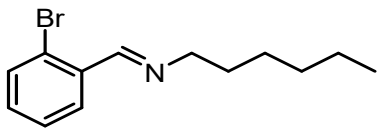

1j

***N*-hexyl-1-(2-bromophenyl)methanimine** (**1j**): ^{1}H NMR (400 MHz, $CDCl_3$) δ 8.62 (q, *J* = 1.2 Hz, 1H), 7.99 (dd, *J* = 7.8, 1.8 Hz, 1H), 7.56 (dd, *J* = 8.0, 1.3 Hz, 1H), 7.33 (tdd, *J* = 7.7, 1.3, 0.7 Hz, 1H), 7.24 (ddd, *J* = 7.9, 7.3, 1.9 Hz, 1H), 3.65 (td, *J* = 7.1, 1.4 Hz, 2H), 1.77 – 1.65 (m, 2H), 1.38 – 1.30 (m, 6H), 0.95 – 0.83 (m, 3H). ^{13}C NMR (101 MHz, $CDCl_3$) δ 159.8, 134.8, 133.0, 131.6, 128.8, 127.6, 124.8, 61.9, 31.6, 30.8, 27. 0, 22.6, 14.1.

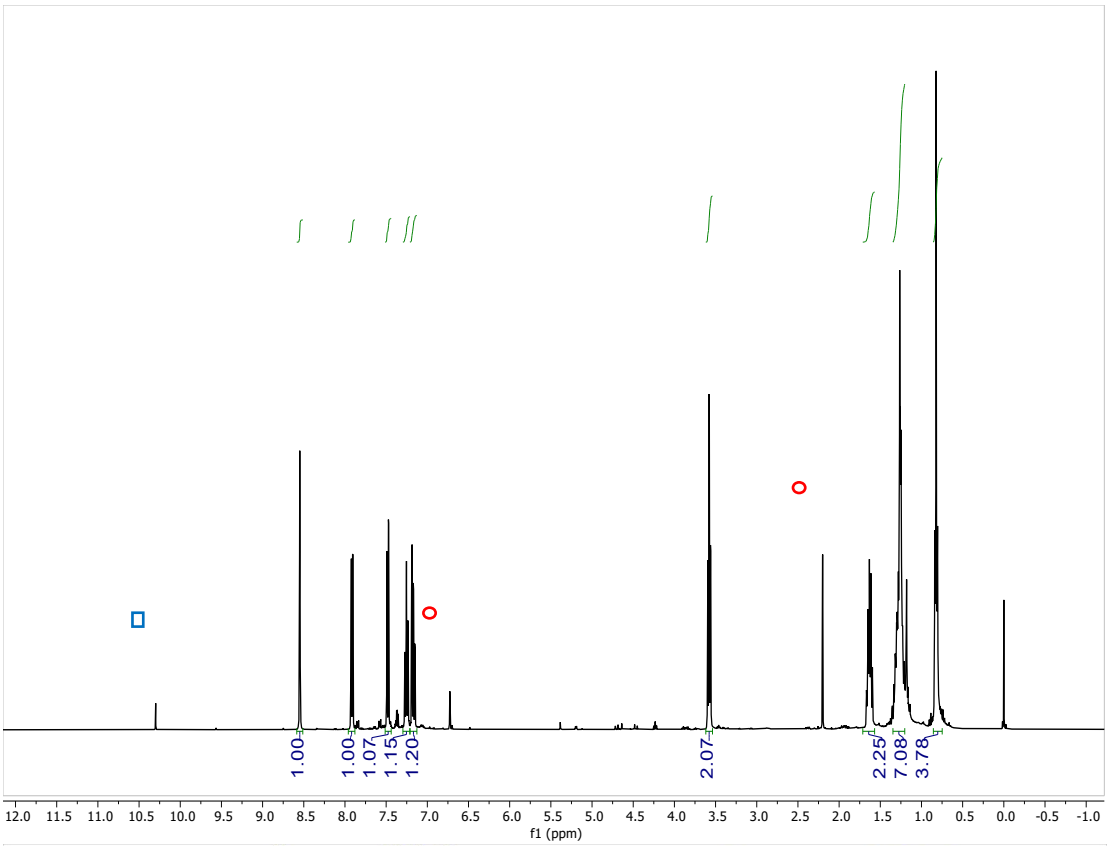
1.00
1.00
1.07
1.15
1.20
2.07
2.25
7.08
3.78
12.0 11.5 11.0 10.5 10.0 9.5 9.0 8.5 8.0 7.5 7.0 6.5 6.0 5.5 5.0 4.5 4.0 3.5 3.0 2.5 2.0 1.5 1.0 0.5 0.0 -0.5 -1.0
f1 (ppm)

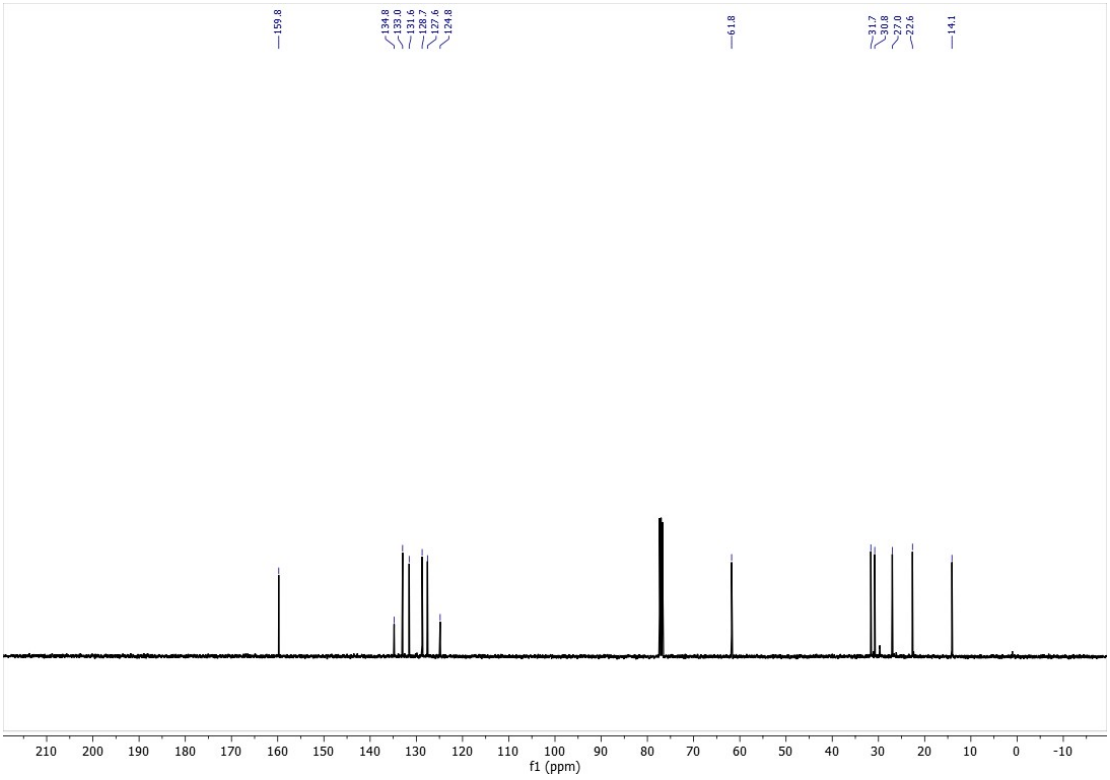
159.8
134.8
133.0
131.6
128.7
127.6
124.8
61.8
31.7
30.8
27.0
22.6
14.1
210 200 190 180 170 160 150 140 130 120 110 100 90 80 70 60 50 40 30 20 10 0 -10
f1 (ppm)

HR-MS: Exact mass ([M+H]$^+$): 268,06954. Found: 268.06848

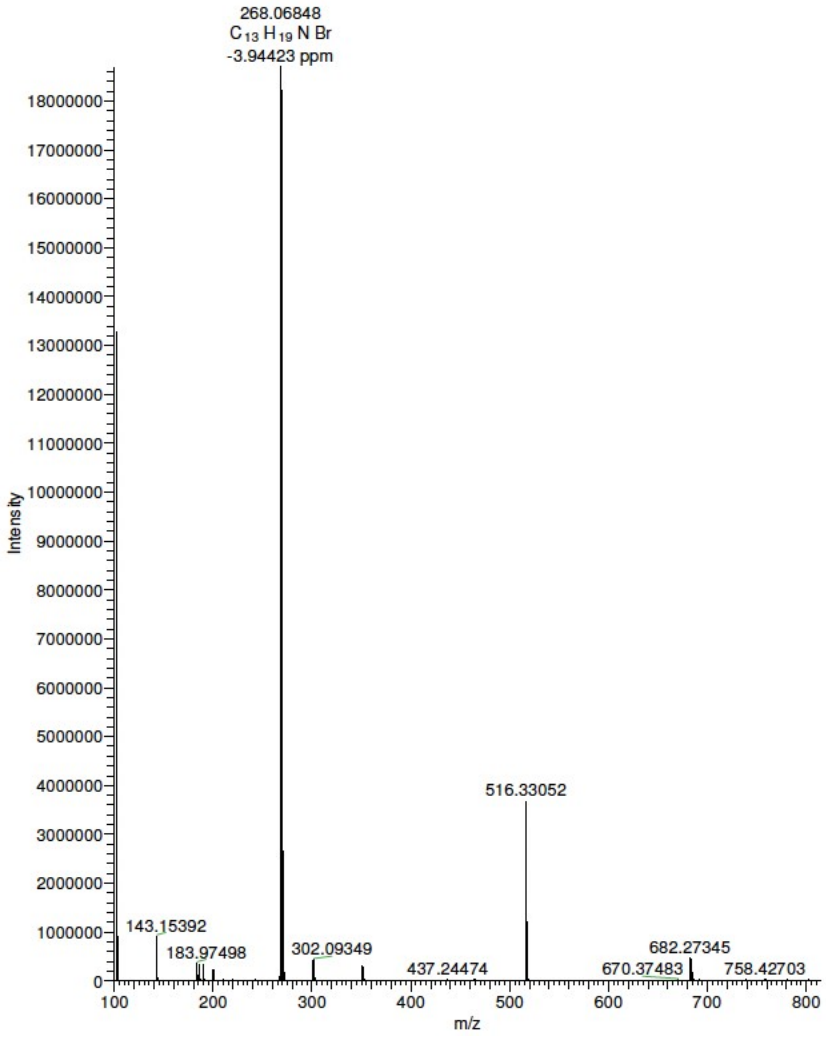

ATR-IR

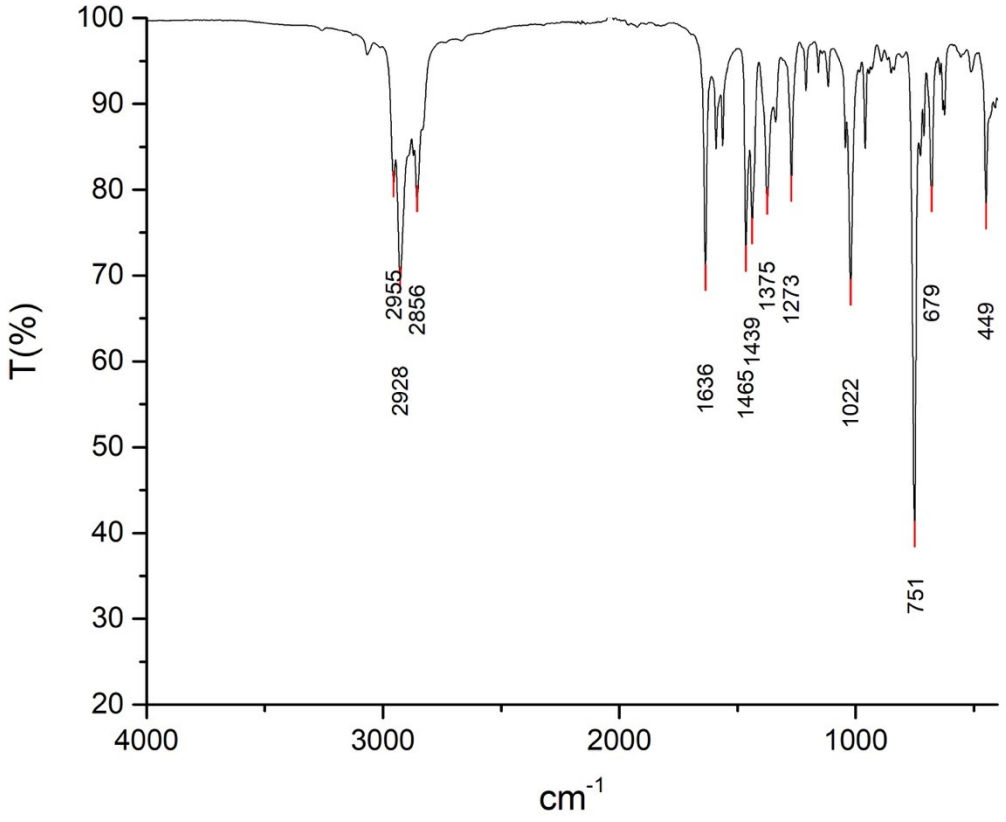

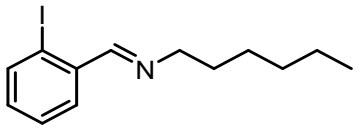

1k

***N*-hexyl-1-(2-iodophenyl)methanimine** (**1k**): ^{1}H NMR (400 MHz, $CDCl_3$) δ 8.42 (d, J = 1.5 Hz, 1H), 7.93 (dd, J = 7.8, 1.8 Hz, 1H), 7.46 (dd, J = 7.6, 1.7 Hz, 1H), 7.09 (td, J = 7.6, 1.8 Hz, 1H), 7.00 (td, J = 7.6, 1.8 Hz, 1H), 3.66 (td, J = 7.0, 1.4 Hz, 2H), 1.71 (p, J = 7.0 Hz, 2H), 1.35 – 1.28 (m, 6H), 0.94 – 0.84 (m, 3H). NMR data are in accordance with literature values.[17]

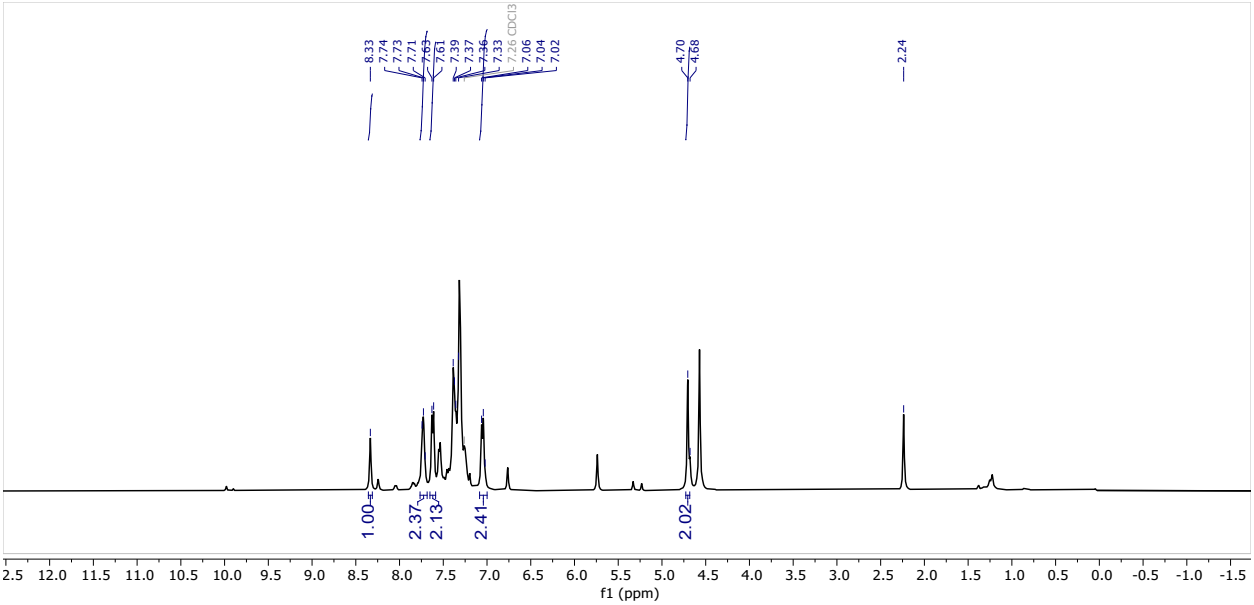

GC-MS trace

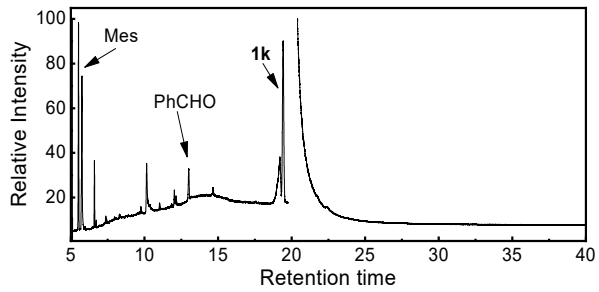

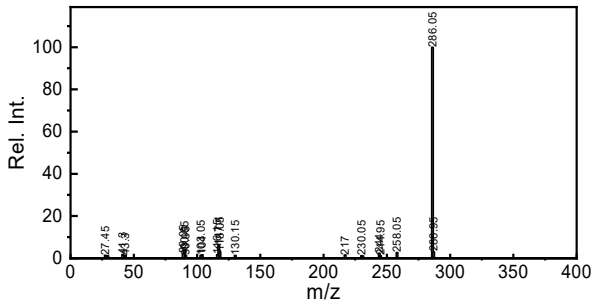

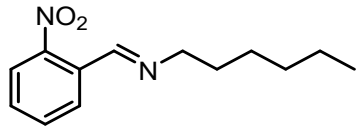

1l

***N*-hexyl-1-(2-nitrophenyl)methanimine** (**1l**): ^{1}H NMR (400 MHz, $CDCl_3$) δ 8.58 (s, 1H), 7.95 – 7.88 (m, 1H), 7.88 (dd, *J* = 7.8, 1.6 Hz, 1H), 7.73 – 7.67 (m, 1H), 7.51 – 7.42 (m, 1H), 3.58 (td, *J* = 7.0, 1.4 Hz, 2H), 1.63 (p, *J* = 7.2 Hz, 2H), 1.25 (ttd, *J* = 13.5, 8.6, 5.6 Hz, 5H), 0.86 – 0.75 (m, 12H). ^{13}C NMR (20.12 MHz, $CDCl_3$): δ 156.39 (1C, *C*H=NR), 148.83 (1C, quat. arom., *C*NO_2), 133.27 (1C, arom.), 131.32 (1C, quat. arom.), 130.38 (1C, arom.), 129.61 (1C, arom.), 124.12 (1C, arom.), 61.70 (1C, N*C*H_2R), 31.57 (1C, R*C*H_2R), 30.59 (1C, R*C*H_2R), 26.91 (1C, R*C*H_2R), 22.56 (1C, R*C*H_2R), 13.99 (1C, R*C*H_3).

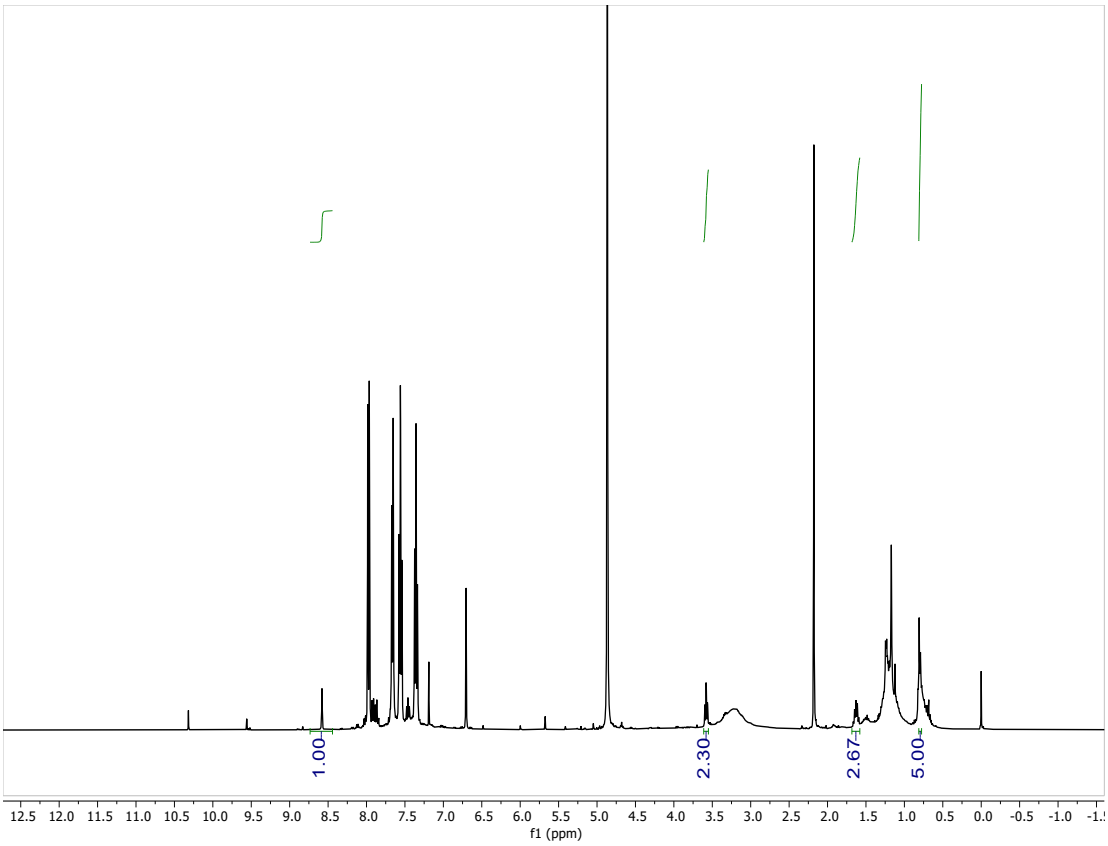
1.00
2.30
2.67
5.00
12.5 12.0 11.5 11.0 10.5 10.0 9.5 9.0 8.5 8.0 7.5 7.0 6.5 6.0 5.5 5.0 4.5 4.0 3.5 3.0 2.5 2.0 1.5 1.0 0.5 0.0 -0.5 -1.0
f1 (ppm)

1D

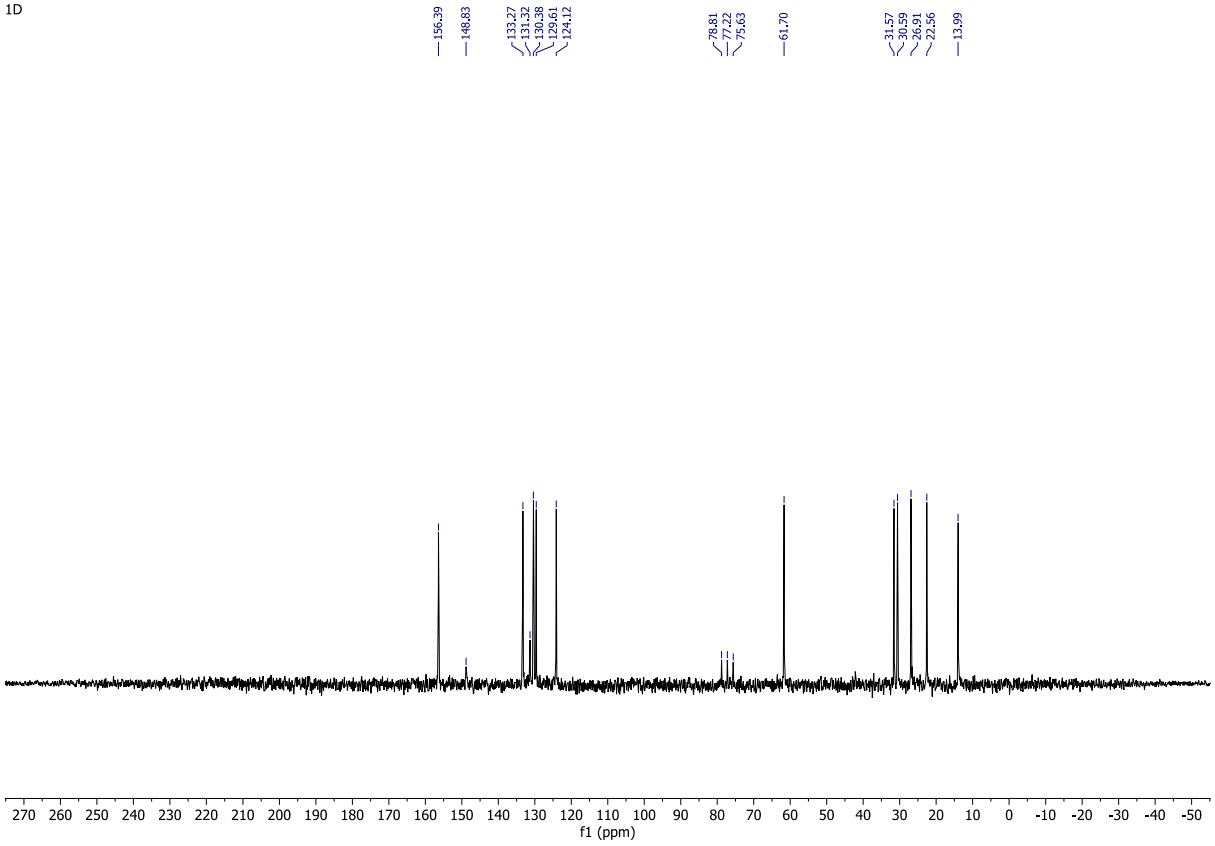

GC-MS trace

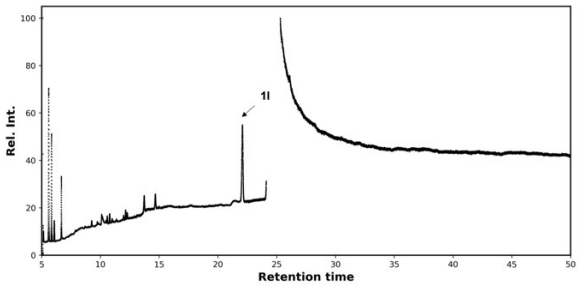

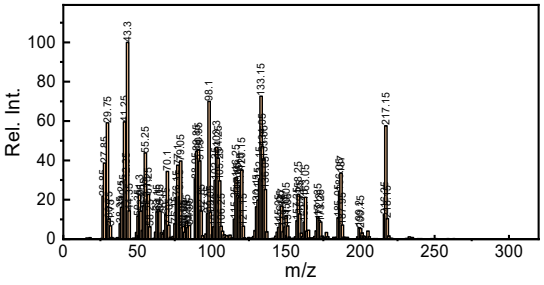

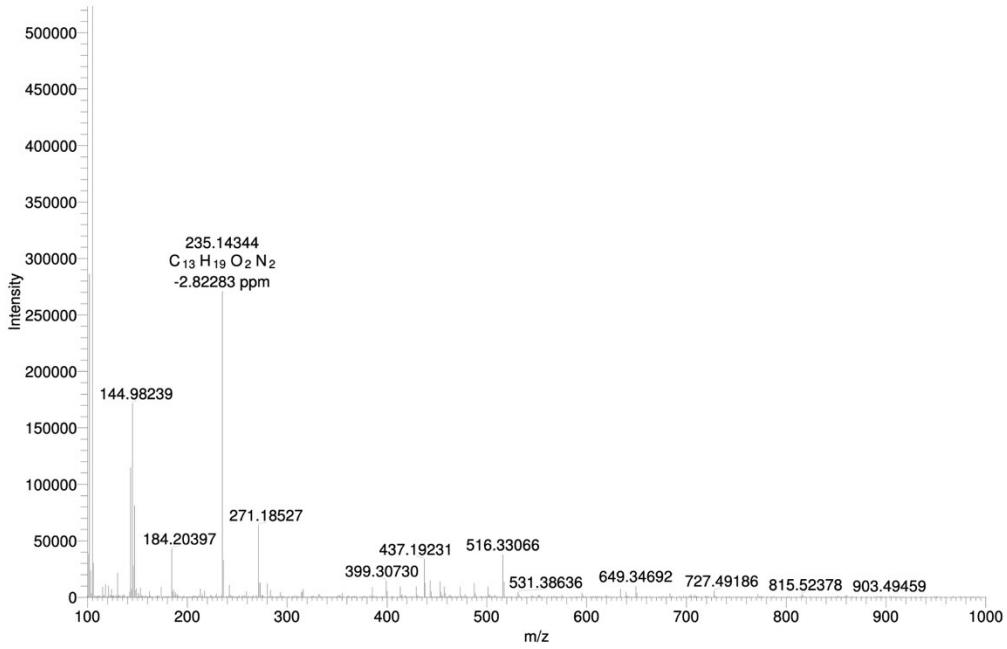

HR-MS: Exact mass ($[M+H]^+$): 235,14410. Found: 235.14344

ATR-IR

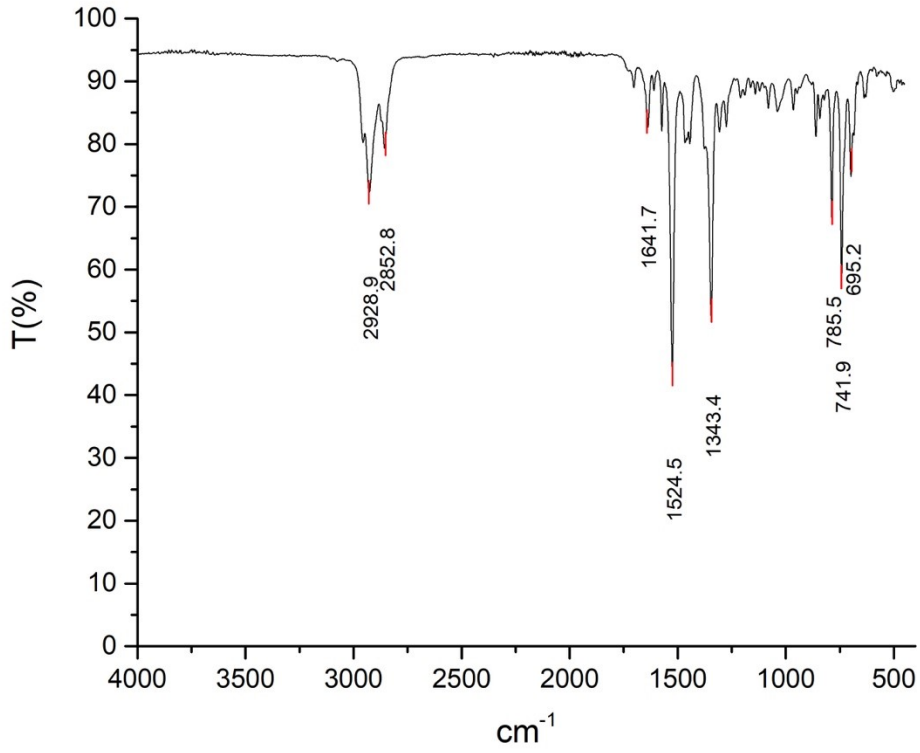

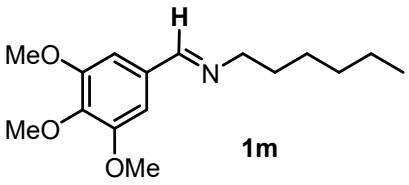

1m

***N*-hexyl-1-(3,4,5-trimethoxyphenyl)methanimine** (**1m**): ^{1}H NMR (400 MHz, $CDCl_3$) δ 8.16 (d, J = 1.4 Hz, 1H, HC=N), 6.99 (s, 2H, CH), 3.93 (s, 3H, C-OCH_3), 3.91 (s, 6H, C-OCH_3), 3.60 (td, J = 7.1, 1.3 Hz, 2H, CH_2), 1.69 (p, J = 7.2 Hz, 2H, CH_2), 1.41 – 1.19 (m, 6H, CH_2), 0.89 (td, J = 5.7, 2.4 Hz, 3H, CH_3). ^{13}C NMR (101 MHz, $CDCl_3$) δ 160.3, 153.4, 140.1, 131.9, 105.0, 61.7, 60.9, 56.2, 31.7, 30.9, 27.0, 22.6, 14.1.

GC-MS trace

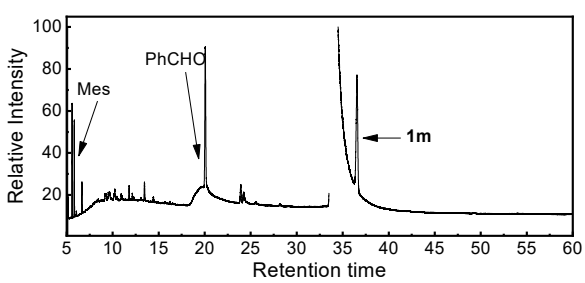

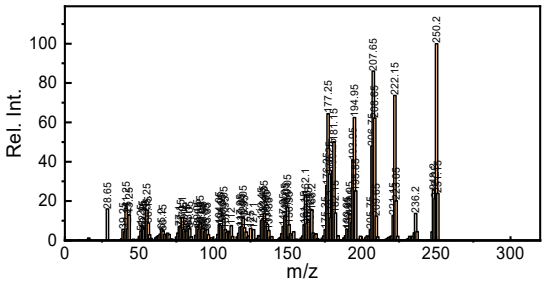

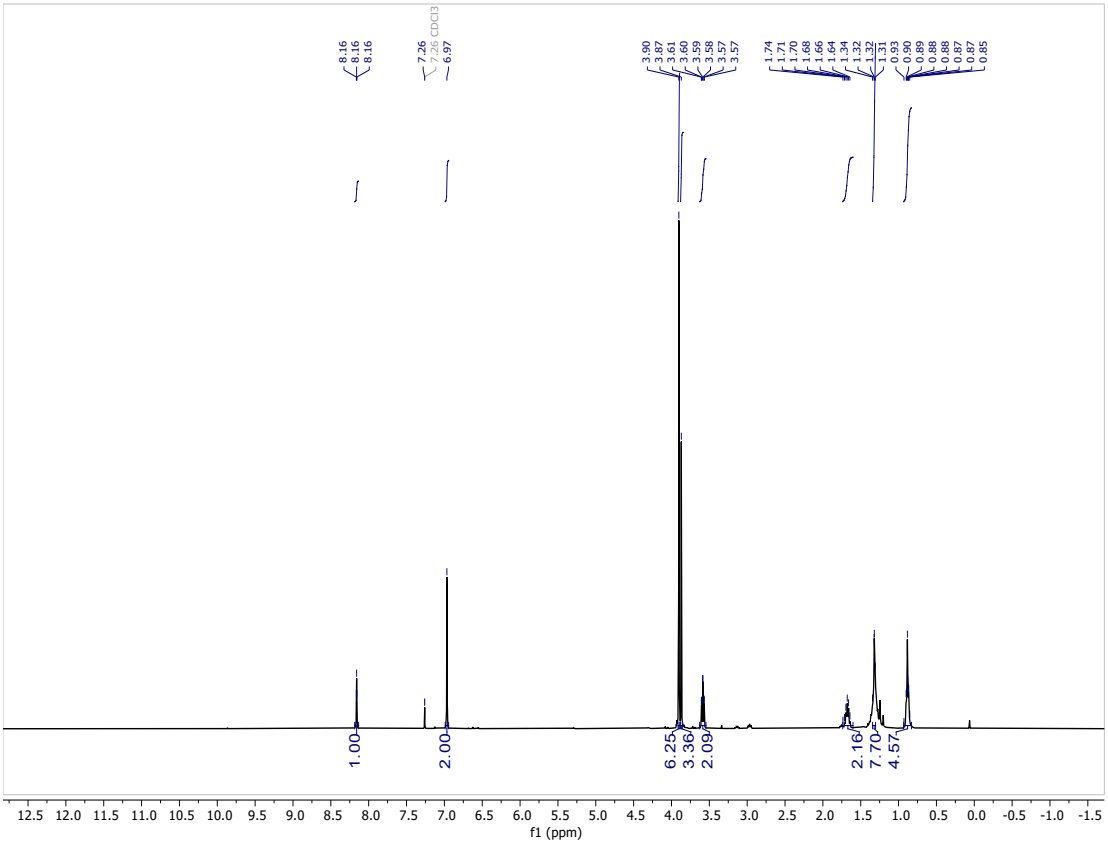

HR-MS: Exact mass ([M+H]$^{+}$): 280,19072. Found: 280.19002

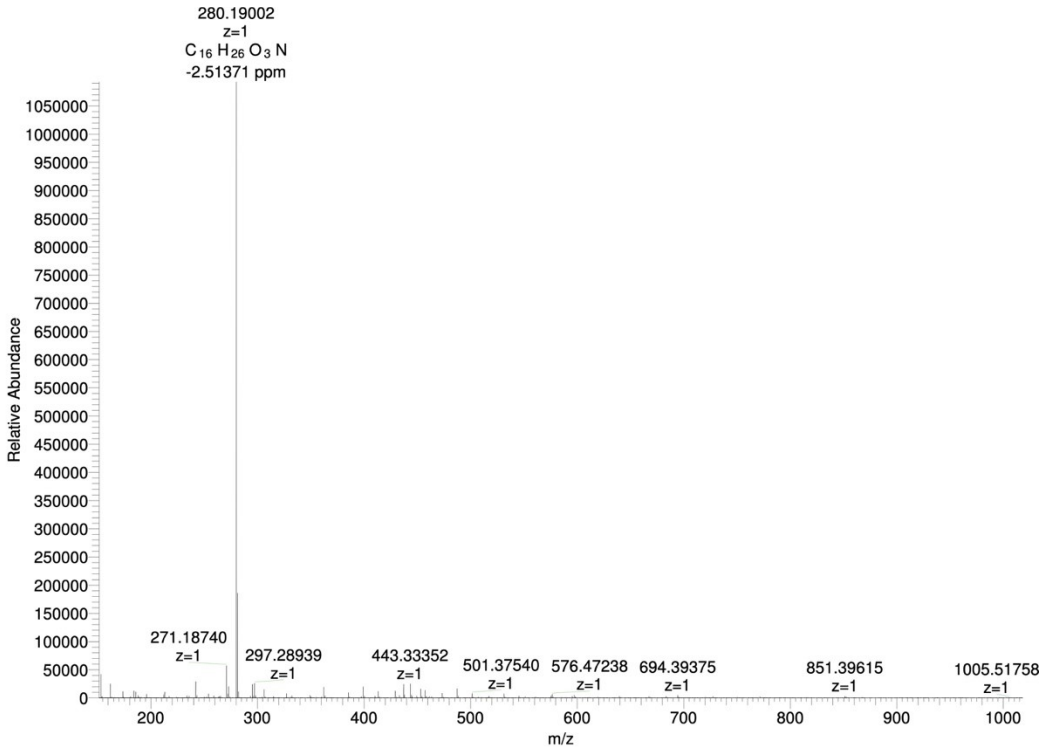
280.19002
z=1
C 16 H 26 O 3 N
-2.51371 ppm
Relative Abundance
m/z
271.18740
z=1
297.28939
z=1
443.33352
z=1
501.37540
z=1
576.47238
z=1
694.39375
z=1
851.39615
z=1
1005.51758
z=1

ATR-IR

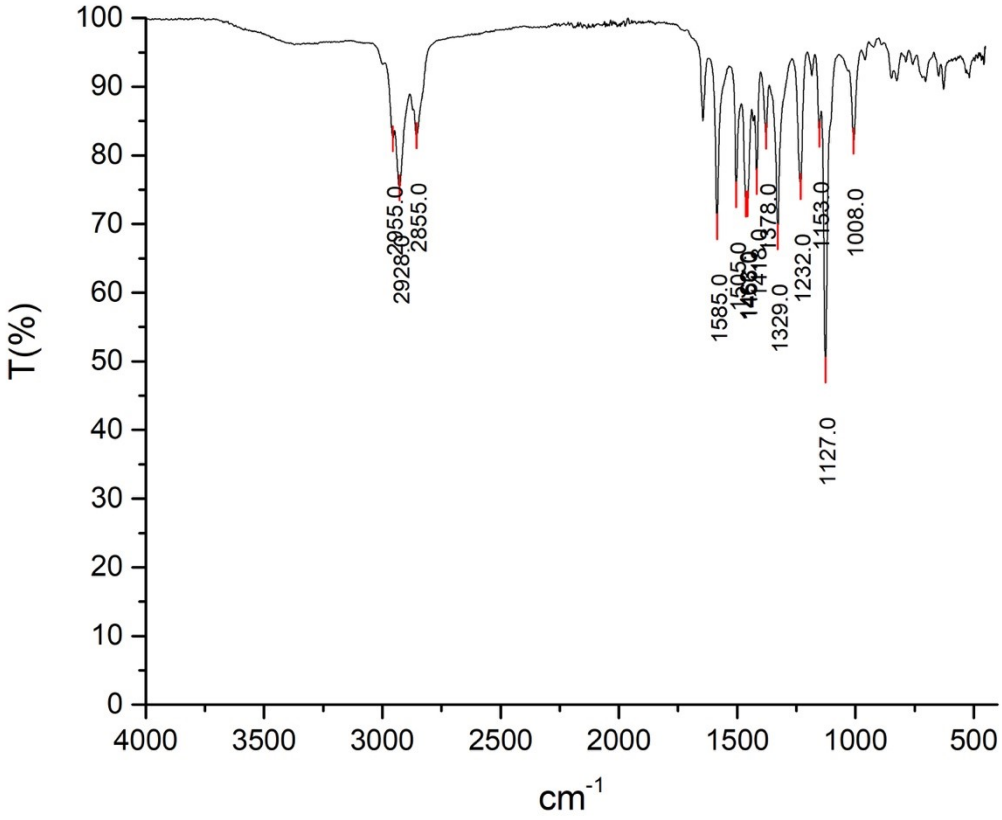

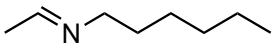

1n

***N*-hexylethan-1-imine** (**1n**): m/z: 127 ([M]$^{\bullet+}$, 8.9%); 112 ([M-CH_3]$^{\bullet+}$, 100%); 98 ([M-C_2H_5]$^{\bullet+}$, 15%); 84 ([M-C_3H_7]$^{\bullet+}$, 22%); 70 ([M-C_4H_9]$^{\bullet+}$, 29%); 56 ([M-C_5H_{11}]$^{\bullet+}$, 37%); 42 ([CH_3CHN]$^{\bullet+}$, 35%).). ^{1}H NMR (80 MHz, $CDCl_3$): δ 7.74 (broad d, 1H, C*H*=NR), 3.36 (d, J = 8.1 Hz, 3H, C*H*$_3$CHNR), 1.97 (broad t, 2H, R=NC*H*$_2$R), 1.34-0.86 (broad m, 11H, $RCH_2CH_2CH_2CH_2CH_3$). In agreement with literature values.[18]

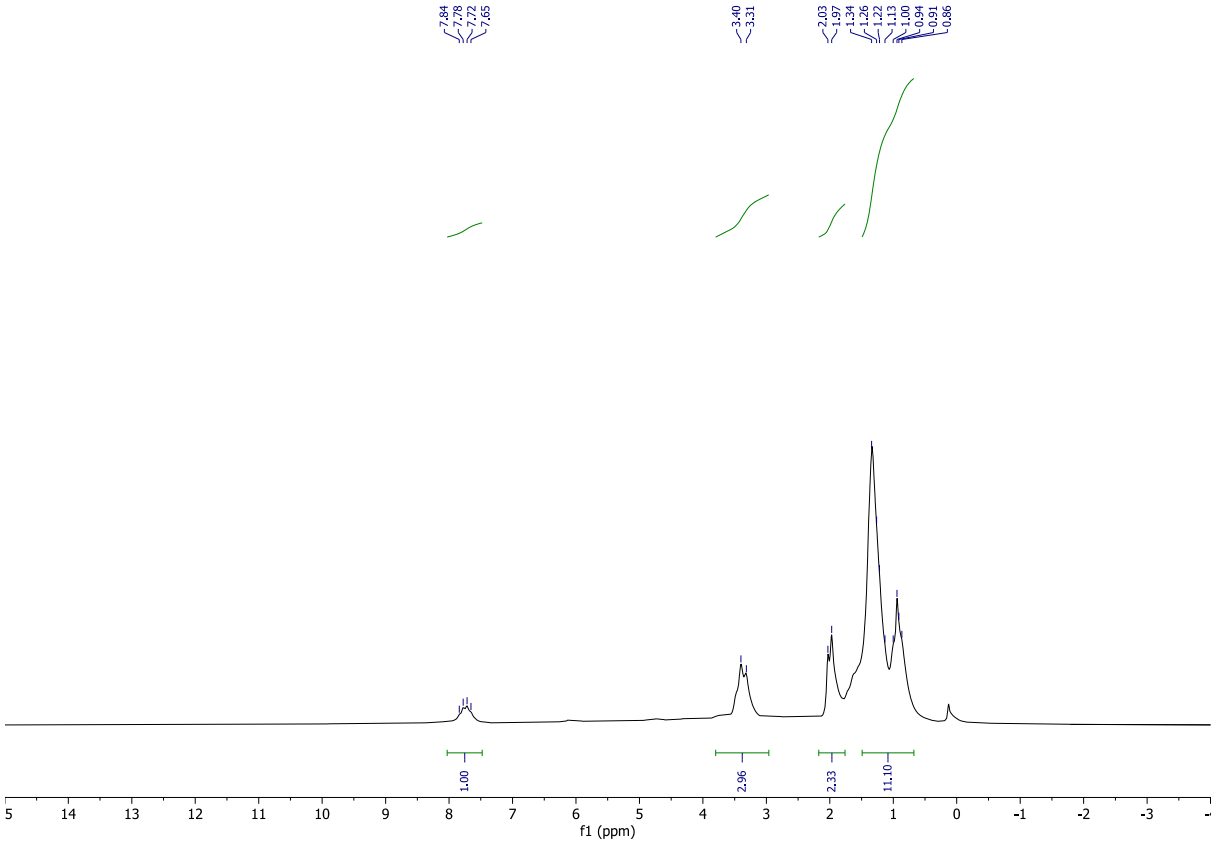

GC-MS trace

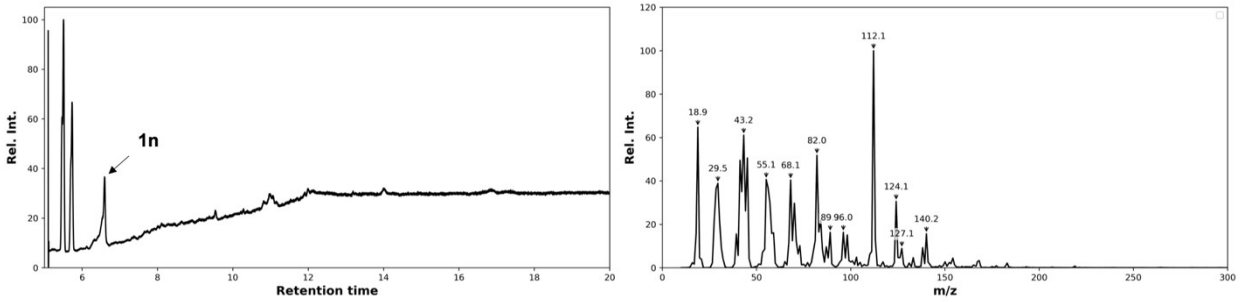

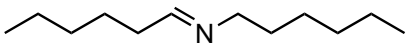

1o

***N*-hexylhexan-1-imine** (**1o**): m/z: 183 ($[M]^{\bullet+}$, 0.5%); 182 ($[M-H]^{\bullet+}$, 1%); 168 ($[M-CH_3]^{\bullet+}$, 2%); 154 ($[M-C_2H_5]^{\bullet+}$, 4%); 154 ($[M-C_3H_7]^{\bullet+}$, 16%); 112 ($[M-C_5H_{11}]^{\bullet+}$, 100%); 98 ($[C_5H_{11}CHN]^{\bullet+}$, 15%). ^{1}H NMR (80 MHz, $CDCl_3$): δ 7.64 (broad t, J = 4.9 Hz, 1H, *CH*=NR), 3.34 (t, J = 6.5 Hz, 2H), 2.81-2.49 (broad m, 4H), 2.34-2.11 (broad m, 2H), 1.67-0.84 (broad m, 16H). In agreement with literature values.[13,19]

GC-MS trace

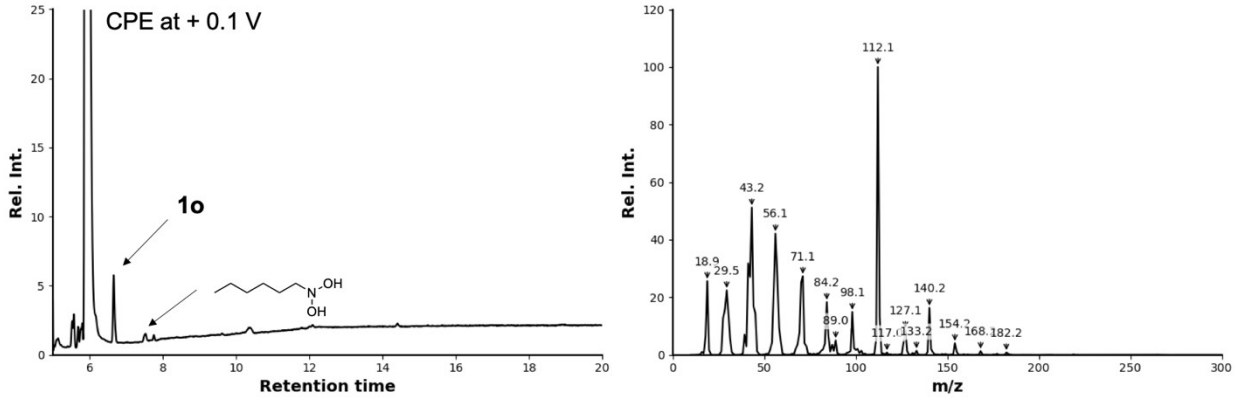

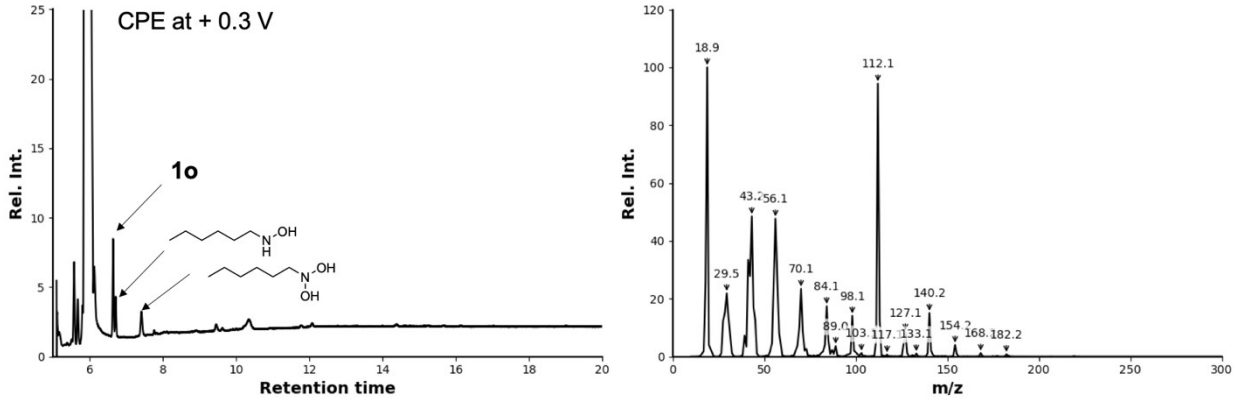

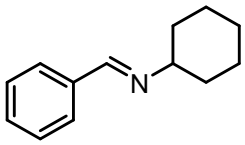

2

***N*-cyclohexyl-1-phenylmethanimine** (**2**) ^{1}H NMR (400 MHz, $CDCl_3$) δ 8.23 (s, 1H), 7.70 – 7.60 (m, 2H), 7.33 – 7.26 (m, 3H), 3.11 (tt, *J* = 10.6, 4.1 Hz, 1H), 1.81 – 1.42 (m, 5H), 1.37 – 1.06 (m, 3H). NMR data are in accordance with literature values.[14]

GC-MS trace

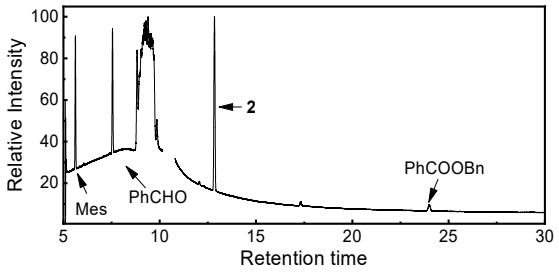

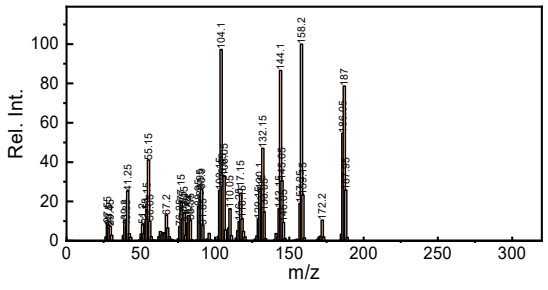

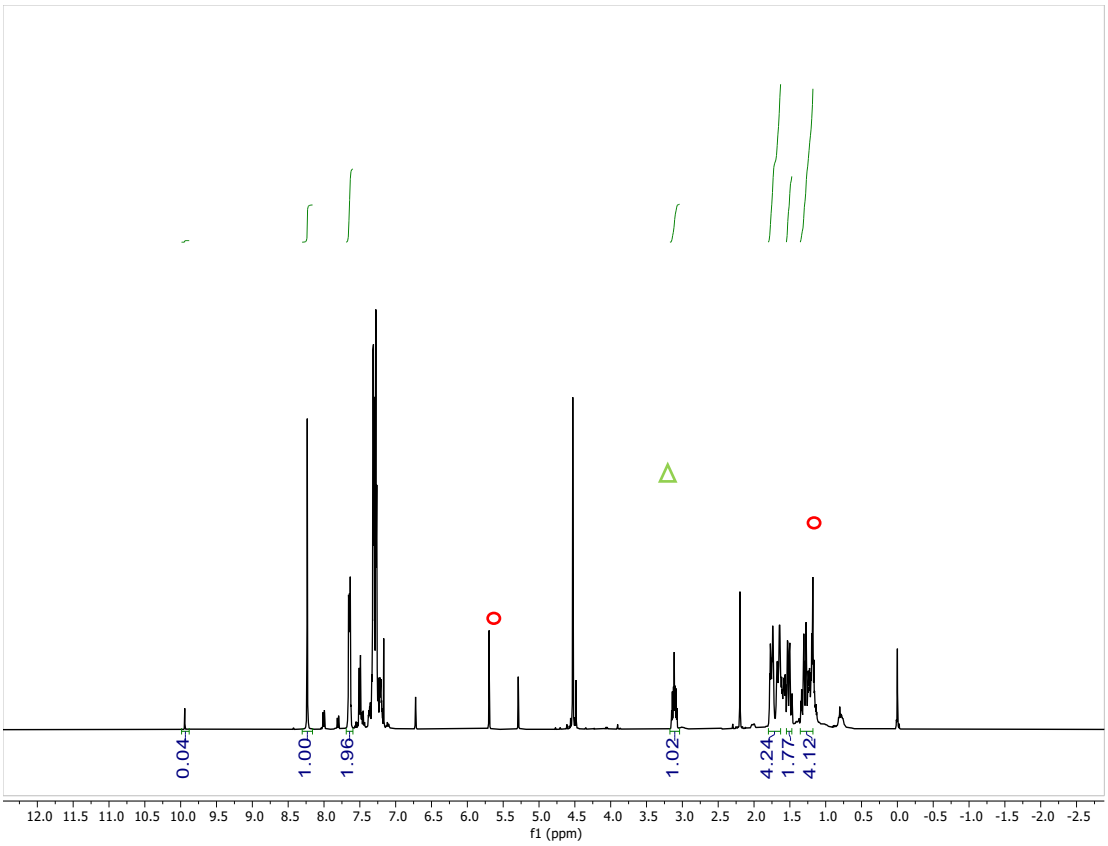

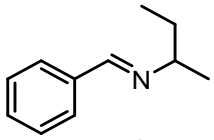

3

***N*-sec-butyl-1-phenylmethanimine** (**3**) ^{1}H NMR (400 MHz, $CDCl_3$) δ 8.19 (d, *J* = 0.6 Hz, 1H), 7.70 – 7.60 (m, 2H), 7.33 – 7.30 (m, 2H), 7.30 – 7.24 (m, 1H), 3.17 – 3.06 (m, 1H), 1.55 (pd, *J* = 7.4, 6.0 Hz, 2H), 1.18 (d, *J* = 6.3 Hz, 3H), 0.77 (t, *J* = 7.4 Hz, 3H). NMR data are in accordance with literature values.[20]

GC-MS trace

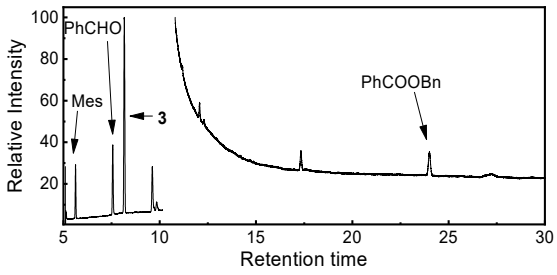

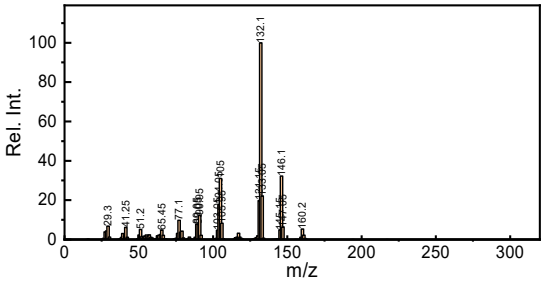

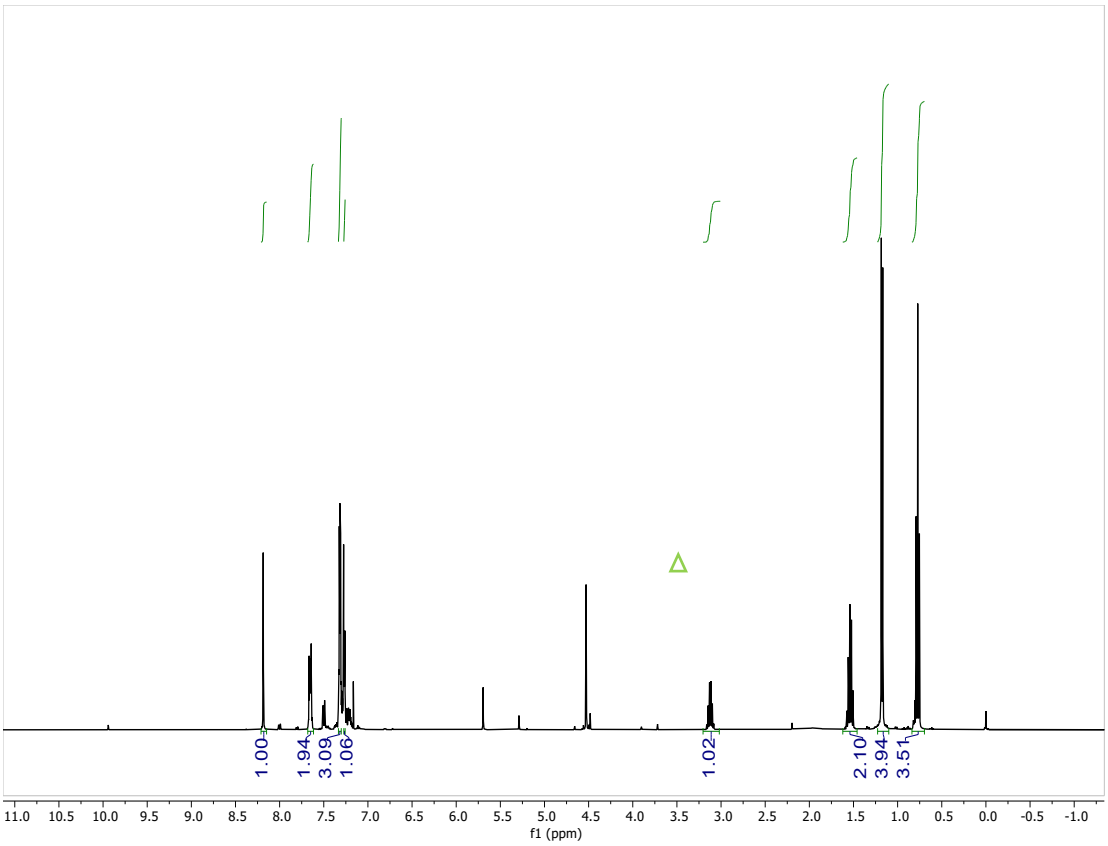

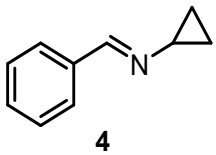

4

***N*-Cyclopropyl-1-phenylmethylanimine** (**4**) ^{1}H NMR (400 MHz, $CDCl_3$) δ 8.31 (s, 1H), 7.62 – 7.55 (m, 2H), 7.32 – 7.20 (m, 3H), 2.90 (tt, *J* = 6.8, 3.5 Hz, 1H), 0.94 – 0.86 (m, 2H), 0.84 – 0.74 (m, 2H). NMR data are in accordance with literature values.[21]

Note: To confirm the possible ring opening in this system, **4** and its corresponding allylic moiety were *in situ* prepared by mixing benzaldehyde with the amine in 1:1 mole ratio in $CDCl_3$ and directly measure by NMR (*vide infra*).

GC-MS trace

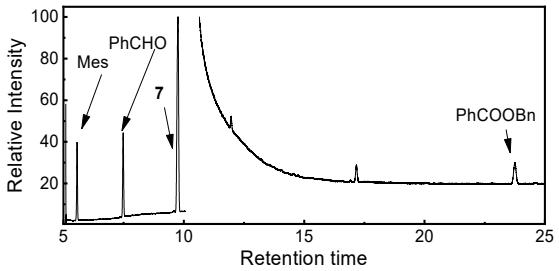

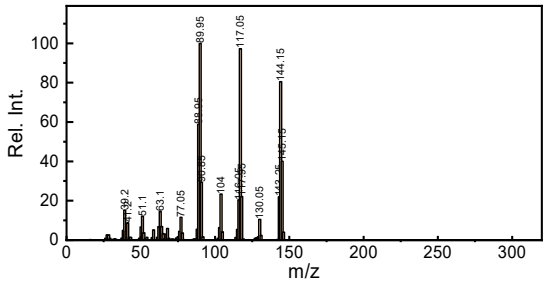

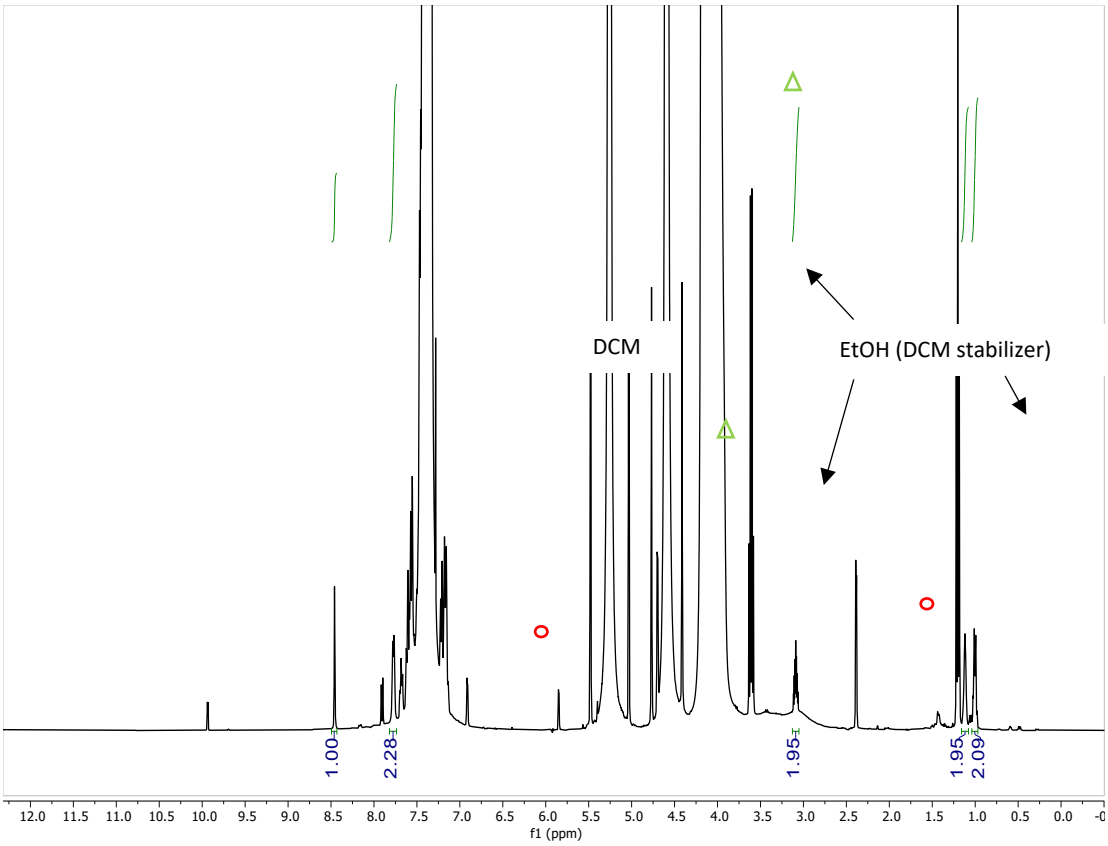
DCM
EtOH (DCM stabilizer)
1.00
2.28
1.95
1.95
2.09
f1 (ppm)

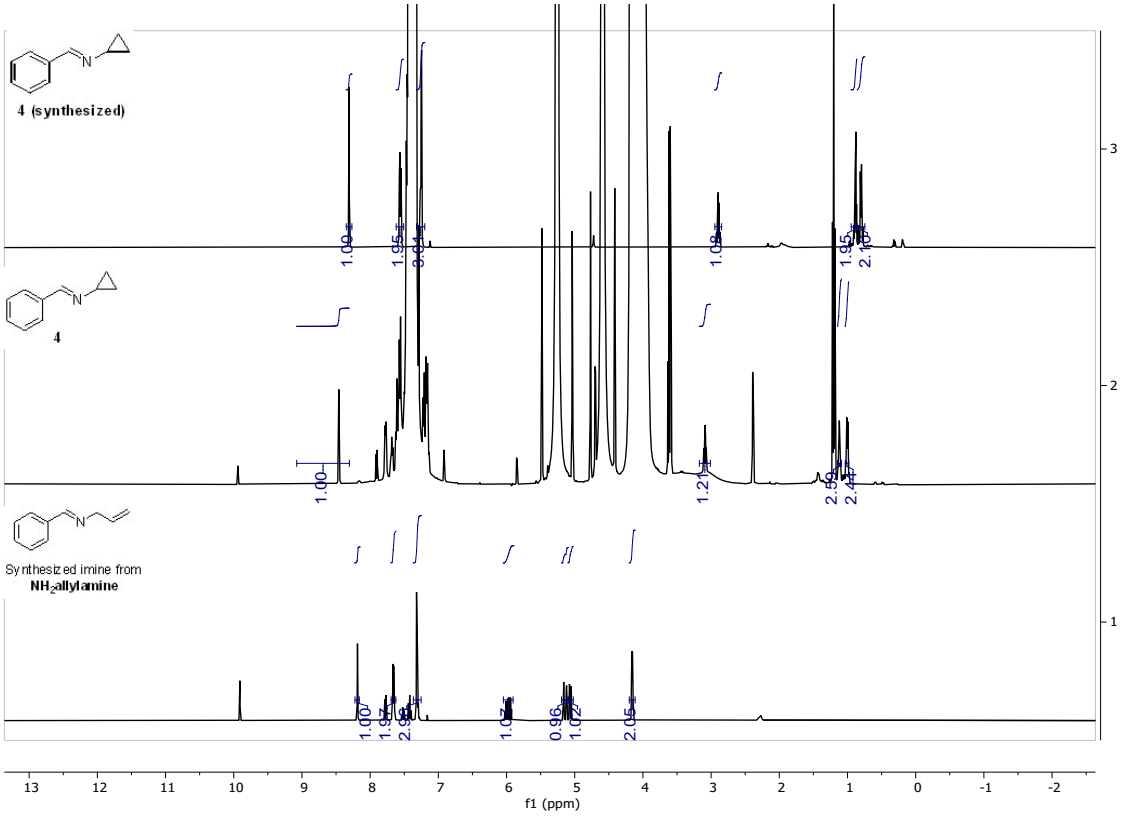
4 (synthesized)
4
Synthesized imine from
NH2allylamine
f1 (ppm)

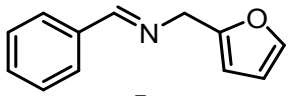

5

***N*-(furan-2-ylmethyl)-1-phenylmethanimine** (**5**) ^{1}H NMR (400 MHz, $CDCl_3$) δ 8.26 (d, *J* = 1.5 Hz, 1H), 7.74 – 7.62 (m, 2H), 7.35 – 7.28 (m, 4H), 6.26 (dd, *J* = 3.2, 1.8 Hz, 1H), 6.19 (dd, *J* = 3.1, 0.9 Hz, 1H), 4.70 (t, *J* = 1.0 Hz, 2H). NMR data are in accordance with literature values.[22]

GC-MS trace

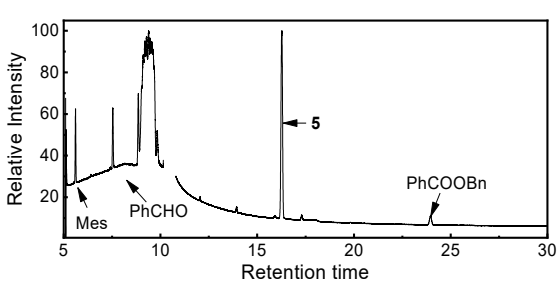

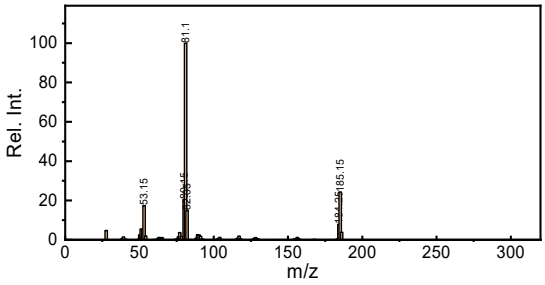

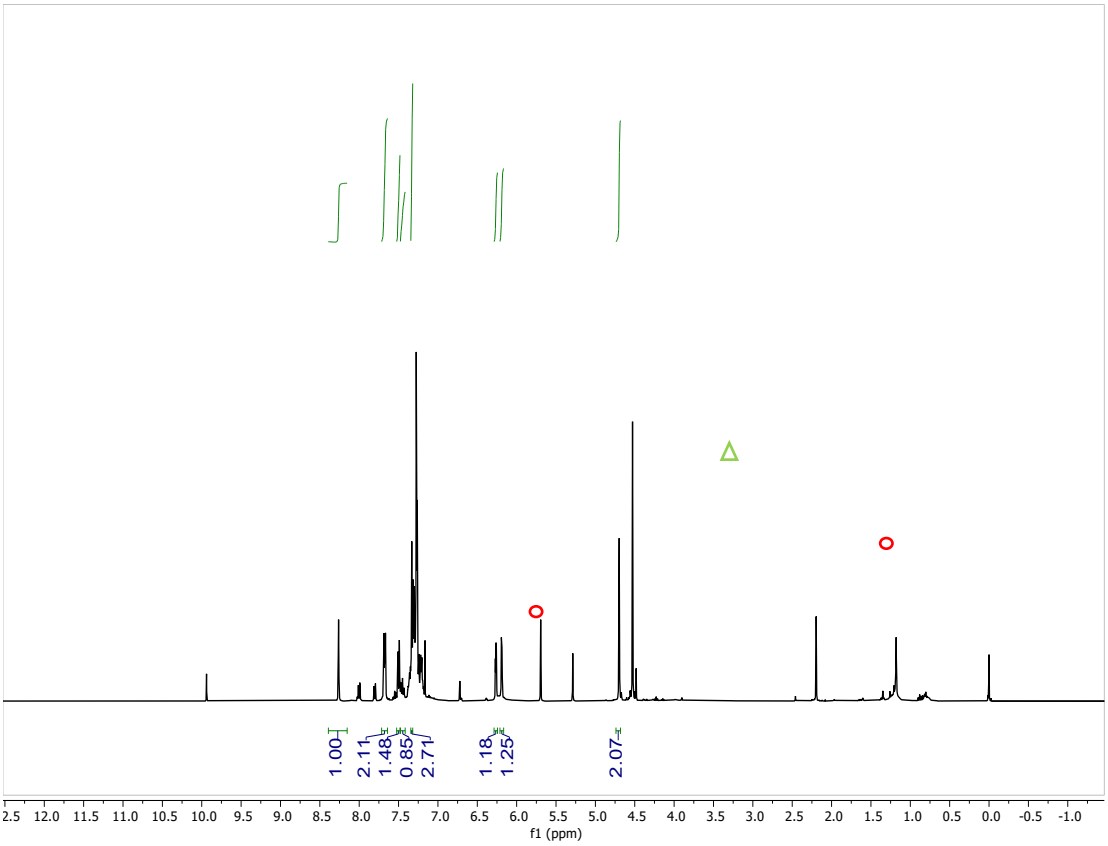

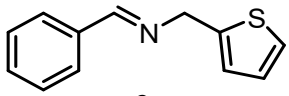

6

1-phenyl-*N*-(thiophen-2-ylmethyl)methanimine (**6**) ^{1}H NMR (400 MHz, $CDCl_3$) δ 8.26 (s, 1H), 7.73 – 7.63 (m, 2H), 7.35 – 7.28 (m, 3H), 7.16 – 7.10 (m, 1H), 6.89 (d, *J* = 3.4 Hz, 2H), 4.88 (d, *J* = 1.5 Hz, 2H). NMR data are in accordance with literature values.[23]

GC-MS trace

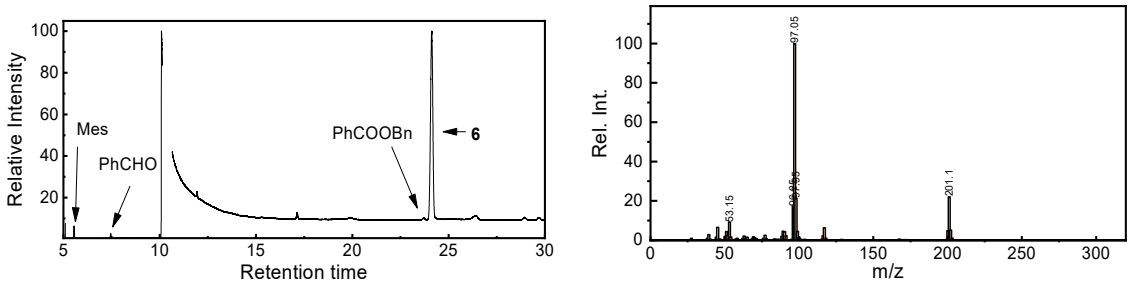

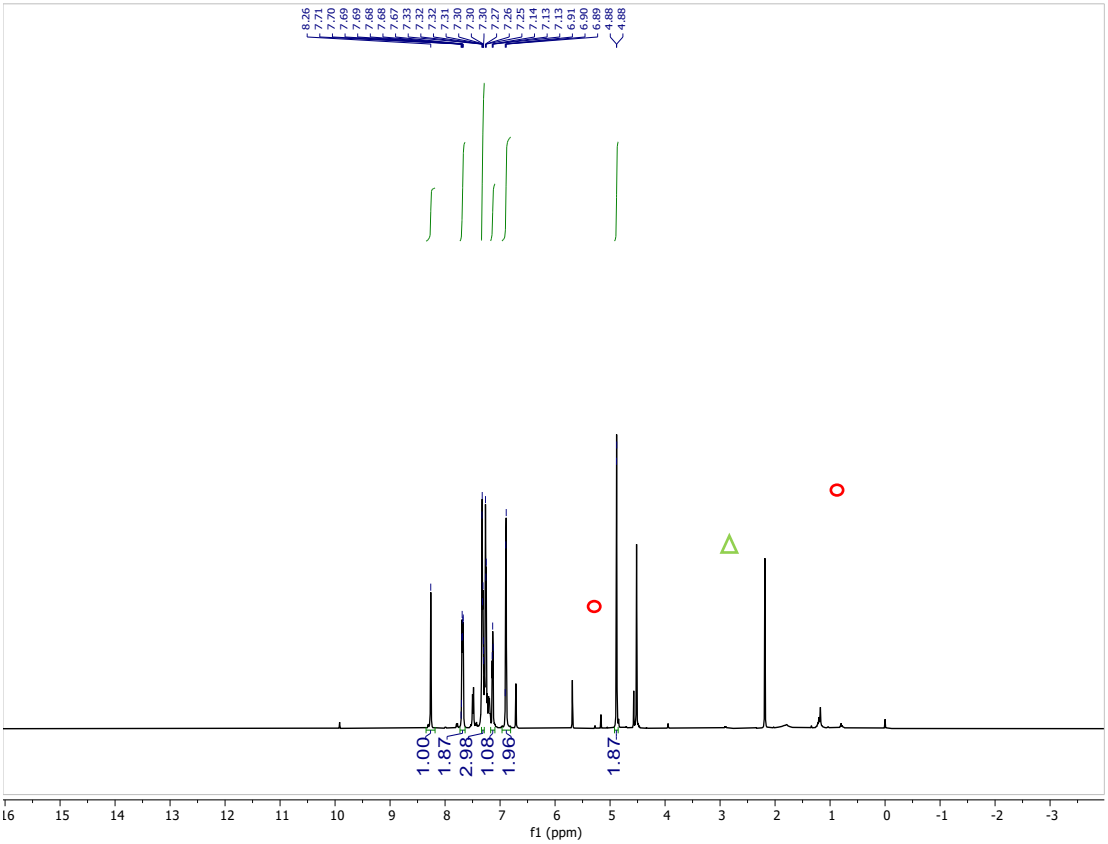

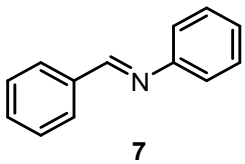

7

***N*,1-diphenylmethanimine (7) GC-MS trace**.

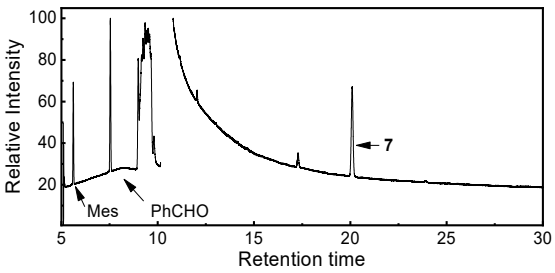
Relative Intensity
Retention time
Mes
PhCHO
7

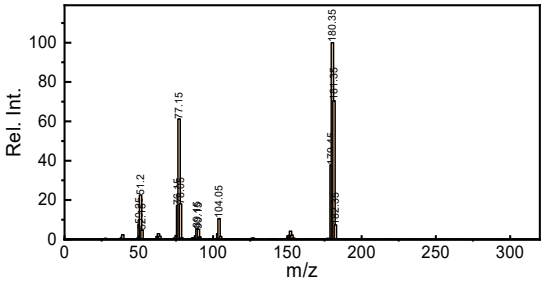
Rel. Int.
m/z
180.35
77.15
104.05

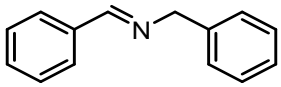

8

***N*-benzyl-1-phenylmethanimine** (**8**) ^{1}H NMR (400 MHz, $CDCl_3$) δ 8.30 (t, *J* = 1.4 Hz, 1H), 7.75 – 7.65 (m, 2H), 7.37 – 7.29 (m, 3H), 7.29 – 7.22 (m, 5H), 4.74 (d, *J* = 1.4 Hz, 2H). NMR data are in accordance with literature values.[22]

GC-MS trace

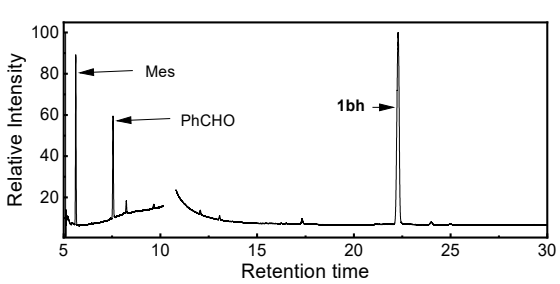

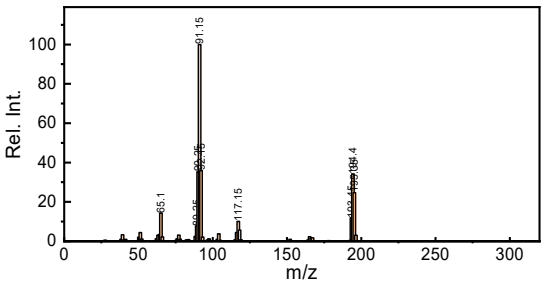

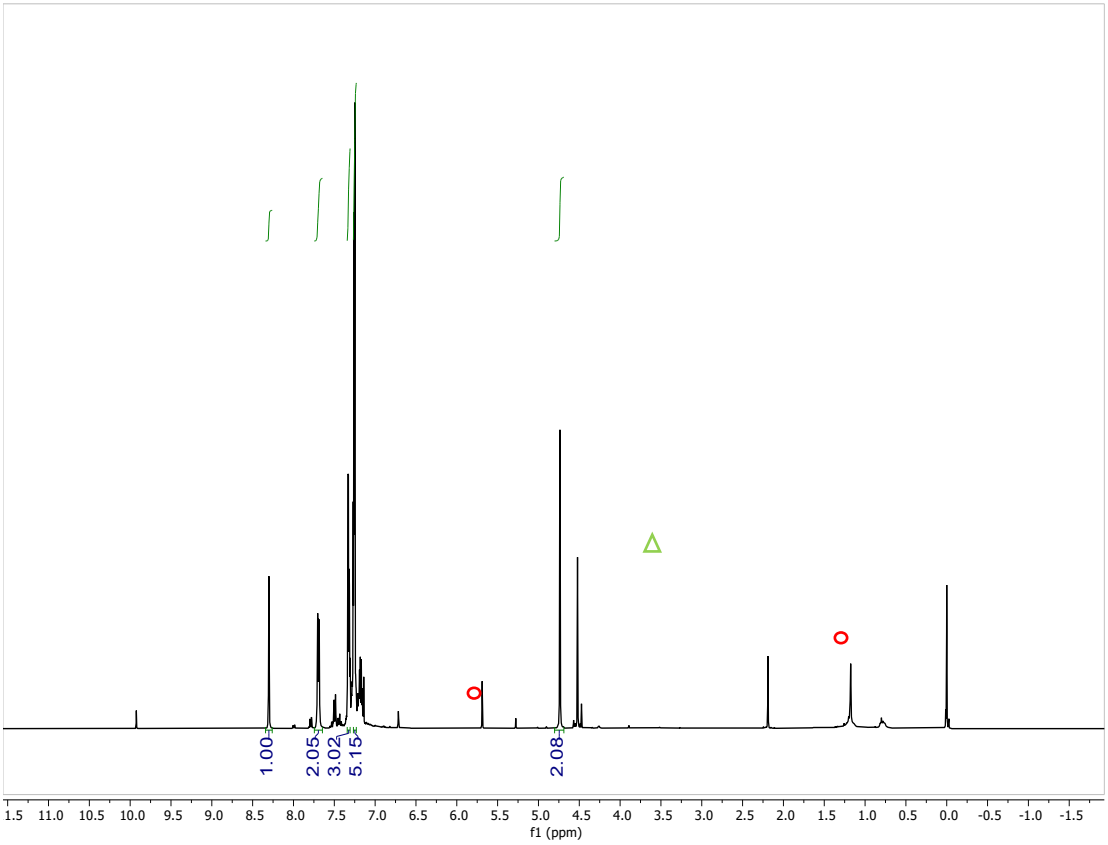

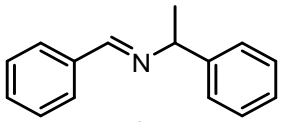

9

1-phenyl-*N*-(1-phenylethyl)methanimine (**9**) ^{1}H NMR (400 MHz, $CDCl_3$) δ 8.28 (s, 1H), 7.73 – 7.66 (m, 2H), 7.40 – 7.33 (m, 2H), 7.33 – 7.30 (m, 2H), 7.27 – 7.23 (m, 3H), 7.19 – 7.11 (m, 1H), 4.46 (q, *J* = 6.6 Hz, 1H), 1.51 (d, *J* = 6.7 Hz, 3H). NMR data are in accordance with literature values.[24]

GC-MS trace

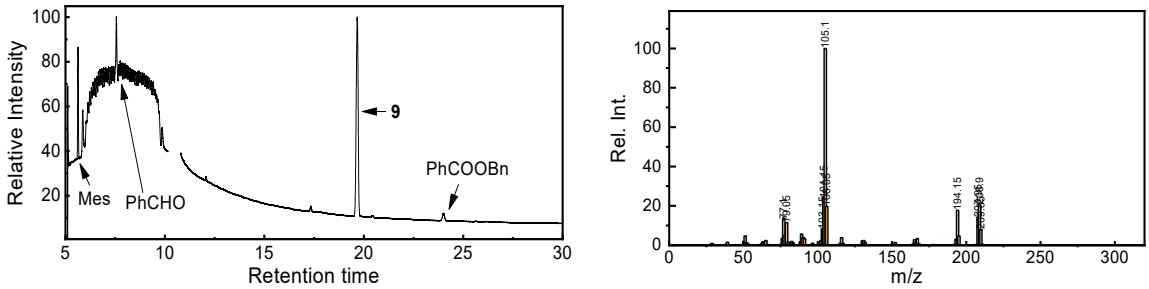

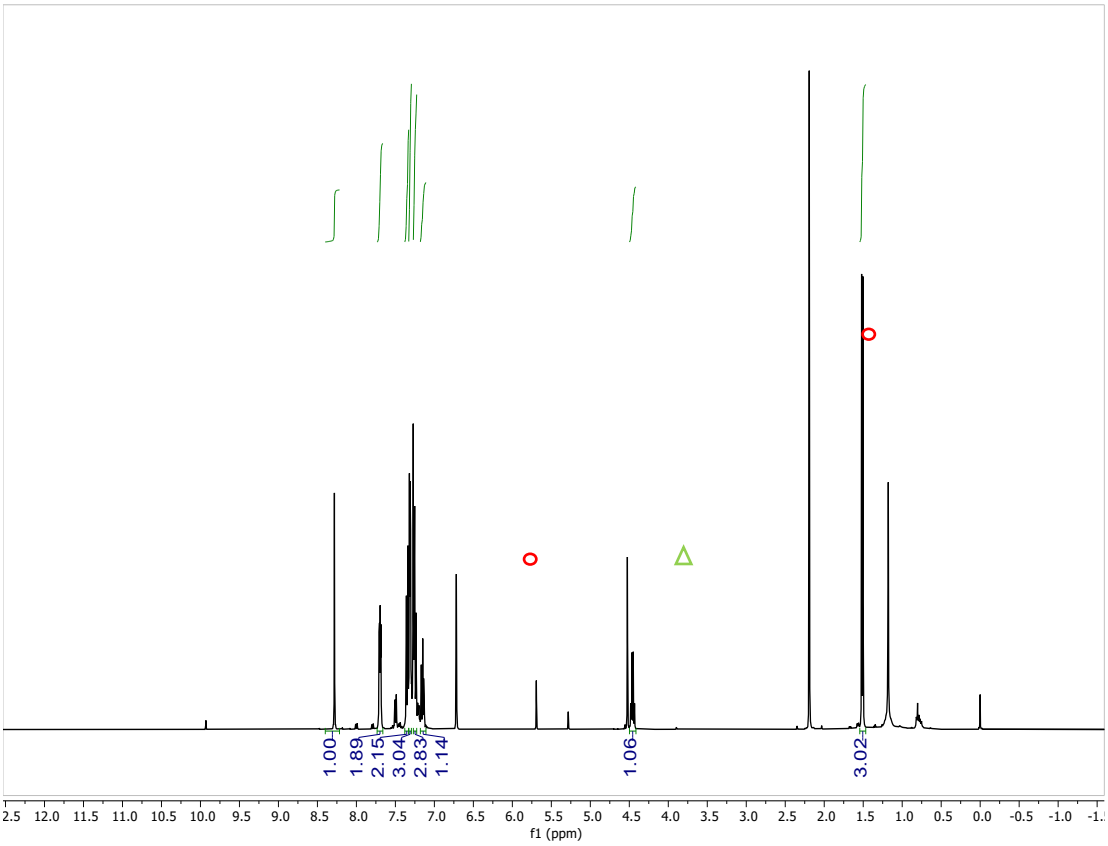

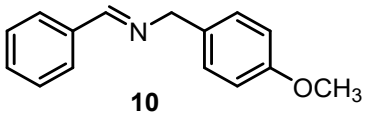

10

***N*-(4-methoxybenzyl)-1-phenylmethanimine** (**10**) ^{1}H NMR (400 MHz, $CDCl_3$) δ 8.39 (d, *J* = 1.4 Hz, 1H), 7.87 – 7.82 (m, 2H), 7.55 – 7.48 (m, 3H), 7.34 – 7.28 (m, 2H), 7.03 – 6.96 (m, 2H), 4.77 (d, *J* = 1.4 Hz, 2H), 3.84 (s, 3H), 2.41 (s, 2H). NMR data are in accordance with literature values.[25]

GC-MS trace

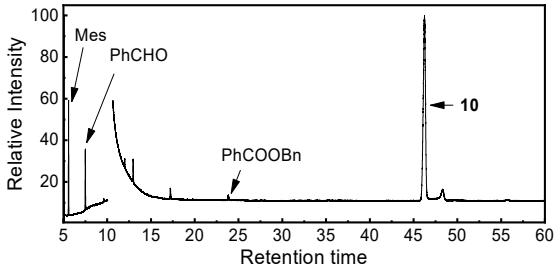

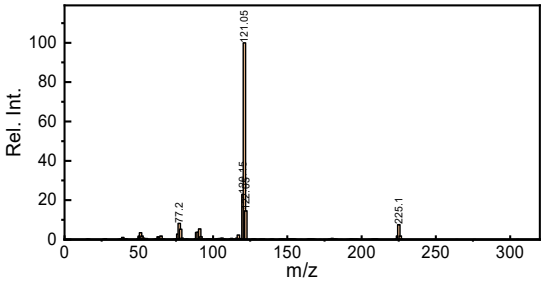

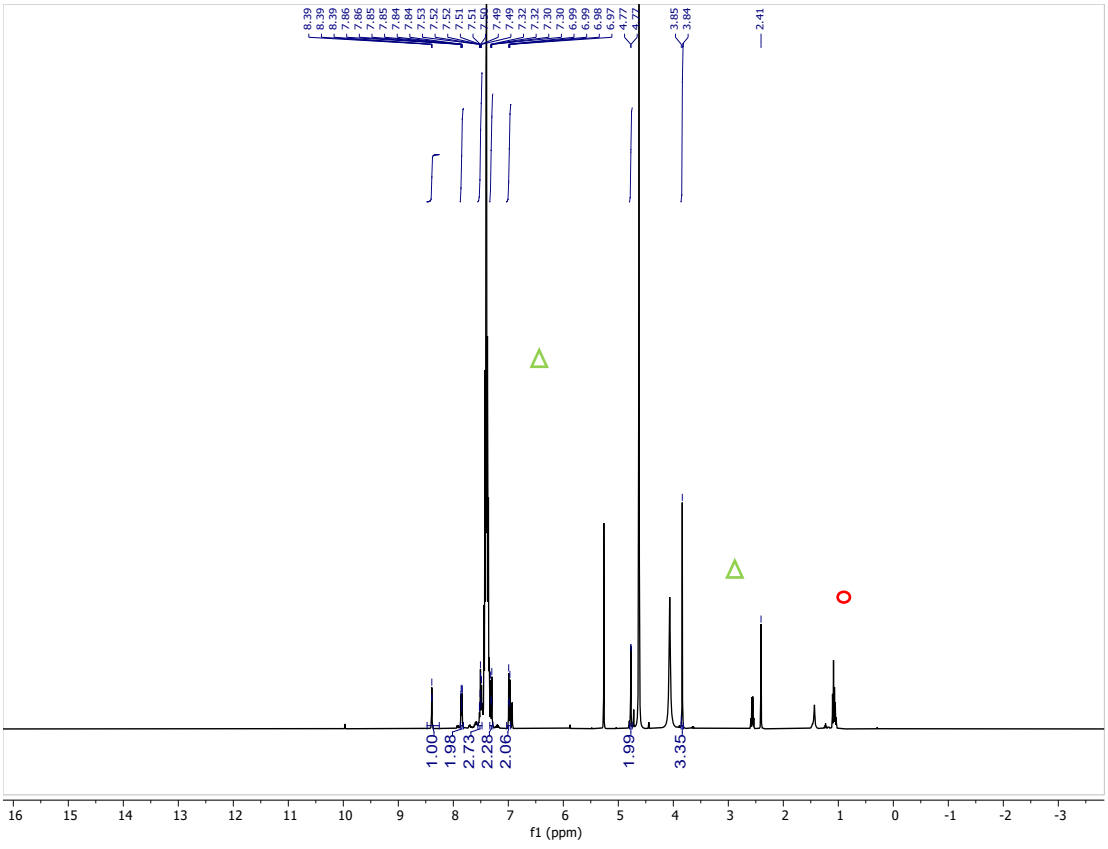

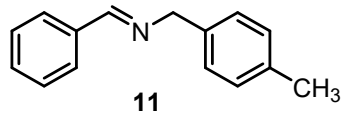

11

***N*-(4-methylbenzyl)-1-phenylmethanimine** (**11**) ^{1}H NMR (400 MHz, $CDCl_3$) δ 8.41 (d, *J* = 1.6 Hz, 1H), 7.95 – 7.87 (m, 2H), 7.54 (dt, *J* = 6.4, 2.5 Hz, 6H), 7.34 (d, *J* = 3.7 Hz, 3H), 4.82 (s, 2H), 2.52 (s, 3H). NMR data are in accordance with literature values.[25]

GC-MS trace

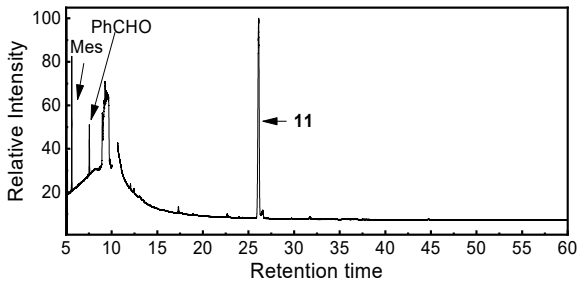

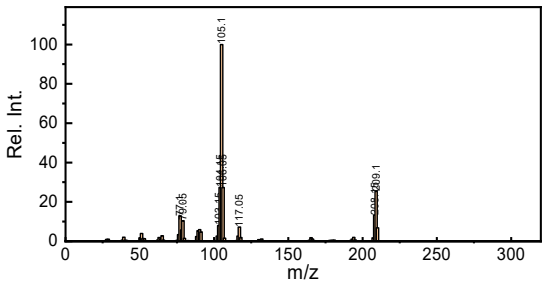

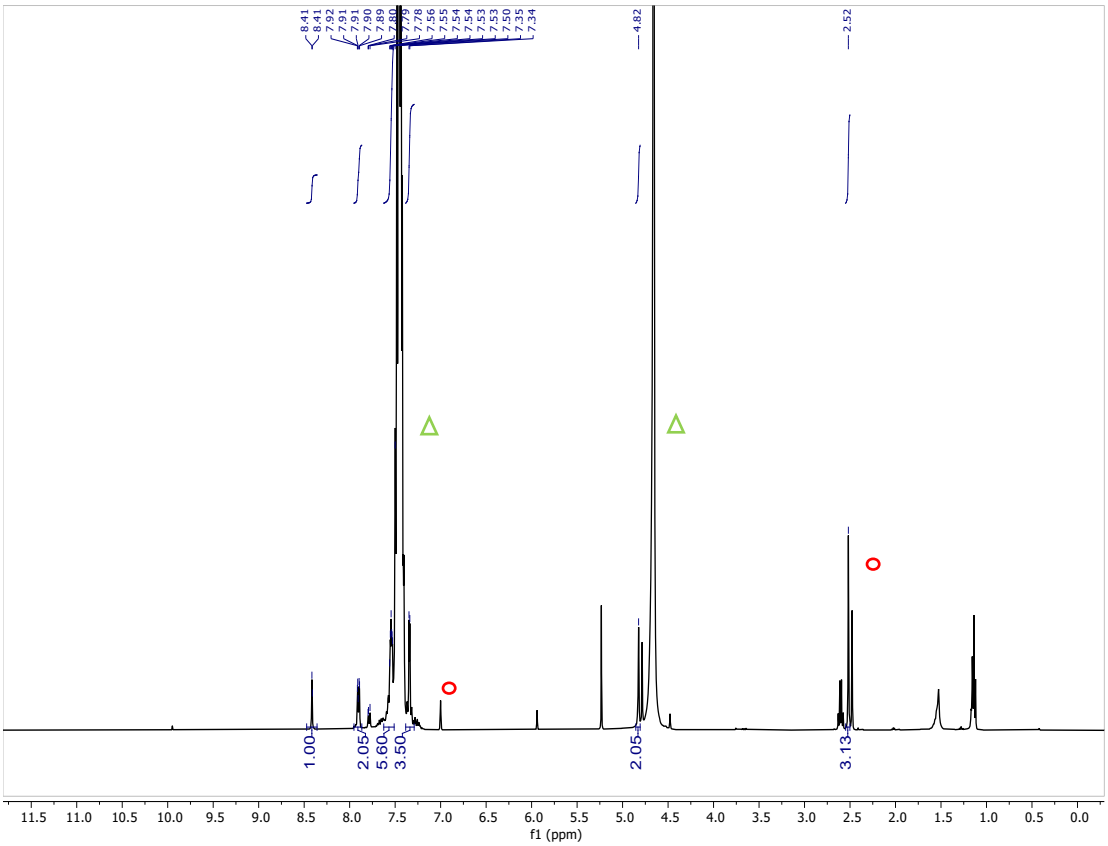

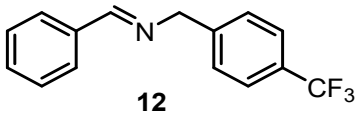

12

***N*-(4-trifluorobenzyl)-1-phenylmethanimine** (**12**) ^{1}H NMR (400 MHz, $CDCl_3$) δ 8.31 (s, 1H), 7.75 – 7.64 (m, 2H), 7.53 – 7.46 (m, 3H), 7.36 (d, *J* = 8.5 Hz, 3H), 7.25 (d, *J* = 4.1 Hz, 1H), 4.75 (s, 2H). ^{19}F NMR (376 MHz, $CDCl_3$) δ -62.31. NMR data are in accordance with literature values.[25]

GC-MS trace

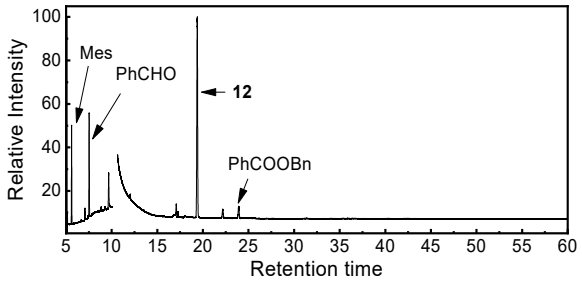

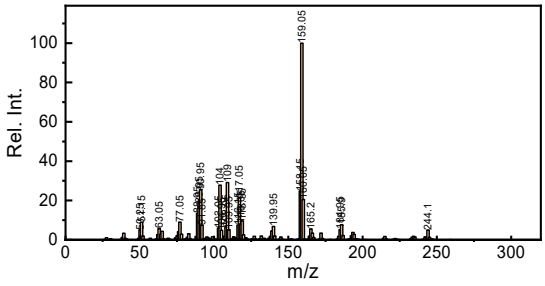

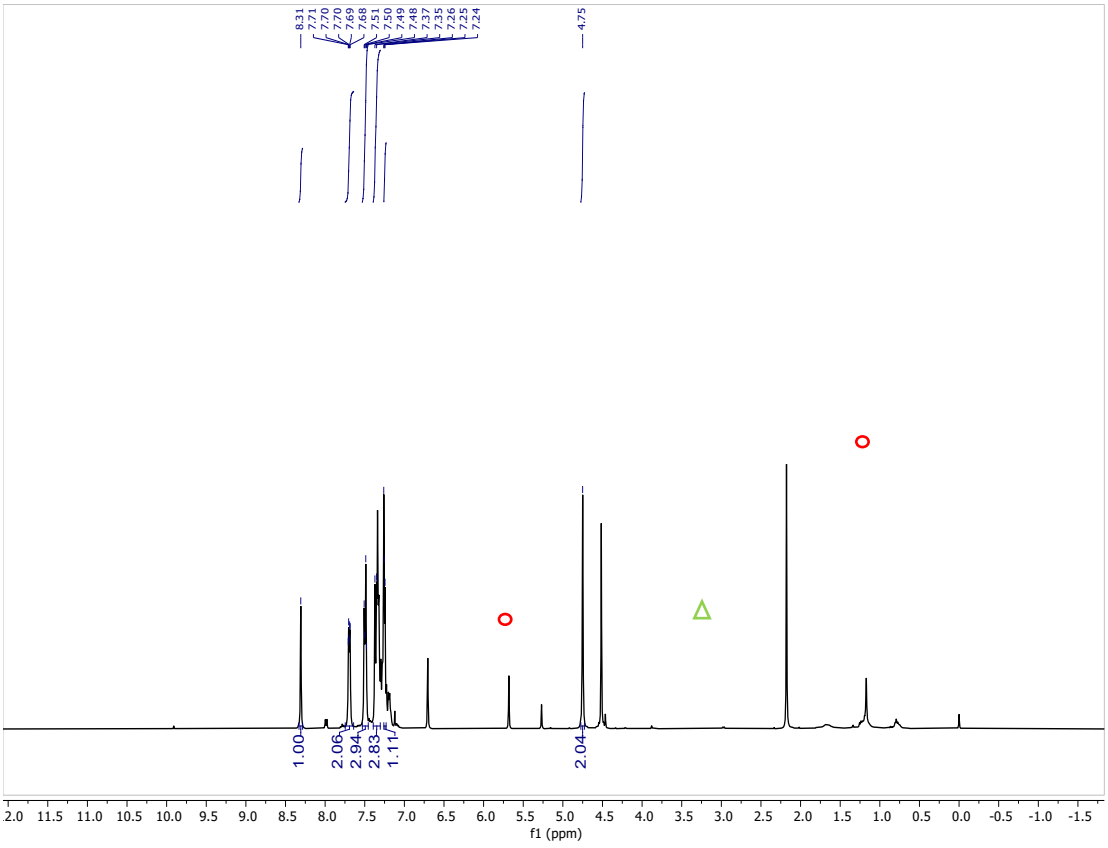

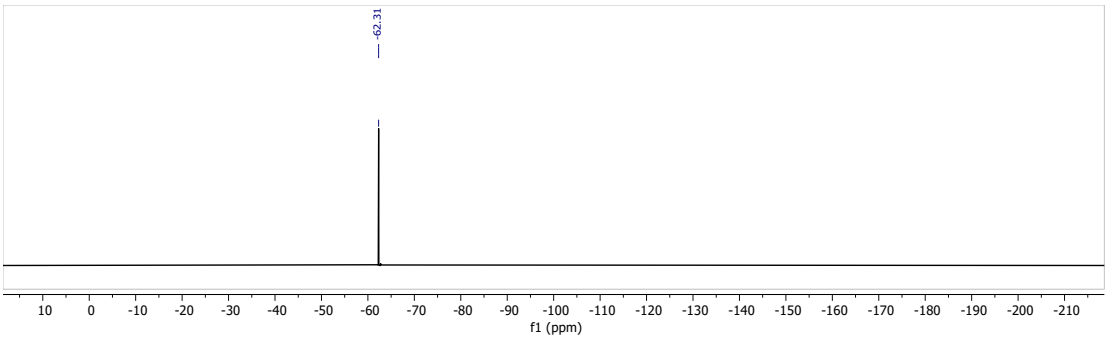

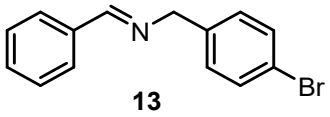

13

***N*-(4-bromobenzyl)-1-phenylmethanimine** (**13**) ^{1}H NMR (400 MHz, $CDCl_3$) δ 8.29 (d, *J* = 1.5 Hz, 1H), 7.69 (dt, *J* = 6.7, 2.2 Hz, 2H), 7.38 – 7.09 (m, 7H), 4.77 (d, *J* = 1.5 Hz, 2H). NMR data are in accordance with literature values.[26]

GC-MS trace

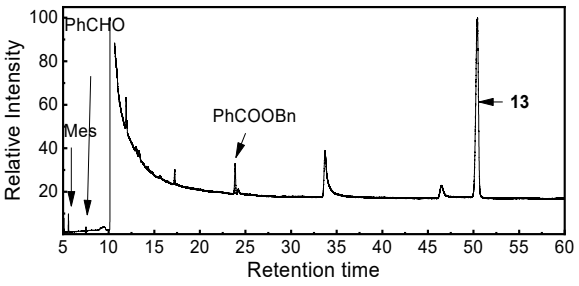

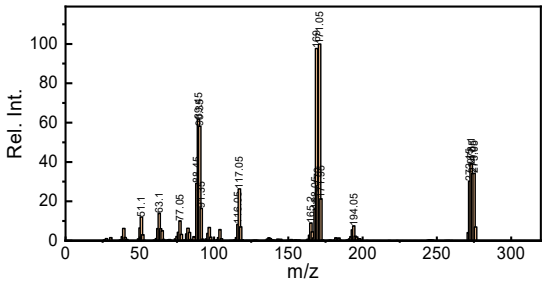

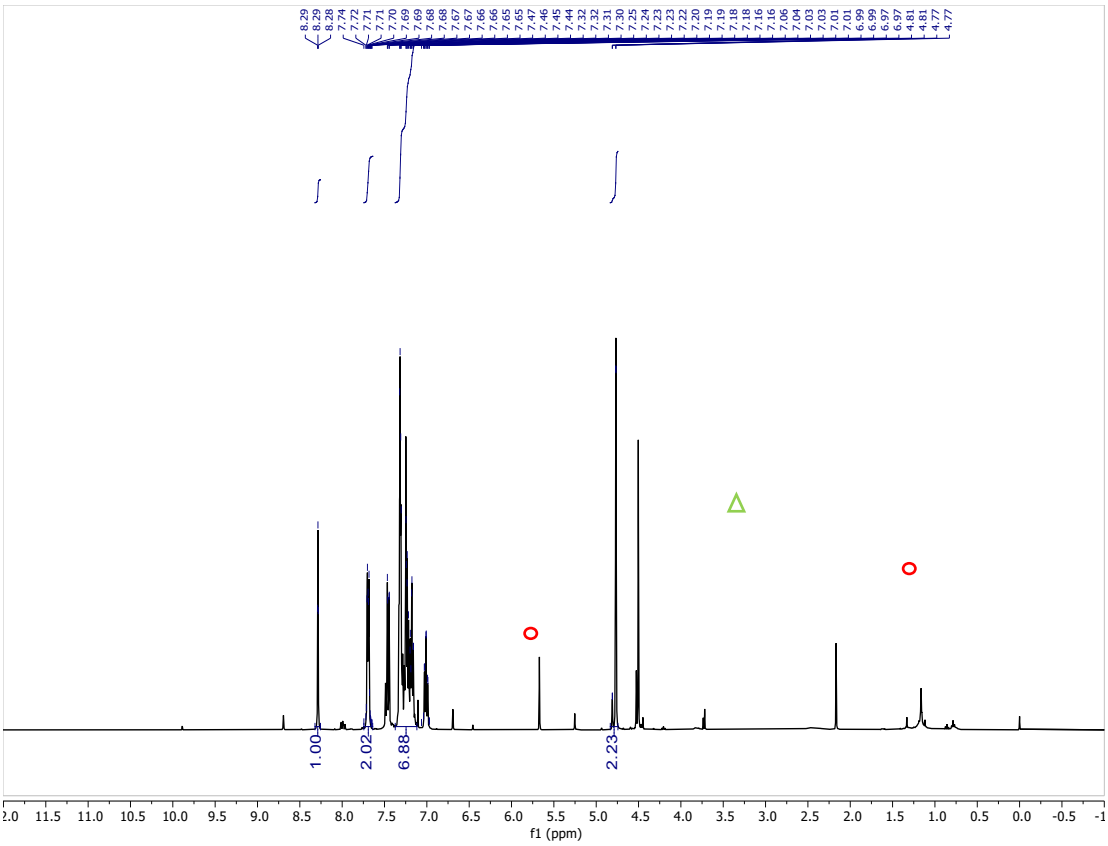

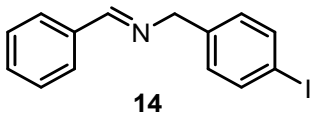

14

***N*-(4-bromobenzyl)-1-phenylmethanimine** (**14**) ^{1}H NMR (400 MHz, $CDCl_3$) δ 8.40 (s, 1H), 7.82 – 7.76 (m, 2H), 7.68 (d, J = 8.0 Hz, 2H), 7.64 – 7.55 (m, 2H), 7.45 (td, J = 5.1, 1.9 Hz, 3H), 7.11 (d, J = 8.0 Hz, 2H), 4.77 (s, 2H). NMR data are in accordance with literature values.[26]

GC-MS trace

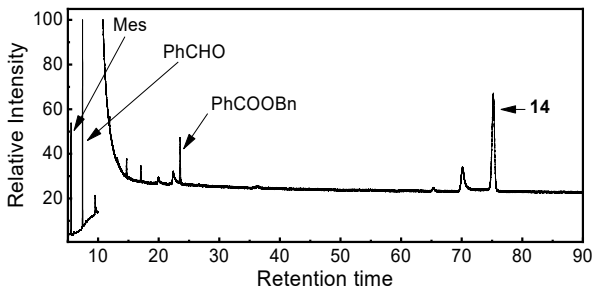

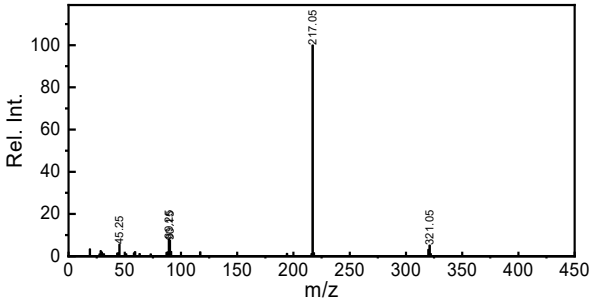

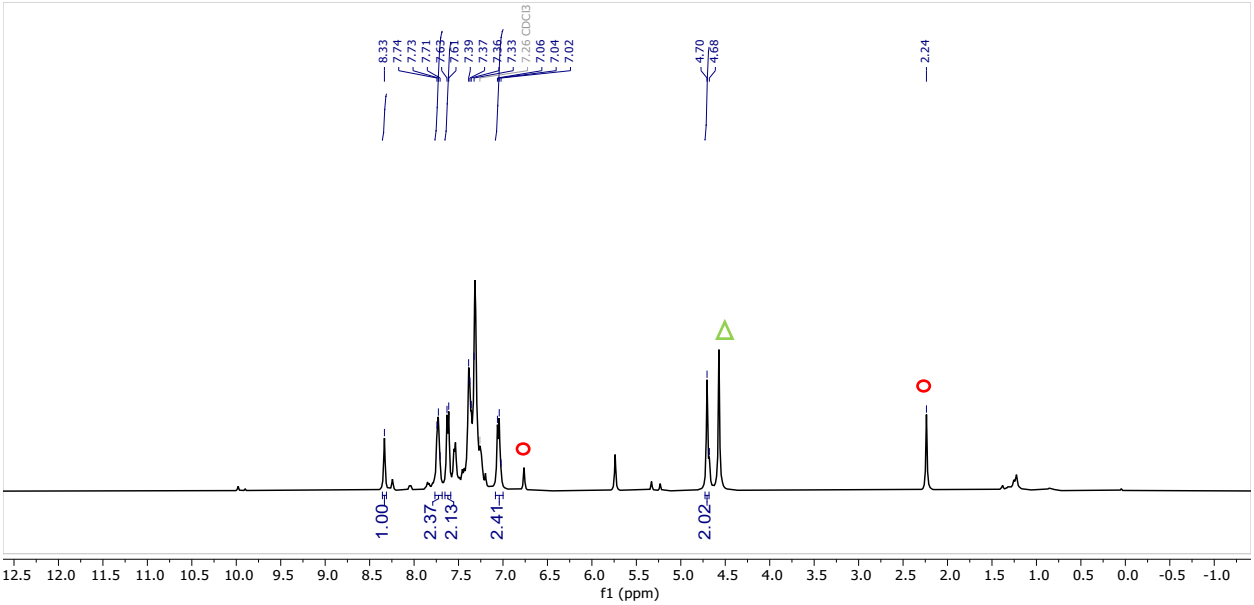

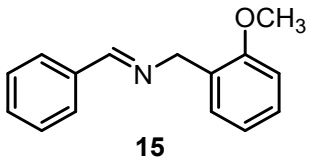

15

***N*-(2-methoxybenzyl)-1-phenylmethanimine** (**15**) ^{1}H NMR (400 MHz, $CDCl_3$) δ 8.25 (d, *J* = 1.5 Hz, 1H), 7.68 (dd, *J* = 6.7, 3.0 Hz, 2H), 7.52 – 7.43 (m, 1H), 7.23 – 7.10 (m, 4H), 6.84 (t, *J* = 7.5 Hz, 1H), 6.77 (d, *J* = 8.2 Hz, 1H), 4.73 (d, *J* = 1.4 Hz, 2H), 3.72 (s, 3H). NMR data are in accordance with literature values.[27]

GC-MS trace

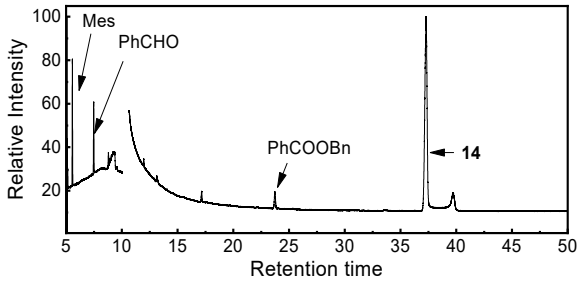

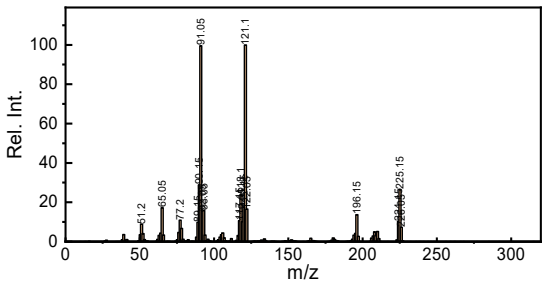

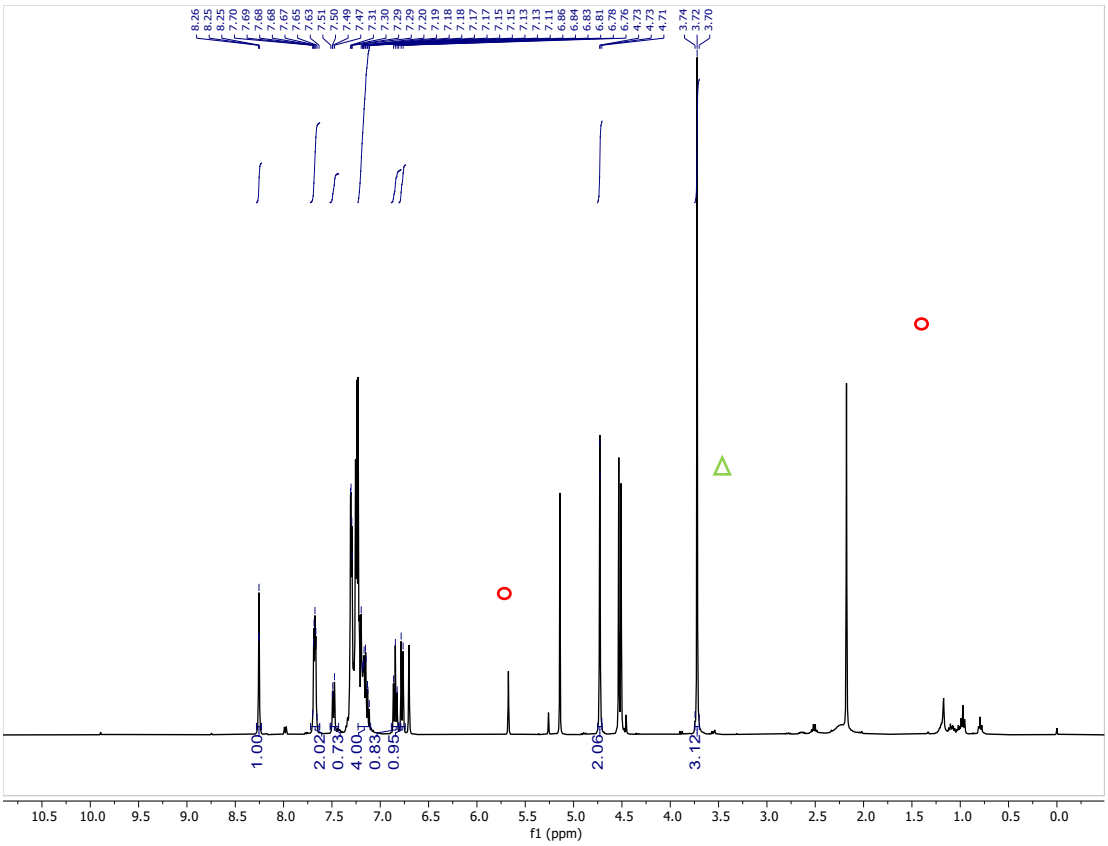

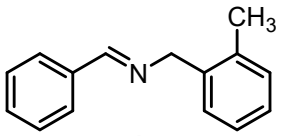

16

***N*-(2-methylbenzyl)-1-phenylmethanimine** (**16**) ^{1}H NMR (400 MHz, $CDCl_3$) δ 8.38 (d, *J* = 1.6 Hz, 1H), 7.91 – 7.84 (m, 2H), 7.58 – 7.34 (m, 7H), 4.85 (d, *J* = 1.5 Hz, 2H), 2.45 (s, 3H). NMR data are in accordance with literature values.[27]

GC-MS trace

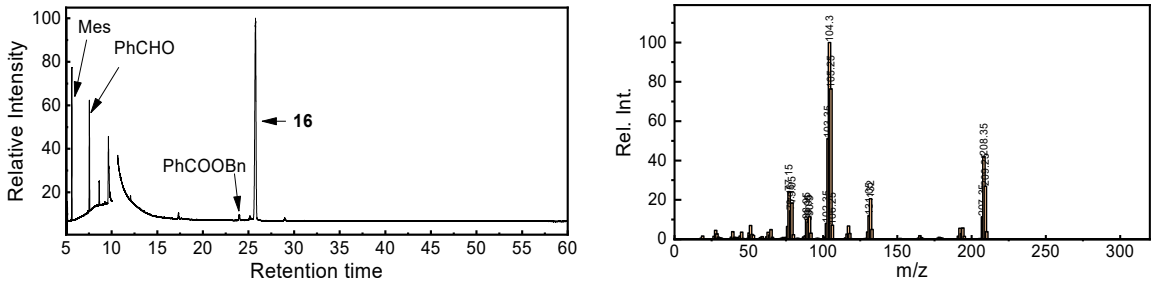

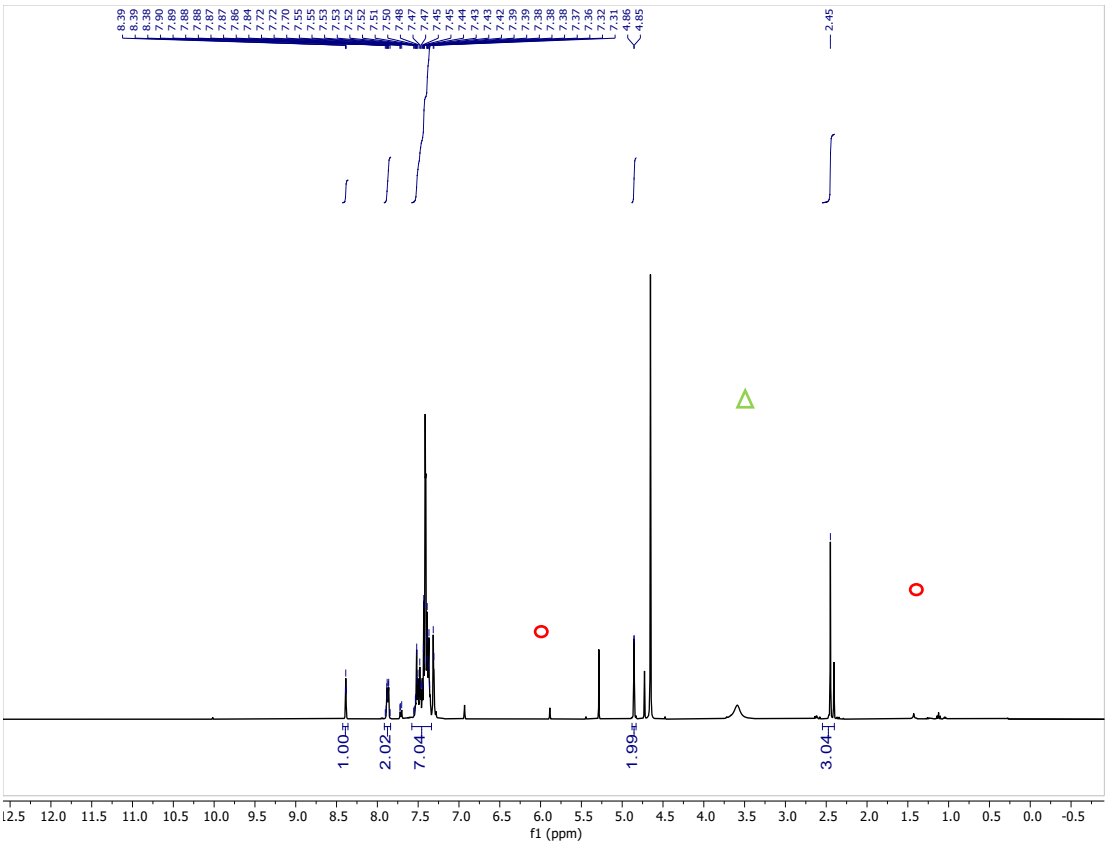

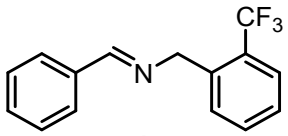

17

***N*-(2-trifluoromethylbenzyl)-1-phenylmethanimine** (**17**) ^{1}H NMR (400 MHz, $CDCl_3$) δ 8.42 (d, *J* = 1.5 Hz, 1H), 7.95 – 7.87 (m, 2H), 7.79 (dd, *J* = 7.8, 1.3 Hz, 1H), 7.69 (d, *J* = 7.8 Hz, 1H), 7.61 (t, *J* = 7.7 Hz, 1H), 7.56 – 7.51 (m, 2H), 7.51 – 7.47 (m, 1H), 7.45 (t, *J* = 1.5 Hz, 2H), 5.07 (s, 2H). ^{19}F NMR (376 MHz, $CDCl_3$) δ -59.67. NMR data are in accordance with literature values.[28]

GC-MS trace

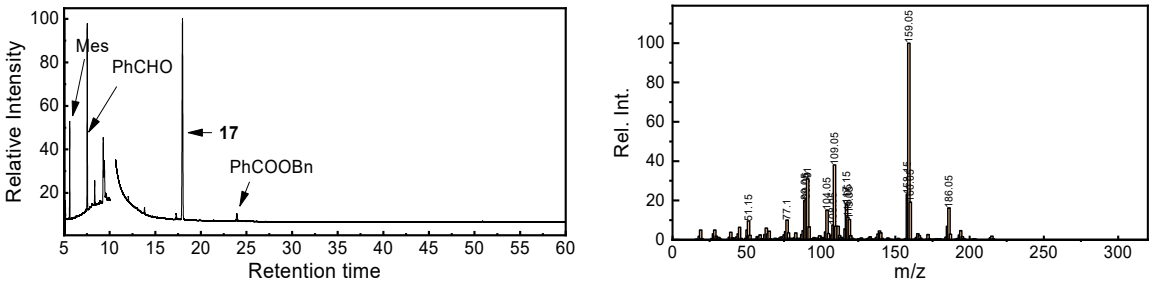

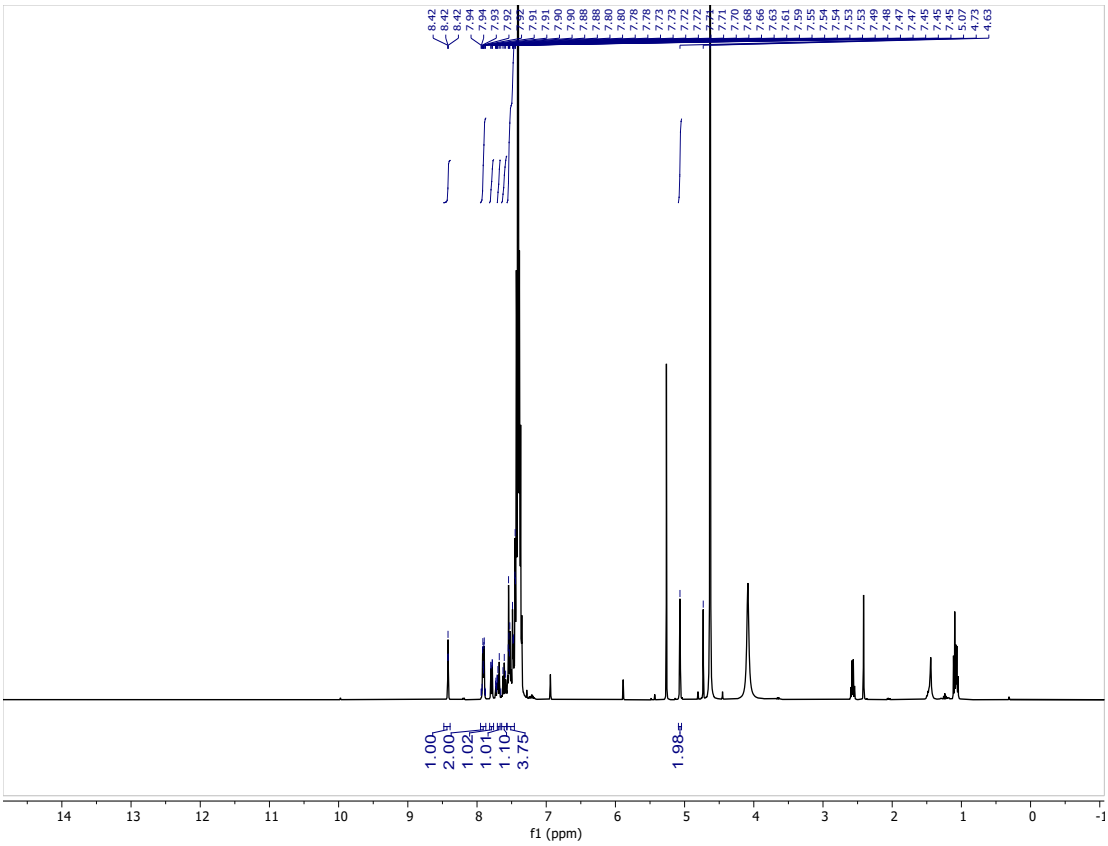
8.42
8.42
8.42
7.94
7.94
7.93
7.92
7.92
7.91
7.91
7.90
7.90
7.88
7.88
7.80
7.80
7.78
7.78
7.73
7.73
7.72
7.72
7.71
7.71
7.70
7.68
7.66
7.63
7.61
7.59
7.55
7.54
7.54
7.53
7.53
7.49
7.48
7.47
7.45
7.45
7.45
5.07
4.73
4.63
1.00
2.00
1.02
1.01
1.10
3.75
1.98
14
13
12
11
10
9
8
7
6
5
4
3
2
1
0
-1
f1 (ppm)

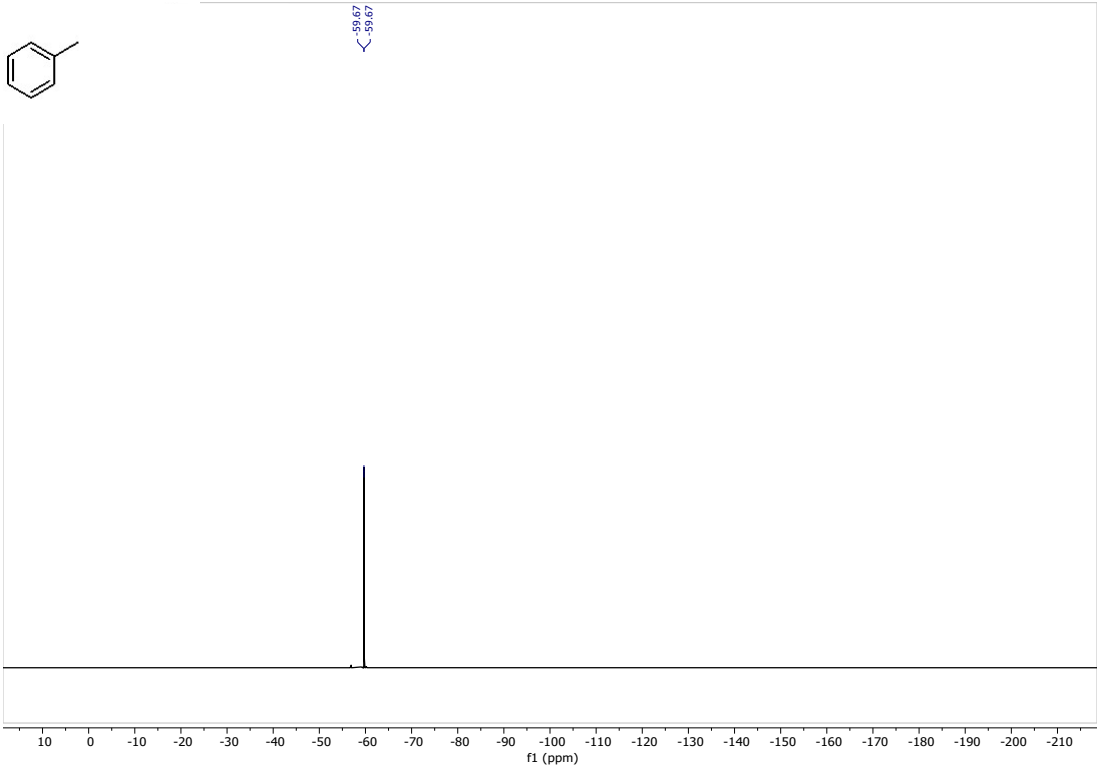
59.67
59.67
10
0
-10
-20
-30
-40
-50
-60
-70
-80
-90
-100
-110
-120
-130
-140
-150
-160
-170
-180
-190
-200
-210
f1 (ppm)

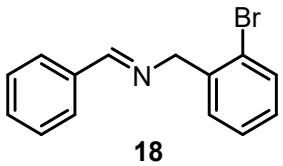

18

***N*-(2-Bromobenzyl)-1-phenylmethanimine** (**18**) ^{1}H NMR (400 MHz, $CDCl_3$) δ 8.47 (d, *J* = 1.5 Hz, 1H), 7.95 – 7.88 (m, 2H), 7.60 (d, *J* = 8.4 Hz, 2H), 7.58 – 7.50 (m, 3H), 7.31 (d, *J* = 8.3 Hz, 2H), 4.82 (s, 2H). NMR data are in accordance with literature values.[29]

GC-MS trace

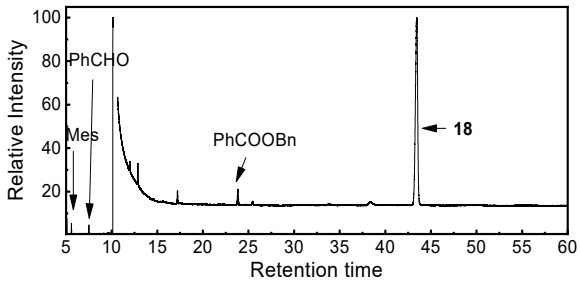

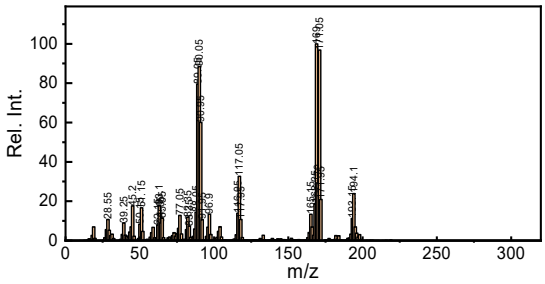

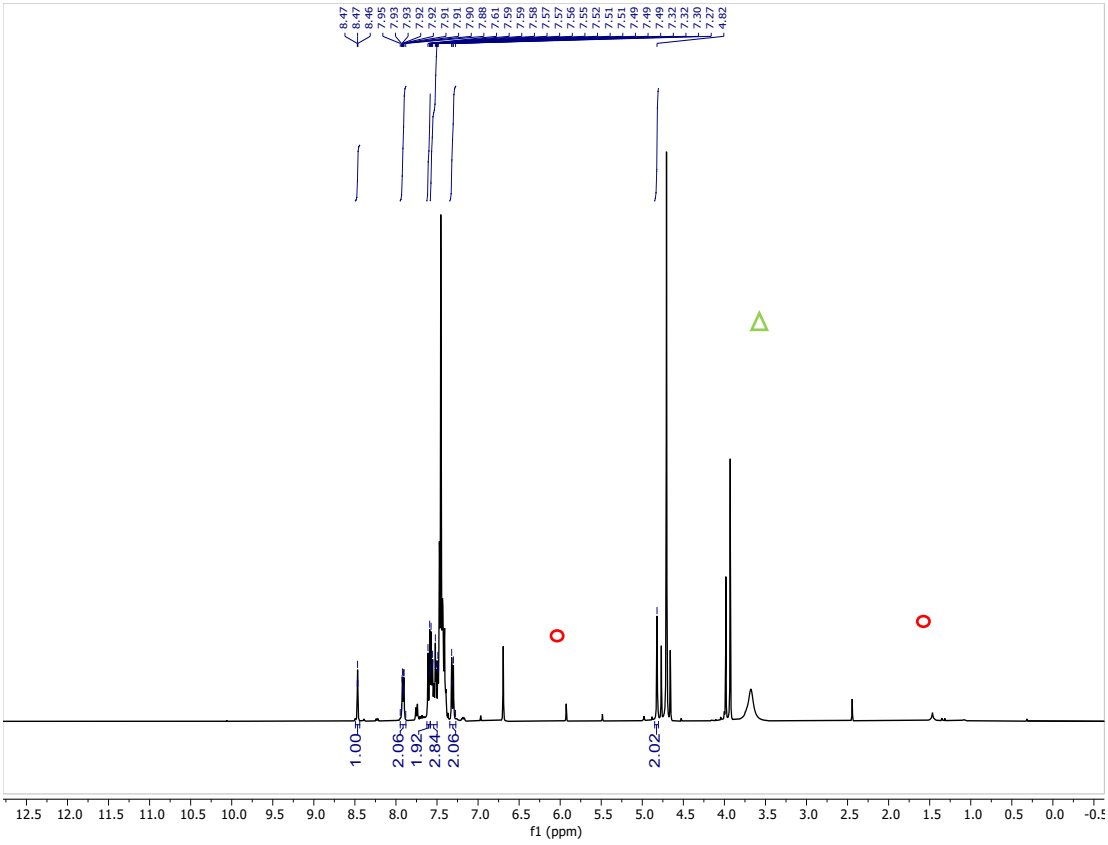

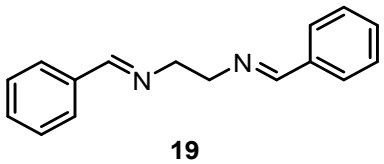

19

***N*,*N*'-(ethane-1,2-diyl)bis(1-phenylmethanimine) (19)** ^{1}H NMR (80 MHz, $CDCl_3$) δ 8.13 (s, 2H), 7.66 – 7.54 (m, 4H), 7.28-7.18 (m, , 6H), 3.85 (s, 2H). NMR data are in accordance with literature values.[30]

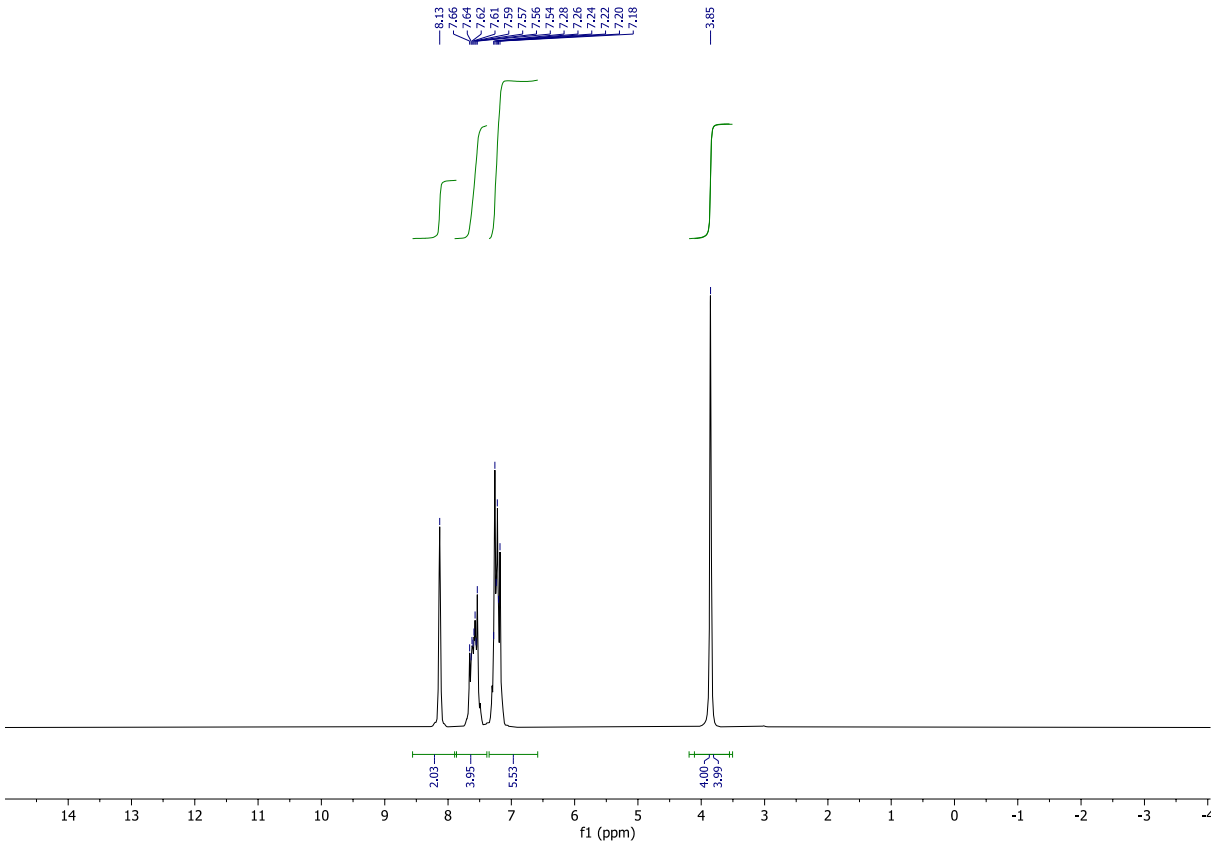

GC-MS trace

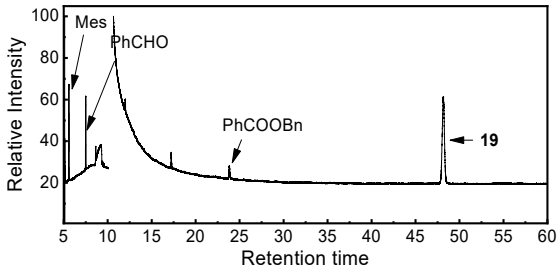

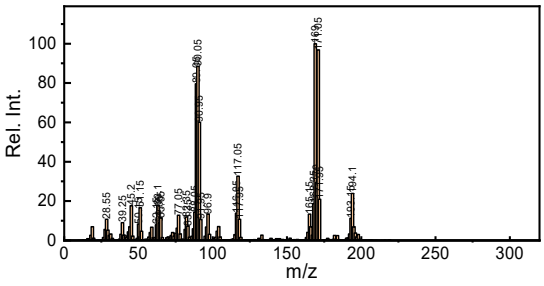

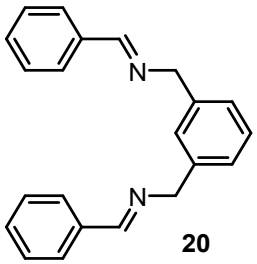

20

***N,N'*-(1,3-phenylenebis(methylene))bis(1-phenylmethanimine)** (**20**) ^{1}H NMR (400 MHz, $CDCl_3$) δ 8.22 (d, *J* = 1.5 Hz, 2H), 7.67 – 7.60 (m, 4H), 7.32 – 7.15 (m, 8H), 7.11 (dd, *J* = 8.3, 1.6 Hz, 2H), 4.67 (d, *J* = 1.4 Hz, 4H). ^{13}C NMR (101 MHz, $CDCl_3$) δ 162.2, 162.1, 139.6, 136.2, 130.9, 128.8, 128.7, 128.7, 128.4, 127.8, 126.8, 65.1.

Note: to confirm the peak of mono substitute imine, the disubstituted diimine was prepared by *in situ* mixing benzaldehyde and corresponding diamine in $CDCl_3$ (*vide infra* for the spectra). The ^{13}C NMR who has never been describe in the literature was measure from this solution.

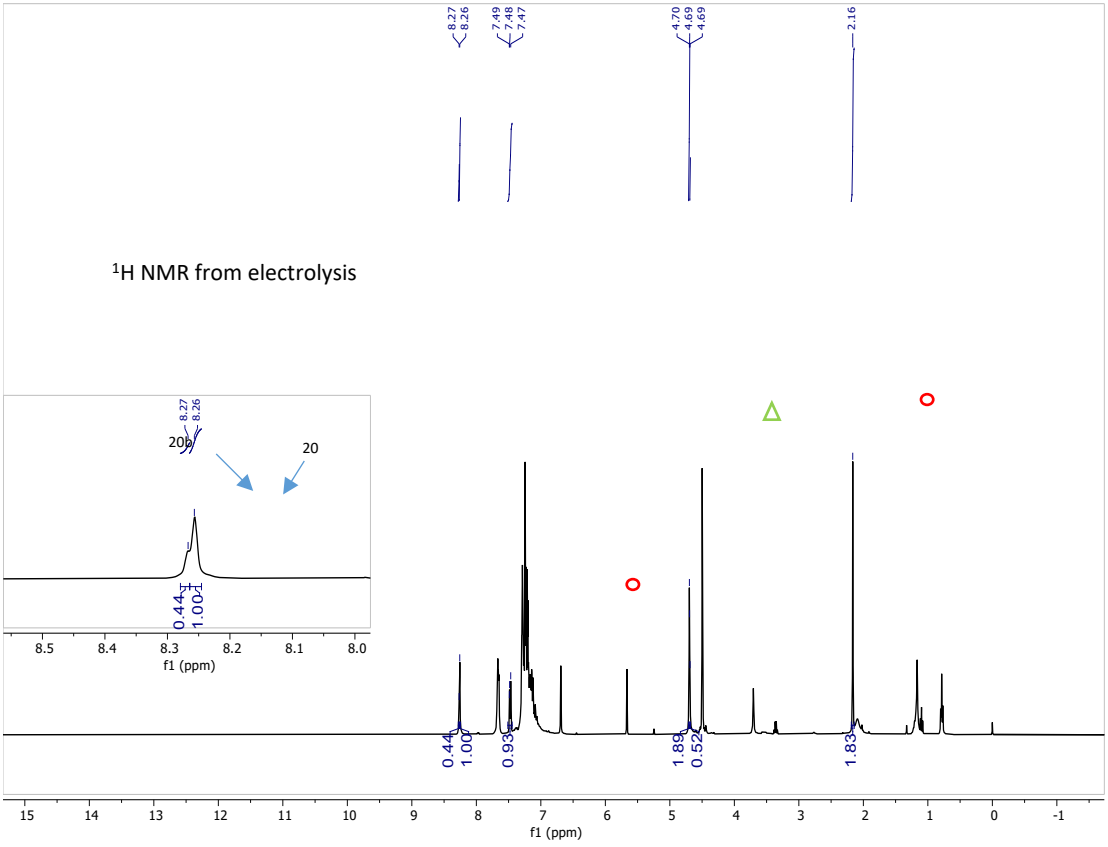

^{1}H NMR of synthesized **20**

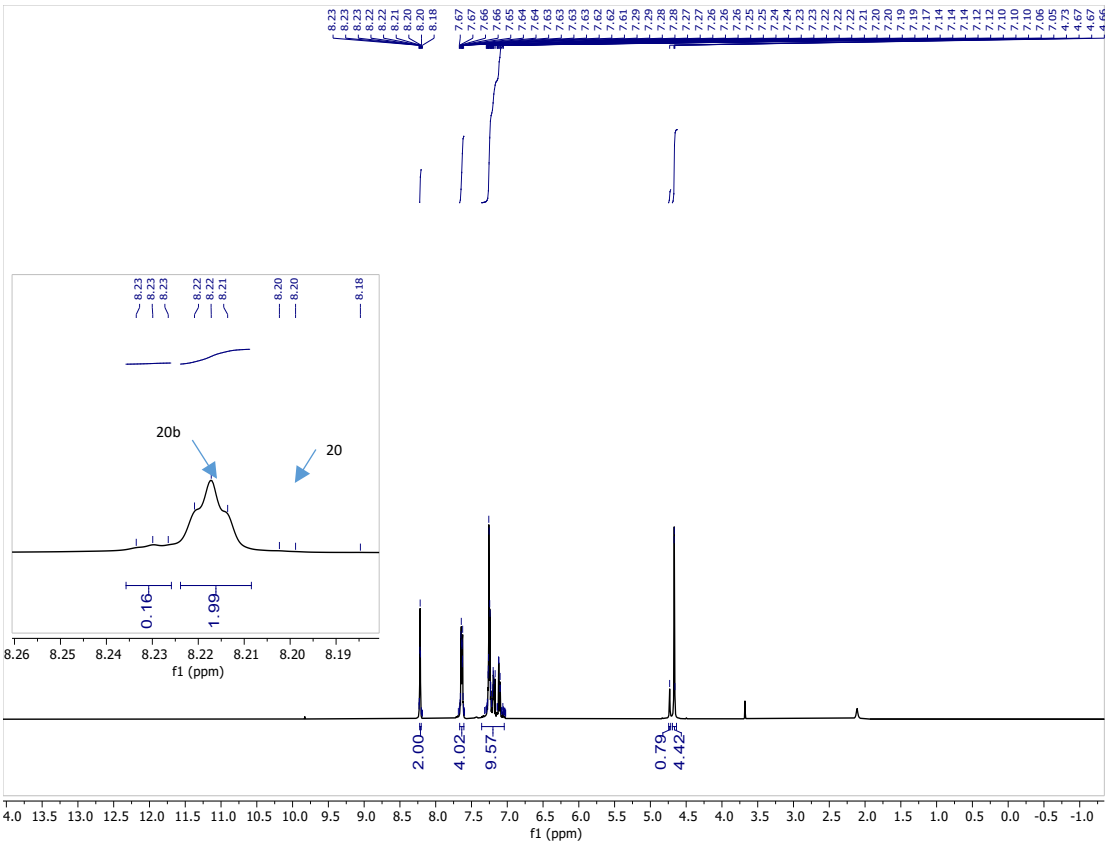

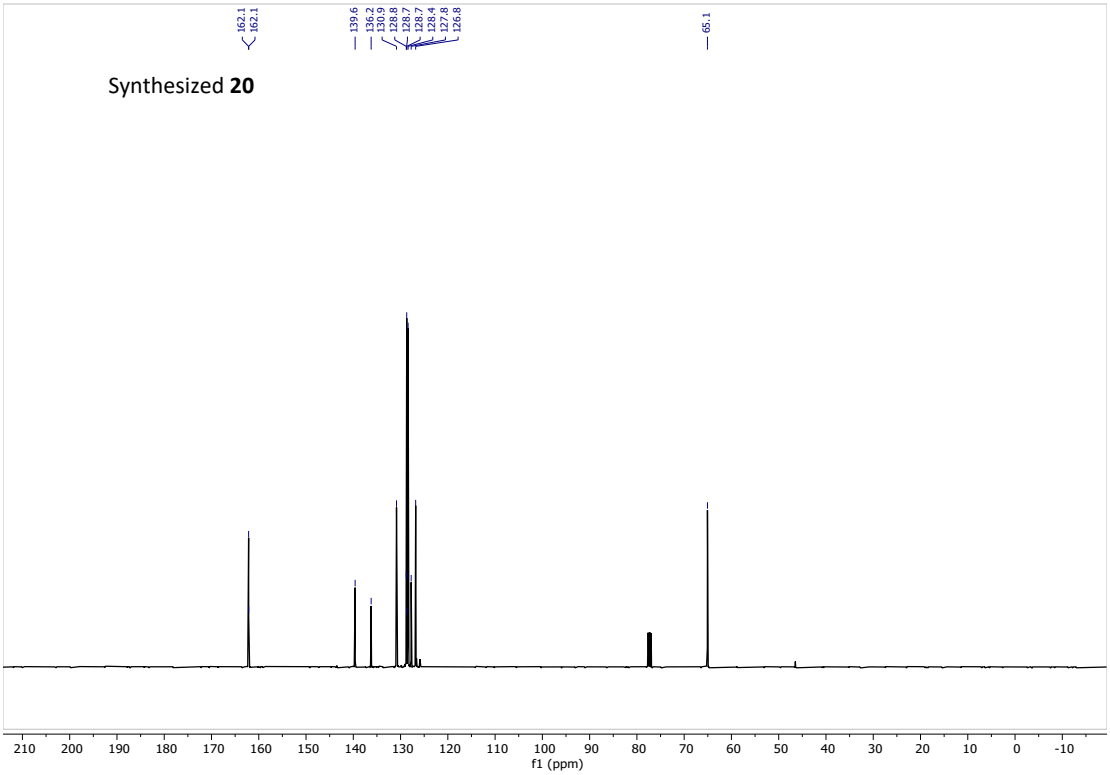

Synthesized **20**

HR-MS: Exact mass ([M+H]$^{+}$): 313.16993. Found: 313.16904

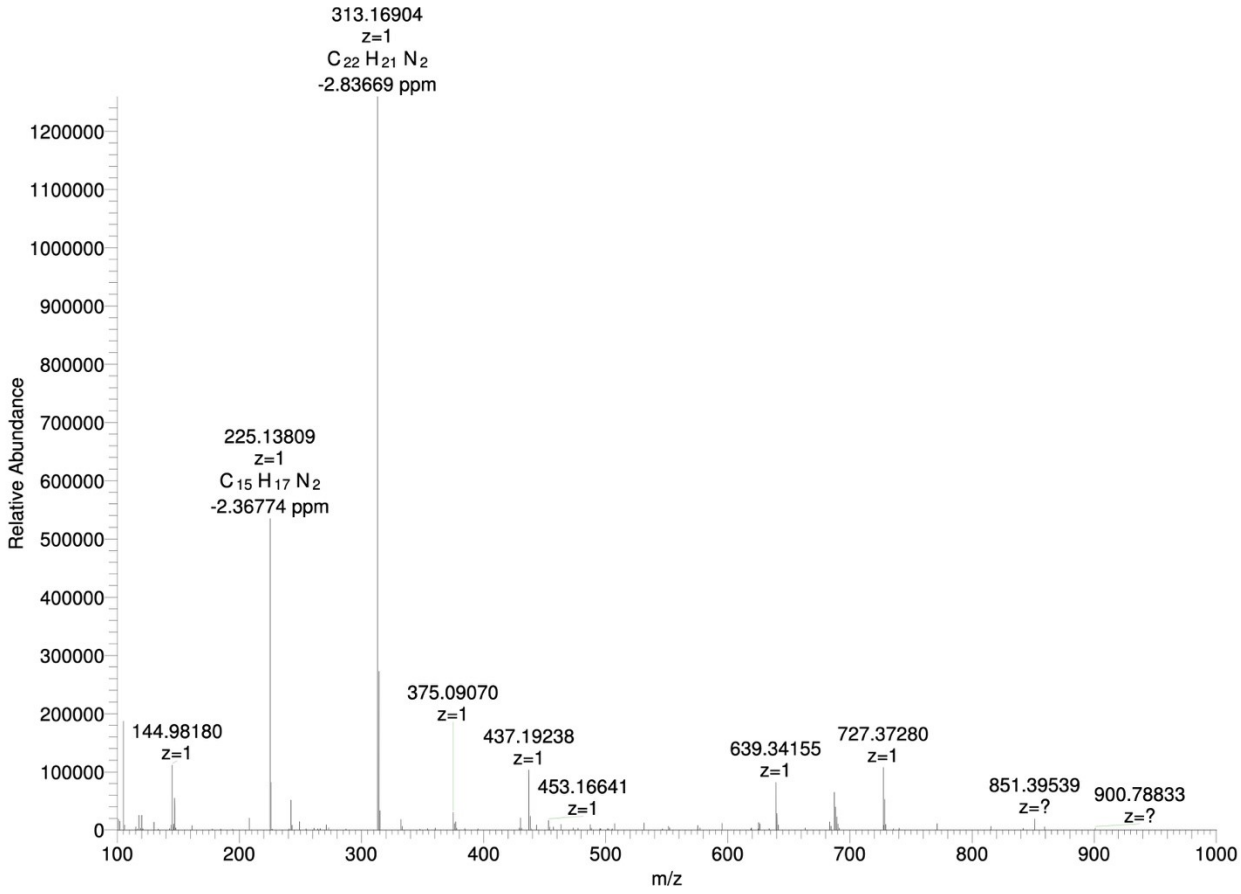
313.16904
z=1
C 22 H 21 N 2
-2.83669 ppm
225.13809
z=1
C 15 H 17 N 2
-2.36774 ppm
375.09070
z=1
144.98180
z=1
437.19238
z=1
453.16641
z=1
639.34155
z=1
727.37280
z=1
851.39539
z=?
900.78833
z=?
Relative Abundance
m/z
0
100000
200000
300000
400000
500000
600000
700000
800000
900000
1000000
1100000
1200000
100
200
300
400
500
600
700
800
900
1000

ATR-IR:

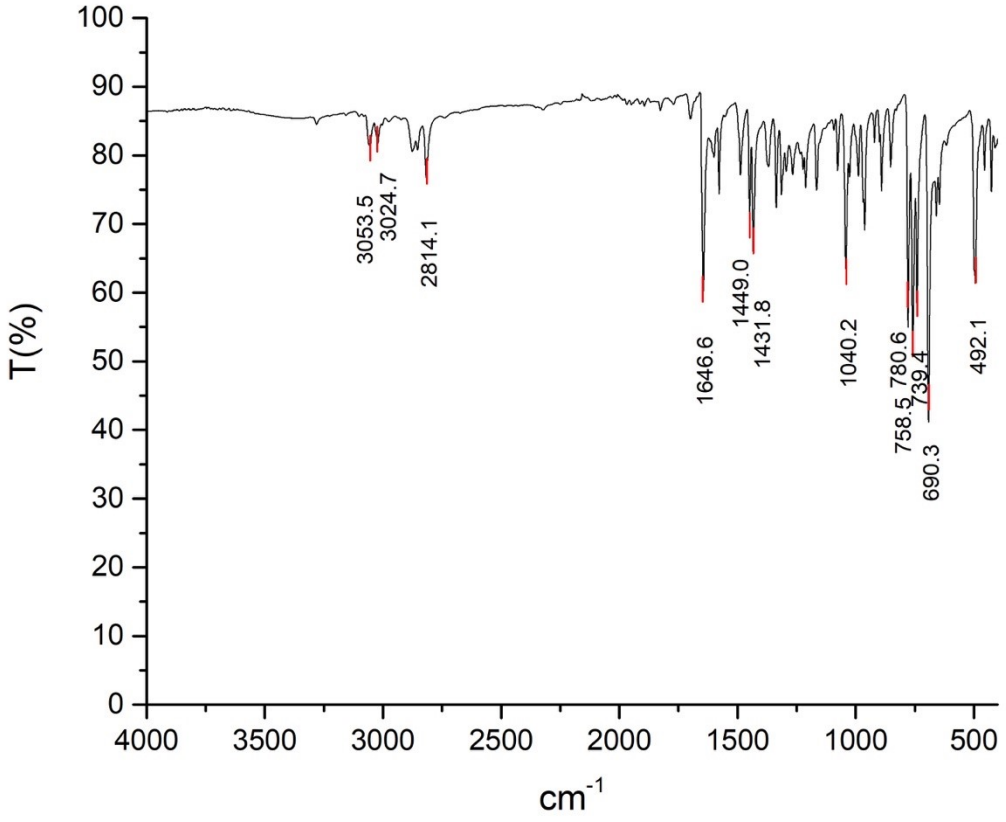

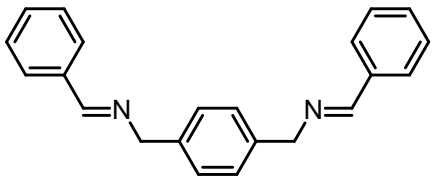

21

***N*,*N*'-(1,4-phenylenebis(methylene))bis(1-phenylmethanimine)** (**21**) ^{1}H NMR (400 MHz, $CDCl_3$) δ 8.46 (d, *J* = 1.6 Hz, 1H), 7.93 – 7.82 (m, 2H), 7.50 (dd, *J* = 5.3, 1.9 Hz, 3H), 7.46 – 7.43 (m, 2H), 4.90 (d, *J* = 1.4 Hz, 2H). NMR data are in accordance with literature values.[31]

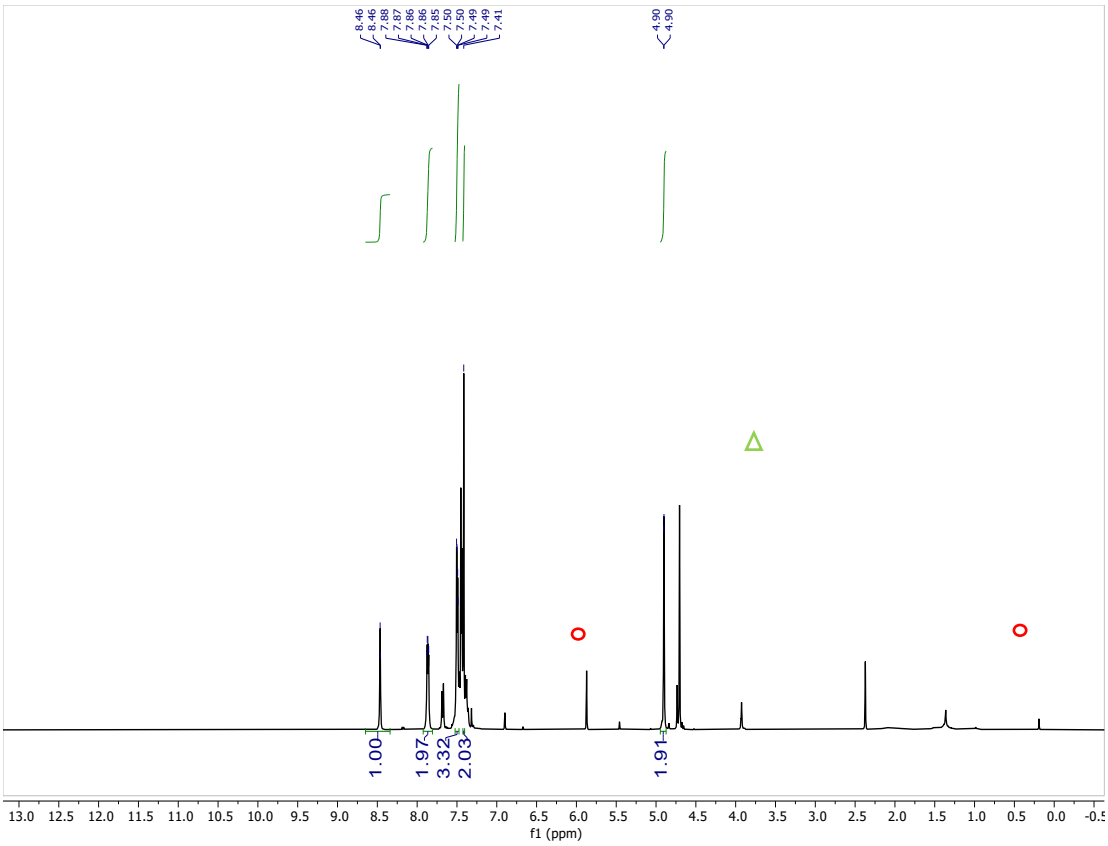

11 References

1 J. Zhang, M. Gandelman, L. J. W. Shimon, H. Rozenberg and D. Milstein, *Organometallics*, 2004, **23**, 4026–4033.
2 C. Gunanathan, Y. Ben-David and D. Milstein, *Science*, 2007, **317**, 790.
3 A. M. Abend, L. Chung, R. T. Bibart, M. Brooks and D. G. McCollum, *Journal of Pharmaceutical and Biomedical Analysis*, 2004, **34**, 957–962.
4 L. Droguet, M. Courty, O. Fontaine, J. M. Tarascon and A. Grimaud, *J. Electrochem. Soc.*, 2022, **169**, 070510.
5 F. Dorchies, A. Serva, D. Crevel, J. D. Freitas, N. Kostopoulos, M. Robert, O. Sel, M. Salanne and A. Grimaud, , DOI:10.26434/chemrxiv-2022-wjsbs-v2.
6 L. Zhu, J. Du, S. Zuo and Z. Chen, *Inorg. Chem.*, 2016, **55**, 7135–7140.
7 V. Briega-Martos, F. J. Sarabia, V. Climent, E. Herrero and J. M. Feliu, *ACS Meas. Au*, 2021, **1**, 48–55.
8 J. L. Jeffrey, J. A. Terrett and D. W. C. MacMillan, *Science*, 2015, **349**, 1532–1536.
9 L. Capaldo, D. Ravelli and M. Fagnoni, *Chem. Rev.*, 2022, **122**, 1875–1924.
10 S. W. Kohl, L. Weiner, L. Schwartsburd, L. Konstantinovski, L. J. W. Shimon, Y. Ben-David, M. A. Iron and D. Milstein, *Science*, 2009, **324**, 74–77.
11 C. A. Huff, J. W. Kampf and M. S. Sanford, *Chem. Commun.*, 2013, **49**, 7147–7149.
12 D. Tocqueville, F. Crisanti, J. Guerrero, E. Nubret, M. Robert, D. Milstein and N. von Wolff, *Chem. Sci.*, 2022, **13**, 13220–13224.
13 B. Gnanaprakasam, J. Zhang and D. Milstein, *Angewandte Chemie International Edition*, 2010, **49**, 1468–1471.
14 T. Higuchi, R. Tagawa, A. Iimuro, S. Akiyama, H. Nagae and K. Mashima, *Chemistry – A European Journal*, 2017, **23**, 12795–12804.
15 C. Dong, A. Uematsu, S. Kumazawa, Y. Yamamoto, S. Kodama, A. Nomoto, M. Ueshima and A. Ogawa, *J. Org. Chem.*, 2019, **84**, 11562–11571.
16 H. Tian, X. Yu, Q. Li, J. Wang and Q. Xu, *Advanced Synthesis & Catalysis*, 2012, **354**, 2671–2677.
17 G. M. Torres, M. De La Higuera Macias, J. S. Quesnel, O. P. Williams, V. Yempally, A. A. Bengali and B. A. Arndtsen, *J. Org. Chem.*, 2016, **81**, 12106–12115.
18 Journal of Applied Polymer Science | Wiley Online Library, https://onlinelibrary-wiley-com.inc.bib.cnrs.fr/doi/10.1002/app.49986, (accessed September 13, 2023).
19 R. D. Patil and S. Adimurthy, *Advanced Synthesis & Catalysis*, 2011, **353**, 1695–1700.

20 G. Zhang and S. K. Hanson, *Org. Lett.*, 2013, **15**, 650–653.
21 M. H. Shaw, N. G. McCreanor, W. G. Whittingham and J. F. Bower, *J. Am. Chem. Soc.*, 2015, **137**, 463–468.
22 L. J. Donnelly, J.-C. Berthet and T. Cantat, *Angewandte Chemie International Edition*, 2022, **61**, e202206170.
23 C. Cheng and M. Brookhart, *J. Am. Chem. Soc.*, 2012, **134**, 11304–11307.
24 Y. Miao, S. V. Samuelsen and R. Madsen, *Organometallics*, 2021, **40**, 1328–1335.
25 H. Li, D. Lupp, P. K. Das, L. Yang, T. P. Gonçalves, M.-H. Huang, M. El Hajoui, L.-C. Liang and K.-W. Huang, *ACS Catal.*, 2021, **11**, 4071–4076.
26 K. C. Nicolaou, C. J. N. Mathison and T. Montagnon, *J. Am. Chem. Soc.*, 2004, **126**, 5192–5201.
27 J. C. Anderson, A. J. Blake, G. P. Howell and C. Wilson, *J. Org. Chem.*, 2005, **70**, 549–555.
28 S. P. Midya, J. Pitchaimani, V. G. Landge, V. Madhu and E. Balaraman, *Catal. Sci. Technol.*, 2018, **8**, 3469–3473.
29 M. Crespo, M. Martinez, J. Sales, X. Solans and M. Font-Bardia, *Organometallics*, 1992, **11**, 1288–1295.
30 T. Földesi, G. Sipos, R. Adamik, B. Nagy, B. L. Tóth, A. Bényei, K. J. Szekeres, G. G. Láng, A. Demeter, T. J. Peelen and Z. Novák, *Org. Biomol. Chem.*, 2019, **17**, 8343–8347.
31 S. H. Doan and T. V. Nguyen, *Green Chem.*, 2022, **24**, 7382–7387.